

PROCESSING AND TRAFFICKING OF THE IRON
REGULATORY PROTEIN, HEMOJUVELIN

By

Julia Elizabeth Maxson

A DISSERTATION

Presented to the Department of Cell & Developmental Biology
And the Oregon Health & Science University
School of Medicine

In partial fulfillment of
The requirements for the degree of

Doctor of Philosophy

April 2011

School of Medicine
Oregon Health & Science University

CERTIFICATE OF APPROVAL

This is to certify that the PhD dissertation of
Julia Elizabeth Maxson
has been approved

Caroline Enns, PhD.

Peter Mayinger, PhD.

Jan Christian, PhD.

Philip Stork, PhD.

David Koeller, MD.

Philip Copenhaver, PhD.

TABLE OF CONTENTS

List of Figures	iii
Acknowledgement	vi
Abbreviations	vii
Abstract	viii
Chapter 1: Introduction.	1
Iron overload disorders	2
Iron absorption and utilization	4
Regulation of systemic iron homeostasis by hepcidin	5
Hemojuvelin is a critical regulator of hepcidin	7
Cleavage of hemojuvelin regulates hepcidin expression	11
Figures	18
Chapter 2: Processing of hemojuvelin requires retrograde trafficking to the Golgi in HepG2 cells.	22
Abstract	23
Introduction	24
Materials and Methods	27
Results	29
Figures	40
Discussion	49
Chapter 3: The GPI-anchor of hemojuvelin potentiates signaling, but is not required for proteolytic processing.	54
Abstract	55
Introduction	56
Materials and Methods	60
Results	64
Figures	71
Discussion	79
Chapter 4: Matriptase-2 and proprotein convertase cleaved forms of hemojuvelin have different roles in the down regulation of hepcidin expression	84
Abstract	85
Introduction	86
Materials and Methods	89
Results	95
Figures	103
Discussion	117
Chapter 5: Conclusions and Future Directions	122

Appendices	
Appendix A: The cytoplasmic domain of neogenin promotes hemojuvelin secretion	133
Appendix B: Truncated HJV constructs have similar glycosylation profiles to WT HJV, but are secreted more rapidly from the cell	138
Appendix C: BMP signaling induces tyrosine phosphorylation, but treatment with Dasatinib does not effect hepcidin expression.	142
Appendix D: The ectodomain of neogenin is shed by proteolytic cleavage.	146
Appendix E: Generation of flag-tagged mouse HJV constructs with mutations in the furin and matriptase-2 cleavage sites.	150
Appendix F: Trafficking of Tf and TfR1.	155
References	158
Curriculum Vitae	167

LIST OF FIGURES

Figure 1.1. Iron transport across intestinal epithelial cells.

Figure 1.2. Hepcidin regulates iron levels.

Figure 1.3. HJV acts as a BMP co-receptor to upregulate transcription of hepcidin.

Figure 1.4. Cleavage of HJV by furin produces a shed form of HJV that inhibits BMP signaling.

Figure 2.1. Release of cellular HJV.

Figure 2.2. Cell-associated HJV has high-mannose oligosaccharides, whereas cellular neogenin has complex oligosaccharides.

Figure 2.3. Secreted HJV has complex oligosaccharides and is derived from the pool of HJV at the plasma membrane.

Figure 2.4. The glycosylation patterns of cellular and secreted HJV in HEK293 and Hep3B cells.

Figure 2.5. Neogenin is necessary for sHJV release but not for the retention of high-mannose oligosaccharides by HJV.

Figure 2.6. Filipin blocks generation of sHJV but does not alter the glycosylation of cell surface HJV.

Figure 2.7. Addition of Furin Convertase Inhibitor does not lead to a buildup of Endo H-resistant HJV in the cell lysate.

Figure 3.1. HJV constructs with transmembrane domains instead of a GPI-anchor are expressed and processed by the cell.

Figure 3.2. HJV secretion does not require a GPI-anchor.

Figure 3.3. Furin-mediated cleavage of HJV chimeras.

Figure 3.4. The GPI-anchor of HJV potentiates hepcidin expression.

Figure S3.1. GPI-linked HJV is primarily basolaterally localized.

Figure S3.2. Treatment of cells expressing the HJV/LDLR chimera with a dynamin inhibitor reduces secretion of sHJV.

Figure 4.1. Cleavage of HJV by matriptase-2 generates one major isoform of soluble HJV in HEK293 cells.

Figure 4.2. The endogenously expressed matriptase-2 in HepG2 cells is able to cleave HJV.

Figure 4.3. Proprotein convertase-mediated cleavage of HJV is blocked by mutation of Arg 332.

Figure 4.4. Matriptase-2-mediated cleavage of HJV is blocked by mutation of Arg 288.

Figure 4.5. Truncation of HJV after Arg 257 or Arg 288 results in ER retention of HJV.

Figure 4.6. sHJV generated by proprotein convertase cleavage suppresses BMP6-induced hepcidin expression, but sHJV produced by matriptase-2 does not.

Figure S4.1: Leupeptin and furin convertase inhibitor block cell surface HJV from being secreted into the medium.

Figure S4.2. Mass spectrometry analysis of sHJV.

Figure S4.3. Mutation of Arg 288 reduces matriptase-2 mediated cleavage of HJV.

Figure S4.4: Truncation of HJV after the proprotein convertase cluster confirms the site of HJV cleavage.

Figure 5.1. Glycosylation of proteins in the secretory pathway.

Figure 5.2. HJV undergoes retrograde trafficking to the Golgi prior to being secreted.

Figure 5.3. Model of trafficking and secretion of the HJV/furin chimera.

Figure 5.4. Model of inhibition of BMP signaling by furin and matriptase-2 cleavage of HJV.

Figure A.1. GPI-linked HJV is primarily basolaterally localized.

Figure A.2. Cellular HJV release requires full-length neogenin.

Figure A.3. HJV constructs lacking a membrane anchor have a similar glycosylation profile to WT HJV, but are secreted more rapidly.

Figure A.4. BMP signaling induces tyrosine phosphorylation, but treatment with Dasatinib does not effect hepcidin expression.

Figure A.5. Shedding of neogenin into the conditioned medium is blocked by TAPI-2.

Figure A.6. Generation of flag-tagged mouse HJV constructs with mutations in the furin and matriptase-2 cleavage sites.

Figure A.7. Pulse chase of TfR1 and Tf.

ACKNOWLEDGEMENTS

Caroline Enns has been an incredible mentor to me. I am always amazed by her unfailing support of my scientific development, the depth of her knowledge and her skill in troubleshoot experiments. The studies in this thesis have been a fruitful collaboration between An-Sheng Zhang and myself. I have been fortunate to have the opportunity to learn from his impressive technical expertise and keen scientific insight. Past and present members of the Enns Lab have given me excellent experimental advice and have made the lab a very enjoyable place to work. The members of my thesis advisory committee have provided invaluable guidance. I would also like to thank my wonderful family and friends who have always supported me in my academic goals.

ABBREVIATIONS AND TERMS

ActRIIA	Activin receptor IIA
Alk2	Activin receptor-like kinase 2
Alk3	Activin receptor-like kinase
BMP	Bone morphogenetic protein
BMPRII	BMP receptor II
CM	Conditioned medium
Dcytb	Duodenal cytochrome b
DMT1	Divalent metal transporter 1
ER	Endoplasmic reticulum
FCI	Furin convertase inhibitor
Fe ²⁺	Ferrous iron
Fe ³⁺	Ferric iron
FNIII	Fibronectin type III
FPN	Ferroportin
GPI-anchor	Glycosylphosphatidylinositol-anchor
H-ferritin	Heavy or heart ferritin
HFE	Hereditary hemochromatosis protein
<i>HFE2/HJV*</i>	Gene symbol for hemojuvelin
HJV	Hemojuvelin
Hp	Hephaestin
IRIDIA	Iron refractory iron deficiency anemia
JH	Juvenile Hemochromatosis
L-ferritin	Light or liver ferritin
MRP2	Multi-drug resistance protein 2
PC	Proprotein convertase
RGM	Repulsive guidance molecule
RGMa	Repulsive guidance molecule a
RGMb	Repulsive guidance molecule b, also known as DRAGON
<i>Rgmc/HJV*</i>	Gene symbol for mouse hemojuvelin.
sHJV	Shed hemojuvelin
siRNA	Small-interfering RNA
SMAD	SMA/mothers against decapentaplegic
STEAP3	Six-transmembrane epithelial antigen of the prostate 3
Tf	Transferrin
Tf-saturation	The degree to which iron is bound to Tf
TfR1	Transferrin receptor 1
TfR2	Transferrin receptor 2
TGFβ	Transforming growth factor beta
TGN	Trans Golgi network
<i>TMPRSS6</i>	Gene symbol for matriptase-2

*For clarity, *HJV* will be used as the gene symbol for human and mouse HJV.

ABSTRACT

Mutations in hemojuvelin (*HJV*) lead to the iron overload disorder juvenile hemochromatosis. *HJV* regulates iron metabolism by activating transcription of the iron regulatory peptide, hepcidin, through the bone morphogenetic protein (BMP) signaling pathway. *HJV* is proposed to act as a co-receptor for BMP ligands, but the exact mechanism by which it potentiates BMP signaling is not clear. To better understand the role of *HJV* in the regulation of iron metabolism, I analyzed its trafficking and processing. *HJV* traffics to the cell surface while avoiding modification by glycosylases and proteases that reside in the Golgi. After reaching the cell surface, *HJV* undergoes retrograde trafficking to the Golgi, where it is further modified and cleaved by furin. *HJV* is cleaved by the furin family of proprotein convertases, which generates a soluble form of *HJV* that antagonizes BMP signaling. Reaching the cell surface prior to cleavage and secretion may allow *HJV* to participate in BMP signaling at the cell surface and allow for greater regulation of cleavage. Since endocytosis of *HJV* precedes secretion and *HJV* is a glycosylphosphatidylinositol (GPI)-anchored protein that endocytoses through a GPI-specific pathway, the GPI-anchor of *HJV* might be necessary for secretion. Interestingly, replacing the GPI-anchor of *HJV* with a transmembrane and cytoplasmic domain did not prevent cleavage of *HJV*. It did, however, block the ability of *HJV* to upregulate hepcidin expression. This finding indicates that the GPI-anchor of *HJV* is important for its ability to signal through the BMP-signaling pathway. In addition to the cleavage of *HJV* by furin, I also show that another protease involved in iron metabolism, matriptase-2, cleaves *HJV* in a liver-derived

cell line and that these cleavages occur in a site-specific manner. Furthermore, regulation of hepcidin expression by furin-mediated cleavage of HJV generates a soluble form of HJV that antagonizes hepcidin expression, while cleavage of HJV by matriptase-2 does not. Cleavage of HJV by matriptase-2 may reduce the amount of cell surface HJV available to participate in BMP signaling. This work is the first to detail the trafficking of HJV and also increases our understanding of the proteolytic cleavage of HJV in response to iron demand.

CHAPTER 1
INTRODUCTION

Iron overload disorders

Iron is a critical nutrient for the majority of organisms. It is required for a variety of biological processes, including oxidative phosphorylation, DNA synthesis and oxygen transport. The majority of iron in the body is bound by heme, which acts as a cofactor for hemoglobin, allowing the transport of oxygen in red blood cells for delivery to tissues (Laidlaw, 1904; Peters, 1912). Lack of iron can result in iron deficiency anemia, a disorder in which there is insufficient hemoglobin production, resulting in a reduced oxygen carrying capacity (Dameshek, 1931; Heath et al., 1932; Minot, 1932). Conversely, too much iron in the body can lead to the iron overload disorder, hereditary hemochromatosis (Sheldon, 1934).

Hereditary hemochromatosis is the most common potentially fatal genetic disorder in people of Northern European origin. In patients with the most common form of hereditary hemochromatosis, excess iron concentrates in organs including the liver, heart and pancreas (Horns, 1949; Sheldon, 1934). Iron accumulation over time is slow, and disease symptoms usually manifest in the fourth or fifth decades of life. Excess iron that has exceeded the bodies storage capacity increases the production of reactive oxygen species that damage proteins, lipids, and nucleic acids (Park et al., 1987). This cellular damage eventually leads to organ damage and dysfunction. Patients with hereditary hemochromatosis typically have cirrhosis or hepatocellular carcinoma associated with liver damage, diabetes secondary to pancreas damage, or arrhythmias or heart failure associated with heart damage (Horns, 1949; Opie, 1899; Sheldon, 1934).

Proteins mutated in hemochromatosis-

Mutations in several proteins lead to hereditary hemochromatosis. The most common are mutations in the hereditary hemochromatosis protein (HFE) (Feder et al., 1996). It is estimated that 1 in 200 to 1 in 300 Caucasians are homozygous for mutations in HFE, the most common of which is C282Y (Merryweather-Clarke et al., 1997). Mutation of C282Y disrupts the interaction of HFE with the beta 2-microglobulin subunit, which is critical for its stability and function. The penetrance of hereditary hemochromatosis due to mutations in HFE varies widely. A recent study found that patients homozygous for C282Y have a 38-50% chance of developing iron overload and a 10-33% chance of having organ damage secondary to iron overload (Whitlock et al., 2006). Mutations in the iron transporter ferroportin (FPN), and the iron regulatory protein transferrin receptor 2 (TfR2) also lead to hereditary hemochromatosis (Camaschella et al., 2000; Montosi et al., 2001). Mutations in the iron regulatory protein hemojuvelin (HJV), and the iron regulatory peptide, hepcidin, both lead to juvenile hemochromatosis (Nicolas et al., 2001; Papanikolaou et al., 2004; Viatte et al., 2005). Juvenile hemochromatosis is a more severe form of iron overload in which symptoms present in patients in their teens and early twenties. These patients primarily have cardiac dysfunction and hypogonadism due to gonad damage, secondary to rapid iron accumulation (Camaschella et al., 2002; De Gobbi et al., 2002).

Iron absorption and utilization

Non-heme and heme iron are both absorbed from the diet by intestinal enterocytes in the duodenum (Figure 1.1). Non-heme iron is reduced from the ferric form (Fe^{3+}) to the ferrous form (Fe^{2+}) by ferrireductases, including duodenal cytochrome b (Dcytb), on the apical side of the enterocyte (McKie et al., 2001). Fe^{2+} is then transported across the apical membrane of the enterocytes by divalent metal transporter 1 (DMT1), a proton symporter (Fleming et al., 1997; Gunshin et al., 2005; Gunshin et al., 1997). Heme iron is transported across the apical membrane by a yet to be discovered transporter.

After transport into the enterocyte, iron can either be stored in ferritin or exported into the blood by FPN. Ferritin is an iron storage protein that forms a cage-like structure made up of 24 subunits of L-ferritin (light or liver ferritin) and H-ferritin (heavy or heart ferritin). This cage can accommodate up to 4500 iron atoms (Theil, 2003). Iron stored as ferritin is cleared from the body during the normal turnover of intestinal epithelial cells. The transport of iron out of enterocytes by FPN (Abboud and Haile, 2000; Donovan et al., 2000; McKie et al., 2000), is coupled to the oxidation of Fe^{2+} iron to Fe^{3+} by the ferroxidases ceruloplasmin and hephaestin, allowing the Fe^{3+} to bind transferrin (Tf), the major iron transport protein in serum (Cherukuri et al., 2005; Harris et al., 1999; Vulpe et al., 1999). The binding of iron to Tf converts apo-Tf into holo-Tf.

Holo-Tf is taken up by cells, where it releases iron, which is incorporated into proteins or stored. In most cell types, Tf binds to transferrin receptor 1 (TfR1), which allows it to be endocytosed. After endocytosis, acidification of the endosome

allows for release of Fe^{3+} from Tf (Klausner et al., 1983). In erythroblasts, Fe^{3+} is then reduced to Fe^{2+} by six-transmembrane epithelial antigen of the prostate 3 (STEAP3) so that it can be transported into the cytosol by DMT1 (Fleming et al., 1998; Ohgami et al., 2005). Iron can then be incorporated into iron-containing proteins or transported to the mitochondria for incorporation into heme. The majority of Tf bound iron is taken up by erythroid precursors in the bone marrow for incorporation into heme. When red blood cells become senescent, they are phagocytosed by macrophages, which release iron back into circulation through FPN (Donovan et al., 2005). Iron in the body is stored primarily in liver hepatocytes under normal physiological conditions where it is stored in ferritin.

Regulation of systemic iron homeostasis by hepcidin

The liver acts as the primary sensor and regulator of iron homeostasis. Iron uptake from the diet must be tightly controlled to maintain sufficient iron for erythropoiesis without saturating iron storage capacity. This is accomplished by production of an iron regulatory hormone, hepcidin, in response to iron loading. Hepcidin is a 25 amino acid peptide hormone produced by the liver (Nicolas et al., 2001; Park et al., 2001; Pigeon et al., 2001). It is a member of the defensin family of antimicrobial peptides, and can cause the sequestration of serum iron to reduce the iron available to microorganisms in response to inflammation. Hepcidin is also down-regulated in response to increased erythropoietic drive (red blood cell production) and hypoxia, which allows for increased iron uptake for incorporation into hemoglobin (Nicolas et al., 2002).

Hepcidin reduces iron transport from the intestine into circulation by regulating the levels of FPN (Nemeth et al., 2004). Hepcidin regulates the levels of FPN by binding to it and inducing its internalization from the cell surface and subsequent lysosomal degradation (Nemeth et al., 2004). Under conditions of high iron, hepcidin production increases in the liver, which leads to decreased FPN and reduced iron transport into the body (Pigeon et al., 2001). When iron is scarce, hepcidin levels are reduced, increasing the amount of FPN and iron transport into the body.

FPN is also present on the basolateral membrane of hepatocytes and on macrophages (Donovan et al., 2005). Consequently, iron release from macrophages into the blood (which recycle iron from senescent red blood cells), and iron efflux from hepatocytes (which store iron), are both regulated by hepcidin. Thus, hepcidin levels control serum iron, and macrophage and hepatocyte iron content.

Hepcidin levels are regulated by serum iron-

Transcription of hepcidin is regulated by the levels of iron in the serum (Figure 1.2). In a normal individual, there is very little free iron in serum, as it is mainly bound by Tf. In humans, approximately 30% of the Tf binding sites are occupied by iron (Andrews and Schmidt, 2007), thus providing a buffering capacity for fluctuation in iron due to iron uptake from the diet or mild hemolysis. The liver is proposed to sense the proportion of holo-Tf in the blood and regulates hepcidin levels accordingly to maintain iron homeostasis (Johnson and Enns, 2004). When Tf saturation is high, transcription of hepcidin is increased, which reduces iron

transport through FPN into the blood and decreases iron uptake from the intestine. When transferrin saturation is low, transcription of hepcidin is decreased, resulting in increased iron transport from the intestine into the blood to restore adequate iron levels. In contrast to normal individuals, hereditary hemochromatosis patients often have low hepcidin levels, despite having nearly 100% Tf saturation

A possible mechanism by which holo-Tf levels are sensed by hepatocytes is through binding to the cell surface HFE/TfR2 complex. TfR2 is similar in structure to TfR1 but does not play a major role in cellular iron uptake. Loss of function mutations in either HFE or TfR2 lead to iron overload and hereditary hemochromatosis, secondary to inappropriately low hepcidin levels (Camaschella et al., 2000; Feder et al., 1996). Holo-Tf may upregulate signaling through HFE/TfR2 and increase hepcidin expression in two ways. First, holo-Tf displaces HFE from TfR1 (Bennett et al., 2000; Lebron et al., 1999; West et al., 2001), allowing HFE to form a complex with TfR2 (Chen et al., 2007). Second, TfR2 protein is stabilized by holo-Tf binding, which may increase signaling (Johnson and Enns, 2004; Robb and Wessling-Resnick, 2004). Although the exact mechanism by which the HFE/TfR2 complex regulate hepcidin transcription is not yet known, signaling through the ERK pathway may be involved in this process (Calzolari et al., 2006).

Hemojuvelin is a critical regulator of hepcidin

In addition to the proposed HFE/TfR2 axis of hepcidin regulation, hepcidin is also regulated through HJV. Mutations in *HJV* lead to severe iron overload, which is

caused by a decrease in hepcidin levels (Papanikolaou et al., 2004). HJV is therefore critical to the regulation of hepcidin and iron homeostasis.

HJV is a member of the repulsive guidance molecule family (RGM) of proteins (Niederkofler et al., 2004). There are two homologues of HJV, RGMa and RGMb, that are expressed in non-overlapping patterns in the developing nervous system and are involved in neuronal guidance, repulsion, and survival (Niederkofler et al., 2004). RGMa and RGMb signal through the bone morphogenetic protein (BMP) signaling pathway (Babitt et al., 2005; Samad et al., 2005; Xia et al., 2005). Because of the original identification of HJV as a homologue of RGMa and RGMb, HJV is also known as Rgmc in the mouse. For the sake of clarity, HJV will be used to refer to both the mouse and human forms. In humans, all RGM family members possess a N-terminal signal sequence, a potential integrin binding motif with the amino acid sequence RGD, three potential N-linked glycosylation sites, a partial von Willebrand factor type D domain, and a C-terminal glycosylphosphatidylinositol-anchor (GPI-anchor) addition sequence. Unlike RGMa and RGMb, HJV is not expressed in neural tissue, but rather is primarily expressed in cardiac and skeletal muscle and to a lesser extent in the liver (Niederkofler et al., 2004). In the liver, HJV regulates hepcidin levels. The function of muscle derived HJV is not known.

HJV regulates hepcidin through the BMP signaling pathway-

HJV is a co-receptor for BMP ligands (Figure 1.3) (Babitt et al., 2006), which are part of the transforming growth factor β (TGF β) family of signaling molecules. BMPs bind to tetrameric receptor complexes composed of two type 1 BMP receptors

and two type II BMP receptors (Shi and Massague, 2003), and cause the activation and phosphorylation of the cytoplasmic portion of the BMP receptors. The BMP receptors can then phosphorylate members of the receptor-activated small body size/mothers against decapentaplegic (SMAD) family of proteins, including SMADs 1, 5 and 8. Phosphorylation of the receptor-activated SMADs allows them to interact with the SH2 domains of co-SMAD (SMAD4). (Wang et al., 2005) Formation of a trimeric complex of the receptor SMADs and SMAD4 allows the complex to traffic to the nucleus, where it binds to BMP response elements to activate transcription. There are multiple BMP response elements in the hepcidin promoter and transcription of hepcidin is increased in response to BMP ligands, particularly BMP2, 4 and 6 (Xia et al., 2008). A subset of BMP type I and type II receptors participate in hepcidin activation, including the BMP type I receptors activin receptor-like kinase 2 (Alk2) and activin receptor-like kinase 3 (Alk3), along with the type II receptors activin receptor IIA (ActRIIA) and BMP receptor II (BMPRII) (Xia et al., 2008). The severe iron overload seen in the liver-specific knockout of SMAD4 demonstrates the importance of this pathway (Wang et al., 2005).

Neogenin binds to HJV-

Members of the RGM family bind to the cell surface receptor neogenin. The interaction of RGMa with neogenin is critical for its role in neuronal development (Matsunaga et al., 2004; Rajagopalan et al., 2004). HJV also binds to neogenin (Zhang et al., 2005), and this interaction is required for HJV-induced BMP signaling to upregulate hepcidin expression (Zhang et al., 2009). Neogenin is a large single-pass

transmembrane protein. It is a Type I membrane protein with its N-terminus outside the cell and its C-terminus inside the cell. The extracellular domain is composed of interleukin-like repeats and 6 fibronectin III-like domains. HJV interacts most strongly with a portion of neogenin corresponding to the fifth and sixth fibronectin III-like domains (Yang et al., 2008).

Neogenin plays a role in the regulation of hepcidin expression in response to iron-

Several lines of evidence suggest that neogenin is important for the regulation of iron homeostasis. Neogenin may be required for BMP induced upregulation of hepcidin expression by HJV in HepG2 cells (Zhang et al., 2009). These findings are controversial, however: another group showed that neogenin is dispensable for hepcidin expression in their system (Xia et al., 2008). Further evidence that neogenin is critical to the maintenance of iron homeostasis comes from the neogenin gene trap mouse (Lee et al., 2010). This mouse has a 90% reduction in the levels of neogenin protein. In these mice, reduced neogenin results in impaired BMP signaling and reduced hepcidin levels that lead to liver iron-overload. Reduced hepcidin in these mice leads to increase FPN stability and inappropriately high transport of iron from the intestine into the blood (Lee et al., 2010).

The mechanism by which neogenin is required for HJV to induce BMP signaling is not yet known. HJV is capable of binding to both BMPs and neogenin, so neogenin could alter the interaction of HJV with BMP ligands or receptors (Yang et al., 2008). Alternately, neogenin is proposed to recruit HJV to lipid rafts (Zhou et al.,

2010). Enhanced signaling of receptor complexes has been shown in lipid rafts, so recruitment of HJV to these domains could potentially enhance signaling (Lajoie et al., 2009).

Neogenin is homologous to another receptor, deleted in colorectal cancer (DCC). DCC is capable of enhancing signaling through the TGF β pathway. DCC is phosphorylated on tyrosine residues in its cytoplasmic domain in response to ligand binding, which leads to recruitment of the signaling molecule LMO4 (Schaffar et al., 2008). Recruitment of LMO4 enhances TGF β signaling by activating the receptor-activated SMADs (Schaffar et al., 2008). By analogy to DCC, binding to downstream signaling components is another mechanism by which neogenin could increase hepcidin expression.

Cleavage of HJV regulates hepcidin expression

The RGM family members are membrane proteins that are tethered by a GPI-anchor (Niederkofler et al., 2004). GPI-linked HJV potentiates BMP signaling to upregulate hepcidin expression. HJV can also be cleaved by proteases in the furin family of proprotein convertases, which releases HJV from its GPI-anchor and allows it to be secreted from cultured cells (Kuninger et al., 2008; Lin et al., 2008; Silvestri et al., 2008a). This secreted form of HJV antagonizes the BMP signaling pathway and reduces hepcidin expression (Figure 1.4) (Lin et al., 2005). Soluble HJV has been detected in the blood of humans and rats (Lin et al., 2005; Zhang et al., 2007). Detection of HJV in the blood is difficult in mice, due to the lack of sensitivity of currently available antibodies. Whether HJV in the blood is derived from the liver or

from muscle is not known, but muscle has been postulated to serve as a source of secreted HJV. Intravenous injection of super physiological levels of purified soluble HJV into mice leads to a decrease in liver hepcidin levels and an increase in iron delivery into the blood (Babitt et al., 2007), leading to the proposal that sHJV competes with cell-associated HJV for binding to BMPs.

The secretion of HJV is regulated by iron. Treatment of hepatoma-derived cell lines expressing HJV with holo-Tf reduces cleavage of HJV (Lin et al., 2005; Silvestri et al., 2007; Zhang et al., 2007). This leads to more signaling through the BMP pathway to increase hepcidin levels, which would reduce iron transport into the blood to maintain iron homeostasis. This represents another level at which hepcidin expression could be regulated by iron.

Furin family of proprotein convertases

Furin is member of the subtilisin super family of serine endoproteases, also known as proprotein convertases. It is a type I transmembrane protein that localizes primarily to the trans Golgi network (TGN). Although the majority of furin is localized to the TGN, it also cycles through the endosomal system to the cell surface (Molloy et al., 1994). Furin undergoes two autocatalytic cleavage events, which release its prodomain and allow furin to cleave its substrates in trans (Thomas, 2002). Furin has a consensus cleavage motif of R-X-K/R-R and a minimal cleavage motif of R-X-X-R (Molloy et al., 1992). Furin is ubiquitously expressed in tissues, including the liver. In the liver other members of the proprotein convertase (PC) family are also expressed including PACE4, PC6 and PC7 (Roebroek et al., 2004;

Wouters et al., 1998). These PCs have similar substrate specificity to furin. A post-embryonic knockout of furin in the mouse liver demonstrated that there was partial or complete redundancy of furin with other PCs (Roebroek et al., 2004).

Regulation of furin expression levels

A model for regulation of HJV cleavage in response to iron has been proposed in which the levels of furin are transcriptionally regulated in response to iron or hypoxia (Silvestri et al., 2008a). In this model, changes in the levels of furin would alter the proportion of uncleaved to soluble HJV and thus regulate BMP signaling and hepcidin levels. Since furin is an enzyme, and most enzymes do not exhibit haploinsufficiency, it is unclear whether a less than 2 fold change in the activity of the furin promoter would have any effect on the rate of endogenous HJV cleavage (Silvestri et al., 2008a). Importantly, BMPs and hepcidin themselves are processed by furin and other proprotein convertases, so changes in furin levels could have opposing effects on multiple components of these pathways. Additionally, the partial or complete redundancy of furin with other liver-expressed PCs (Roebroek et al., 2004), may further reduce the effect of small changes in furin levels on HJV cleavage.

Neogenin is required for the cleavage of HJV

In addition to potentiating HJV signaling through the BMP pathway, neogenin is involved in the cleavage of HJV. Knockdown of neogenin by siRNA results in a reduction in HJV secretion (Zhang et al., 2007; Zhang et al., 2008). Treatment of cells with a soluble protein fragment containing the fibronectin III 5-6 domains of

neogenin blocks the interaction of full-length cellular neogenin with HJV, resulting in a reduction of HJV cleavage (Zhang et al., 2008). Potentiation of BMP signaling and involvement in HJV cleavage would be expected to have opposite effects on the regulation of hepcidin levels. While this may initially seem paradoxical, many receptor complexes are degraded following signaling as a mechanism of limiting the signal. In this vein, neogenin may potentiate HJV/BMP signaling, which in turn leads to down regulation of the signaling complex by promoting cleavage of HJV and thus appropriately limiting the signal.

Matriptase-2 regulates iron metabolism-

Another protease, matriptase-2, has recently been linked to the regulation of iron homeostasis. Matriptase-2 was recently identified as the mutated gene in the mask mouse (Du et al., 2008). The mask mouse has hair loss secondary to iron deficiency anemia, due to a deletion of the serine protease domain of matriptase-2 (Du et al., 2008). Matriptase-2 mutant mice have inappropriately high levels of hepcidin. The resulting microcytic anemia is refractory to oral iron. Similar phenotypes were observed in a matriptase-2 knockout mouse, demonstrating that the mutations are due to a loss of function (Folgueras et al., 2008). Patients with mutations in the gene for matriptase-2, *TMPRSS6*, also have iron refractory iron deficiency anemia (IRIDA) (Finberg et al., 2008).

One proposed mechanism for the regulation of iron metabolism by matriptase-2 is that it could participate in cleavage of HJV. Studies in cultured cells show that overexpression of matriptase-2 degrades HJV, producing a ladder of

cleavage products (Silvestri et al., 2008b). Degradation of HJV would reduce hepcidin levels, resulting in increased iron uptake. Whether HJV is degraded by matriptase-2 *in vivo* is not known. Matriptase-2 was also shown in this study to bind to HJV (Silvestri et al., 2008b). Double knockout HJV^{-/-} TMPRSS6^{-/-} mice are anemic (Finberg et al., 2010). While the authors of this work propose that this shows that matriptase-2 is upstream of HJV, it may also indicate that there are other iron regulatory proteins that are cleaved by matriptase-2. These data indicate that matriptase-2 may be important in the regulation of HJV.

Summary of the thesis-

Although HJV clearly plays an important role in the regulation of iron metabolism, relatively little is known about its trafficking or processing. HJV is cleaved by furin or related proprotein convertase family members (Kuninger et al., 2008; Lin et al., 2008; Silvestri et al., 2008a). Since furin is localized primarily in the TGN, it could cleave HJV in the biosynthetic pathway (Molloy et al., 1994). However, cleavage of HJV during its initial trafficking to the cell surface could cause HJV to be secreted from cells before it reaches the cell surface to act as a BMP co-receptor. To determine whether HJV is cleaved before it reaches the cells surface, Chapter 2 of this thesis examines the trafficking of HJV. I showed that GPI-linked HJV reaches the cell surface without being cleaved. HJV then undergoes retrograde trafficking to the Golgi prior to being cleaved by furin family members and shed from the cell.

HJV and its related RGM family members are GPI-linked proteins (Niederkofler et al., 2004) and GPI-linkage can impart specific trafficking patterns

on proteins. HJV endocytoses through a clathrin and dynamin independent pathway characteristic of GPI-linked proteins (Zhang et al., 2008). Since HJV endocytoses from the cell surface and then undergoes retrograde trafficking to the Golgi prior to being cleaved and secreted, the GPI-anchor of HJV could direct cleavage of HJV. In Chapter 3 of this thesis, I tested whether the GPI-anchor of HJV is required for cleavage. I showed that GPI-linkage of HJV is not required for furin-mediated cleavage of HJV. GPI-linked proteins are thought to cluster in specific membrane domains to increase signaling. The GPI-anchor of HJV could therefore potentiate its signaling through the BMP pathway. In Chapter 3, I also show that the GPI-anchor is required for HJV to upregulate hepcidin expression.

In addition to cleavage of HJV by furin, matriptase-2 may also play a role in the down-regulation of cell surface HJV levels. Matriptase-2 is an important regulator of iron homeostasis, because matriptase-2 deficient mice have inappropriately high hepcidin levels and anemia (Du et al., 2008; Folgueras et al., 2008). These phenotypes could be accounted for by reduced HJV cleavage, which would lead to an increase in BMP signaling and hepcidin expression. Chapter 4 investigates the role of matriptase-2 in the cleavage of HJV. I showed that matriptase-2 cleaves HJV in a site-specific manner. This cleavage accounts for the smaller of the two HJV secreted products seen in the liver-derived HepG2 cell line. The larger product is the result of cleavage by the furin family of proprotein convertases. Furthermore, the cleavage of HJV by matriptase-2 reduces hepcidin expression in a manner distinct from furin cleavage. These studies into the

trafficking and processing of HJV provide important insight into the role of HJV in the regulation of hepcidin expression and iron metabolism.

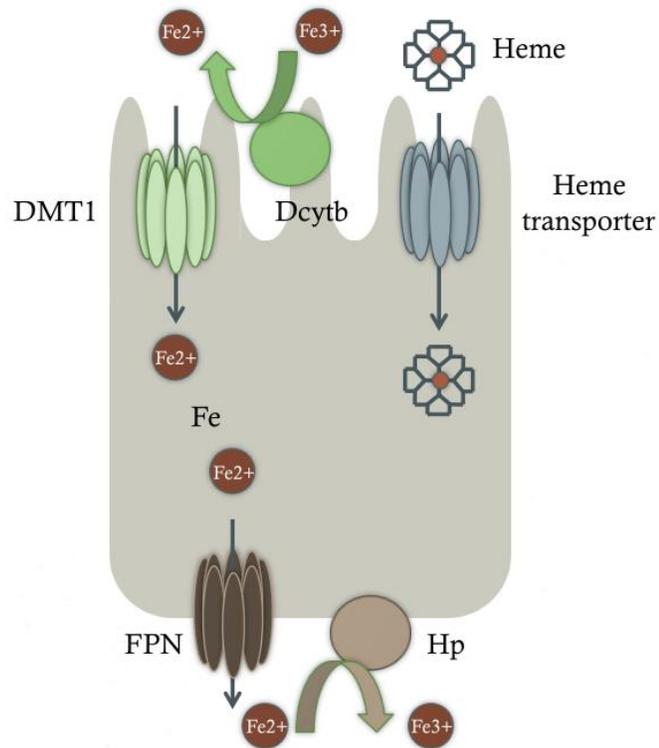


Figure 1.1. Iron transport across intestinal epithelial cells.

Iron is reduced from the Fe³⁺ form to the Fe²⁺ form by duodenal cytochrome b (Dcytb) or other ferrireductases. It can then be transported across the intestinal apical membrane into the cell by DMT1. Heme is also transported from diet across the apical brush border membrane by an unknown transporter. Once inside the cell iron is utilized, stored in ferritin, or transported across the basolateral membrane and into the blood by FPN. This transport is coupled to oxidation of Fe²⁺ to Fe³⁺ by the ferroxidases hephaestin (Hp) or ceruloplasmin.

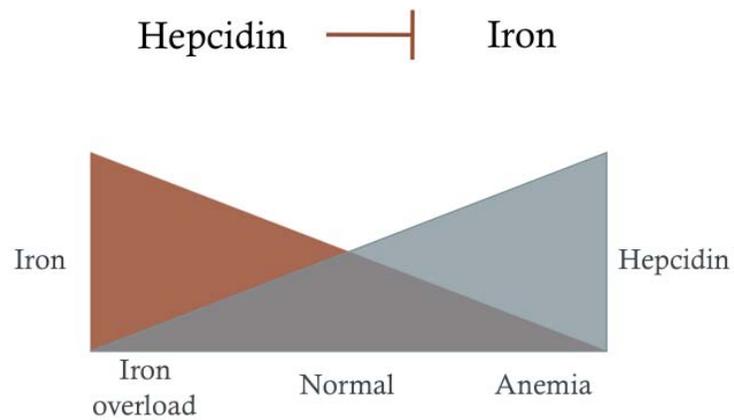


Figure 1.2. Hepcidin negatively regulates iron levels in the blood.

Hepcidin binds to the iron transporter FPN located on the basolateral membrane of intestinal epithelial cells (as well as on hepatocytes and macrophages) and induces its internalization and lysosomal degradation, decreasing the transport of dietary iron into the blood. . In patients with abnormally low levels of hepcidin too much iron is taken into the body resulting in iron overload. Conversely, inappropriately high levels of hepcidin can cause anemia due to low iron transport into the blood.

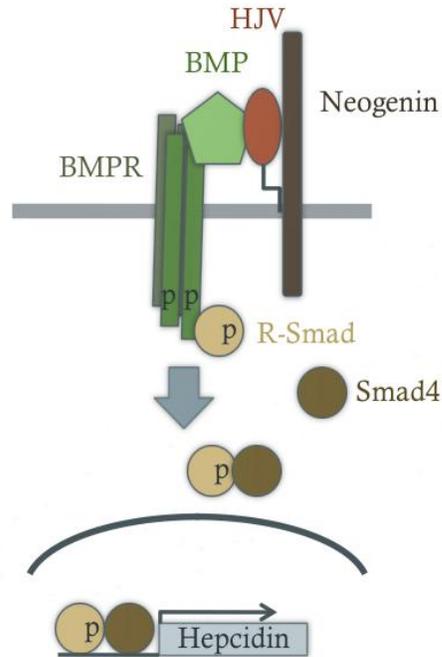


Figure 1.3. HJV acts as a BMP co-receptor to upregulate transcription of hepcidin. HJV binds to BMP ligands and increases their signaling through the BMP co-receptor complex. This increased signaling leads to phosphorylation of the receptors and then subsequent phosphorylation of receptor activated smads (R-Smads 1, 5 or 8). This leads to translocation of a complex of receptor activated Smads and Smad4 to the nucleus where they bind to the hepcidin promoter and activate transcription of hepcidin.

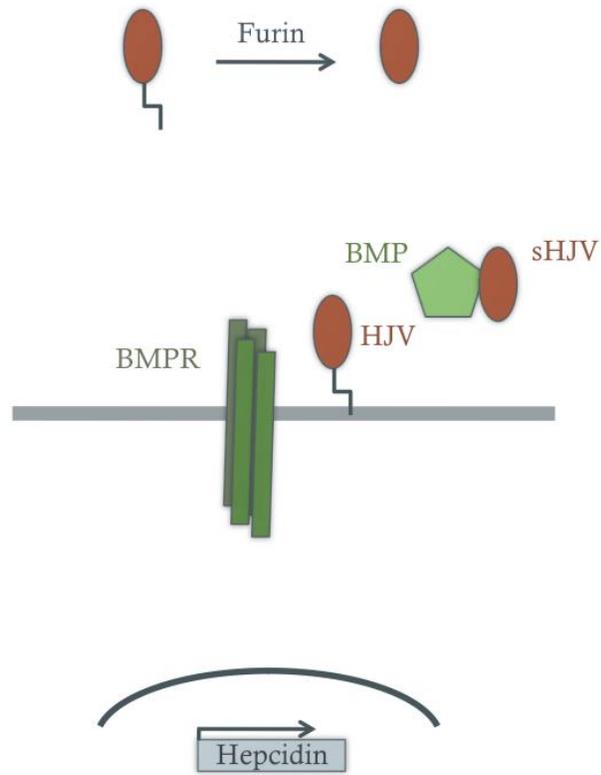


Figure 1.4. Cleavage of HJV by furin produces a shed form of HJV that inhibits BMP signaling. HJV is cleaved within its protein sequence by the furin family of proprotein convertases, which releases HJV from its GPI anchor and allows it to be shed from cells. This shed form of HJV negatively regulates BMP signaling and hepcidin expression, possibly by acting as a decoy that binds to BMP ligands and sequesters them away from the receptor complex.

CHAPTER 2

Processing of hemojuvelin requires retrograde trafficking to the Golgi in HepG2 cells

Julia Maxson¹, Caroline A. Enns¹, and An-Sheng Zhang¹

¹Department of Cell and Developmental Biology, Oregon Health & Science University, Portland, OR 97239 USA

Corresponding Author: An-Sheng Zhang, Department of Cell and Developmental Biology L215, 3181 SW Sam Jackson Park Rd, Portland, OR 97239; fax: (503) 494-4253; e-mail: zhanga@ohsu.edu

Published in Blood, 19 February 2009. Volume 113, Number 8, Pages 1786-1793.

Abstract

Hemojuvelin (HJV) was recently identified as a critical regulator of iron homeostasis. It is either associated with cell membranes through a GPI-anchor or released as a soluble form. Membrane anchored HJV acts as a co-receptor for bone morphogenic proteins (BMPs) and activates the transcription of hepcidin, a hormone that regulates iron efflux from cells. Soluble HJV antagonizes BMP signaling and suppresses hepcidin expression. In this study we examined the trafficking and processing of HJV. Cellular HJV reached the plasma membrane without obtaining complex oligosaccharides, indicating that HJV avoided Golgi processing. Secreted HJV, in contrast, has complex oligosaccharides and can be derived from HJV with high mannose oligosaccharides at the plasma membrane. Our results support a model in which retrograde trafficking of HJV prior to cleavage is the predominant processing pathway. Release of HJV requires it to bind to the transmembrane receptor neogenin. Neogenin does not, however, play a role in HJV trafficking to the cell surface, suggesting that it could be involved either in retrograde trafficking of HJV or in cleavage leading to HJV release.

Introduction

Iron is an indispensable nutrient in most organisms, but is also toxic when in excess. Iron homeostasis is maintained by an elegant control mechanism that coordinates iron absorption from the intestine, iron recycling from senescent red blood cells and mobilization of iron stores from liver hepatocytes. Hemojuvelin (HJV) is central to this process. HJV is a GPI-linked protein and has Asn-linked glycosylation sites in its extracellular domain (Niederkofler et al., 2004). It is mainly expressed in muscle and to a lesser extent in the liver (Niederkofler et al., 2004; Papanikolaou et al., 2004). Clinical studies demonstrated that homozygous or compound heterozygous mutations in the HJV gene (*HFE2*) lead to juvenile hemochromatosis, a severe iron overload disorder, indicating that HJV plays an important role in the regulation of iron homeostasis (Papanikolaou et al., 2004).

HJV regulates serum iron levels by modulating expression of hepcidin, a hepatocyte-derived peptide hormone. The marked suppression of hepcidin expression in juvenile hemochromatosis patients and HJV knockout mice indicates that HJV is a critical upstream regulator of hepcidin expression (Huang et al., 2005; Niederkofler et al., 2005; Papanikolaou et al., 2004). Hepcidin regulates serum iron levels by decreasing iron efflux from intestinal epithelial cells, macrophages and hepatocytes (Huang et al., 2005; Lin et al., 2005; Niederkofler et al., 2005; Papanikolaou et al., 2004). Thus, HJV activates transcription of hepcidin, which decreases serum iron levels by limiting iron efflux.

There are two forms of HJV, a membrane-anchored GPI-linked form and a secreted soluble form (sHJV) that is generated by furin-mediated cleavage of GPI-

HJV (Kuninger et al., 2006; Lin et al., 2005; Lin et al., 2008; Niederkofler et al., 2004; Silvestri et al., 2008a; Zhang et al., 2005). Both forms of HJV regulate hepcidin transcription and iron metabolism though they have opposite effects. GPI-linked HJV increases transcription of hepcidin through the bone morphogenic protein (BMP) signaling pathway by acting as a co-receptor for BMP ligands (Babitt et al., 2006; Lin et al., 2007; Xia et al., 2008). Disruption of BMP signaling by hepatocyte-specific knockout of Smad4, a central mediator of the BMP signaling pathway, results in decreased hepcidin expression and iron overload in mice (Wang et al., 2005). Conversely, sHJV decreases the level of hepcidin mRNA in primary human hepatocytes (Lin et al., 2007). Moreover, injection of sHJV into mice decreases BMP signaling and hepcidin expression and increases the amount of serum and liver iron (Babitt et al., 2007). Soluble HJV could antagonize BMP signaling by competing with membrane-associated HJV for binding to BMP ligands, preventing them from interacting with cell-associated HJV and therefore inhibiting hepcidin expression (Babitt et al., 2007; Lin et al., 2007). Since the GPI-linked and soluble forms of HJV have opposing roles, regulation of HJV processing is important for the control of iron homeostasis.

Generation of sHJV requires neogenin, a transmembrane receptor in the immunoglobulin superfamily (Zhang et al., 2007). HJV binds to neogenin (Kun Hashimoto et al., 2008; Yang et al., 2008; Zhang et al., 2005), specifically to the membrane-proximal fifth and sixth fibronectin type III (FNIII) domains (Yang et al., 2008). Knockdown of neogenin blocks HJV release but does not affect trafficking of HJV to the plasma membrane (Zhang et al., 2008). Neogenin is unable to interact

with the G320V mutant form of HJV, the most common disease-causing mutation in type 2A juvenile hemochromatosis patients (Papanikolaou et al., 2004; Zhang et al., 2005). Although neogenin is necessary for HJV release, the role that it plays in this process is not known.

HJV is endocytosed through a cholesterol-dependent and dynamin-independent pathway (Zhang et al., 2008). Endocytosis of HJV is blocked by filipin, which depletes cholesterol and has been shown to block the endocytosis of other GPI-linked proteins (Chadda et al., 2007; Nichols et al., 2001; Zhang et al., 2008). Filipin also blocks generation of sHJV (Zhang et al., 2008).

In the current study, we sought to understand how HJV trafficking leads to its release and investigate how neogenin affects this process. Using a hepatic cell line as a model system, we showed that HJV trafficked to the plasma membrane without acquiring complex oligosaccharides and that neogenin was not required for this process. Moreover, cell-surface HJV acquired complex oligosaccharides before it was released into the media. Furthermore, blocking HJV cleavage using a furin inhibitor did not lead to a buildup of Endo H-resistant HJV in the cell, suggesting that cleavage precedes complex glycosylation.

Materials and Methods

Cell culture

HepG2 and Hep3B cells were purchased from ATCC (Manassas, VA) and maintained in MEM/10% FCS/1 mM pyruvate/1x non-essential amino acids (complete medium). HEK293 (Human Embryonic Kidney 293) cells (ATCC) were grown in DMEM/10% FCS/1 mM pyruvate. HepG2 cells stably transfected with wild type HFE2 (HJV), G320V mutant HFE2 (G320V) or pcDNA3 empty vector (control) were generated previously (Zhang et al., 2007). The stably transfected cells were maintained in complete medium with 800 µg/mL G418. tTA-HJV-HepG2 cells were generated by cloning HFE2 into a tetracycline-inducible pcDNA4 vector, which was then stably transfected into tTA-HepG2 cells (Feng and Longmore, 2005). They were maintained in complete medium with 800 µg/mL G418 and 5 µg/mL blasticidin and induced to express HJV using 2 µg/mL doxycycline. Neogenin/HJV-HEK293 cells, stably expressing both neogenin and HJV, were maintained in DMEM with 10% FCS and 800 µg/mL G418.

Endo H and PNGase F digestion

Endo H and PNGase F were used to analyze the Asn-linked oligosaccharides on HJV and neogenin protein in cell lysate, conditioned medium, and streptavidin bead eluate. Briefly, samples prepared were incubated with Endo H or PNGase F (New England Biolabs) according to manufacturer's instruction. After 4 hours of incubation at 37°C, the digested samples were subjected to western blot analysis of HJV and neogenin as described for immunodetection.

Immunodetection

Cell lysates, conditioned medium or streptavidin eluates were separated by SDS-PAGE under reducing conditions, followed by transfer onto a nitrocellulose membrane. Membranes were probed with affinity-purified rabbit anti-HJV antibody (0.22 µg/mL) (generated against residues 1-401 of HJV as described previously (Zhang et al., 2008)), rabbit anti-neogenin antibody (0.4 µg/mL, Santa Cruz Biotechnology), goat anti-Tf serum (generated against purified human Tf, 1:10,000) or mouse anti-β-actin antibody (1:10,000, Chemicon International), followed by immunodetection using a corresponding horseradish peroxidase (HRP)-conjugated secondary antibody (Chemicon International) and chemiluminescence (Super Signal, Pierce). Alternatively, HJV was detected using an Alexa Fluor 680 goat anti-rabbit secondary antibody (1:10,000, Invitrogen) and visualized using an Odyssey Infrared Imaging System (Licor).

Results

Release of sHJV constitutes the major pathway of cellular HJV turnover.

HJV exists in either cell-associated or soluble forms. Soluble HJV is generated by furin-mediated cleavage of cellular HJV (Lin et al., 2008; Silvestri et al., 2008a). Because the soluble and cell-associated forms of HJV have opposing effects on iron homeostasis, we analyzed the trafficking and processing of HJV. HepG2 cells stably expressing human HJV (HJV-HepG2) were used as a model system. HepG2 cells are a human hepatoma cell line, which express many proteins involved in iron metabolism but do not express HJV detectably by immunoblot (Knowles et al., 1980; Zhang et al., 2007). HJV-HepG2 cells express HJV, which undergoes active release (Zhang et al., 2007).

The kinetics of the loss of cell-associated HJV and the appearance of HJV in the media was examined. HJV-HepG2 cells were treated with cycloheximide (100 $\mu\text{g}/\text{mL}$) to block protein synthesis, and HJV levels in the cell lysate or one-third of conditioned medium at 0, 1, 2, 4 and 6 hours were detected by immunoblot. HepG2 cells transfected with an empty vector were used as a control for the specificity of the antibody against HJV. The amount of HJV in the cell lysate exhibited a rapid decrease over time (Figure 2.1A). Conversely, sHJV in the media was detected starting at 1 hour and continued to accumulate for at least 6 hours implicating a precursor-product relationship. The two bands seen for secreted HJV are consistent with the literature (Kuninger et al., 2006; Zhang et al., 2007).

In order to more precisely determine the rate of disappearance of HJV from the cell, a pulse-chase experiment was performed. HJV-HepG2 cells were

metabolically labeled with ^{35}S -(met/cys) for 30 minutes, then incubated with complete media for 0, 0.5, 1, 2, 3, 4, 5 and 6 hours (Figure 2.1B). HJV was then immunoprecipitated from cell lysates and analyzed by SDS-PAGE. HJV disappeared from the cell lysate quickly with a turnover of approximately one hour, consistent with the cycloheximide results (Figure 2.1A).

As an independent estimate of the approximate time interval between HJV synthesis in the endoplasmic reticulum (ER) and HJV release into the media, we generated a tTA-HJV-HepG2 cell line in which the expression of HJV is under the tight control of the tTA inducible promoter. HJV expression was induced using doxycycline. Cellular HJV was detectable by western blot at 4 hours post induction, while secreted HJV was evident in the medium at 6 hours post induction (Figure 2.1C). These results indicate that HJV release into the media occurs within 2 hours of synthesis.

Since cellular HJV turnover could also result from lysosomal degradation of HJV, HJV-HepG2 cells were treated with 100 $\mu\text{g}/\text{mL}$ cycloheximide with or without 100 nM bafilomycin A to determine the relative contributions of sHJV release and intracellular degradation to the disappearance of HJV from cells. Bafilomycin A is an inhibitor of the vacuolar H^+ -ATPase, which dissipates the pH gradient in the intracellular organelles and blocks protein degradation in lysosomes (Yoshimori et al., 1991). After 0, 1, 2, 3, 4, 5 and 6 hours of incubation at 37°C, HJV in the cell lysate and in the media was detected by western blot. Only a slight increase in the accumulation of cellular HJV was noticeable at 3 and 4 hours when bafilomycin A was present (Figure 2.1D). Bafilomycin A did not significantly alter HJV release.

These results suggest that while lysosomal turnover of HJV is detectable, release of sHJV is the major mechanism of HJV loss from cells.

Distinct processing of HJV and neogenin

HJV is modified after synthesis by addition of a GPI anchor. GPI-linked proteins are synthesized in the ER where they are linked to a GPI anchor before being targeted to the plasma membrane. In addition to acquiring a GPI-anchor, HJV is a glycoprotein with three potential Asn-linked glycosylation sites. To investigate the routes of HJV and neogenin trafficking, we analyzed the maturation of Asn-linked oligosaccharides on both HJV and neogenin by digestion with either Endo H, which cleaves high mannose oligosaccharides added co-translationally in the ER, or PNGase F, which cleaves both high-mannose and Golgi-modified complex oligosaccharides. In these experiments, extracts from HJV-HepG2 cells were digested with Endo H or with PNGase F (Figure 2.2A). A shift in the molecular weight of the HJV and neogenin, as detected by western blot analysis, indicates that oligosaccharides have been removed. Neogenin was sensitive to PNGase F but resistant to Endo H, indicating that it obtained complex oligosaccharides during its transit through the Golgi (Figure 2.2A). Cellular HJV was unexpectedly found to be sensitive to both Endo H and PNGase F, indicating that it has high mannose oligosaccharides. The pattern of glycosylation of wild-type HJV was identical to the G320V mutant HJV, which does not associate with neogenin and remains primarily in the ER (Silvestri et al., 2007; Zhang et al., 2005). These results suggest that cellular HJV has high mannose

oligosaccharides, which have not been processed in the Golgi, whereas cellular neogenin obtains complex oligosaccharides in the Golgi.

To compare the kinetics of neogenin and HJV trafficking through the biosynthetic pathway, pulse-chase experiments were performed for neogenin and HJV. Neogenin/HJV-HEK293 cells, which stably express neogenin, were used because the level of endogenous neogenin in HJV-HepG2 cells is insufficient for visualization by pulse-chase. Neogenin/HJV-HEK293 cells were metabolically labeled for 30 min and then incubated in complete medium for 0, 20, 60 and 105 minutes. The samples were immunoprecipitated with an anti-neogenin antibody and then digested with Endo H or mock digested. Neogenin was completely Endo H-sensitive at the conclusion of the 30-minute pulse, after which a chase was initiated. At 20 minutes after the chase some of the neogenin is Endo H-sensitive and some is resistant, and by 60 minutes it is completely Endo H-resistant (Figure 2.2B, upper panel), indicating that it has progressed through the Golgi. To analyze the Endo H sensitivity of HJV, HJV-HepG2 cells were labeled for 30 minutes and then chased for 0, 30, 60, 90, 120 and 180 minutes and immunoprecipitated. HJV remained Endo H-sensitive in the cell lysate for at least three hours after the 30-minute labeling (Figure 2.2B, lower panel).

To determine if HJV reaches the cell surface within the time period in which it remains Endo H-sensitive, we induced HJV expression in tTA-HJV-HepG2 cells for 0, 2, 3, 4, 5, and 6 hours and then detected biotinylated cell surface HJV by western blot (Figure 2.2C). HJV reaches the cell surface within two hours of synthesis and did not further accumulate on the cell surface. These results indicate that HJV remains

Endo H sensitive throughout its biosynthetic pathway to the cell surface (Figure 2.2B, lower panel).

Since HJV remains Endo H sensitive for at least three hours and HJV reaches the cell surface within 2 hours, we next examined the Asn-linked glycosylation status of cell-surface HJV and neogenin. Cell-surface proteins were biotinylated at 4°C followed by a streptavidin pull down and Endo H or PNGase F digestion (Figure 2.2D). Cell-surface HJV and neogenin had similar Asn-linked glycosylation patterns as they did in the whole cell lysates (Figure 2.2B). HJV therefore did not obtain complex oligosaccharides in the Golgi, indicating that it is inaccessible to Golgi resident glycosylases en route to the cell surface.

Cell surface HJV undergoes retrograde trafficking prior to being secreted.

Since our studies indicated that the oligosaccharides on the GPI-linked form of HJV are not processed to a complex form, we examined the glycosylation pattern of the secreted form of HJV. The secreted HJV in the media was subjected to Endo H and PNGase F digestion, followed by detection of HJV by western blot. Interestingly, the secreted HJV was resistant to Endo H but sensitive to PNGase F (Figure 2.3A), indicating that the secreted form of HJV acquired complex oligosaccharides before it was released. These results raised two possibilities. HJV may obtain complex oligosaccharides prior to being secreted by undergoing retrograde trafficking to the TGN and Golgi, where its oligosaccharides would be processed to a complex form and HJV could be cleaved by furin. Alternatively, secreted HJV may represent a

subset of HJV that obtains complex oligosaccharides and is cleaved in the Golgi en route to the cell surface.

To determine whether retrograde trafficking occurs, cell surface proteins were labeled with sulfo-NHS-biotin, a cell impermeant form of biotin. After 0, 4 and 8 hours of incubation at 37°C, the conditioned medium and cell lysates were collected. The biotinylated proteins in the cell lysate at 0 hour (total biotinylated) and in the media at 4 and 8 hours were isolated with streptavidin beads and subjected to Endo H or PNGase F digestion, followed by immunodetection of HJV. Biotinylated cell surface HJV was subsequently detected in the media, indicating that secreted HJV can be derived from the pool of HJV at the cell surface. The secreted HJV derived from the cell surface was Endo H-resistant (Figure 2.3B).

This finding suggests that cell surface HJV undergoes retrograde transport to an intracellular compartment where the oligosaccharides are modified. Furthermore, the change in size from 50 kDa in the cell lysates to 38 kDa in the conditioned medium indicates that HJV is cleaved prior to being released. The two species of secreted HJV are not caused by differential N-linked glycosylation since both species are still present after PNGase F digestion, indicating that the difference between the species is due to either another post-translational modification or to cleavage at more than one site. There is variability in the number of bands seen for secreted HJV. Multiple cleaved bands in the conditioned medium have previously been shown (Kuninger et al., 2006; Silvestri et al., 2007; Zhang et al., 2007). Additionally, HJV has an acidic autocatalytic cleavage site, which could account for

the lowest molecular mass of the multiple cleavage products seen in Figure 2.3A (Niederkofler et al., 2004; Zhang et al., 2005).

Since the formation of complex oligosaccharides occurs in Golgi/TGN compartment, these results suggest that HJV release requires retrograde trafficking of HJV from the cell surface to the Golgi/TGN where it acquires complex oligosaccharides and is exposed to furin cleavage before it is secreted. Since no HJV with complex oligosaccharides is detected in the cell lysate, we hypothesize that once HJV obtains complex oligosaccharides it is rapidly secreted.

Secreted HJV has complex oligosaccharides in multiple cell types.

The release of sHJV with complex oligosaccharides could be specific to HepG2 cells. To test this possibility, the glycosylation status of HJV was analyzed in HEK293 and Hep3B cells. HEK293 cells are derived from human embryonic kidney, and Hep3B is a relatively undifferentiated human hepatoma cell line. Neither endogenously expresses detectable HJV by immunoblot analysis. HJV was transiently transfected into both cell lines. Proteins from cell lysates and media were subjected to Endo H and PNGase F digestions. Consistent with the findings in HepG2 cells (Figure 2.2A), cellular HJV in both Hep3B and HEK293 cells was Endo H-sensitive, whereas the secreted HJV was Endo H-resistant (Figure 2.4A & B). Thus, complex oligosaccharides on secreted HJV occur in several cell types.

Blocking the interaction of HJV with neogenin does not alter the glycosylation status of cellular HJV.

HJV could traffic through the Golgi and be protected from oligosaccharide modification and furin cleavage by binding to a chaperone protein. Since neogenin is known to bind to HJV, we sought to determine whether neogenin was necessary for HJV to maintain high-mannose oligosaccharides in the cell lysates. Endogenously expressed neogenin in HJV-HepG2 cells was knocked down using a siRNA specific for neogenin. After knockdown, neogenin was not detectable by western blot (Figure 2.5A). For the parallel control transfected with scrambled siRNA see Figure 2.2A which is from the same blot and exposure. Endo H and PNGase F digestions revealed that knockdown of neogenin does not affect the glycosylation pattern of HJV. This result as well as the finding that knockdown of neogenin had no effect on HJV trafficking to the plasma membrane (Zhang et al., 2008), ruled out the possibility that neogenin serves as a chaperone to protect HJV from modification in the Golgi/TGN in the biosynthetic pathway.

To determine if disruption of the interaction between HJV and neogenin at the cell surface affects the processing of HJV, HJV-HepG2 cells were treated with a soluble portion of the neogenin ectodomain. These soluble portions of the ectodomain compete with endogenous neogenin for binding to HJV and consequently block HJV release (Zhang et al., 2008). Initially, two neogenin fragments were used to compete with endogenous neogenin for binding to HJV, a larger fragment comprising the FNIII repeats 1-6, or a smaller fragment consisting of only repeats 5-6. These fragments bind to HJV with 500 and 5 nM affinity, respectively (Yang et al., 2008). HJV-HepG2 cells were treated with either form of soluble neogenin overnight and conditioned medium was collected to verify that

soluble neogenin blocked HJV release (Figure 2.5B). Cell lysates were collected and subjected to Endo H or PNGase F digestion. Cell-associated HJV was both Endo H- and PNGase-sensitive with or without soluble neogenin (Figure 2.5B). Thus, cellular HJV retains high mannose oligosaccharides independent of neogenin. When cells are incubated with the full-length ectodomain of neogenin, not only was release of sHJV blocked, but the level of cell-associated HJV also increased, indicating that generation of sHJV is a major pathway of HJV turnover in cells (Figure 2.5C). The interaction of HJV with full-length neogenin appears to be necessary for the processing of HJV after HJV reaches the cell surface and is consistent with the hypothesis that only HJV complexed to full-length neogenin is capable of undergoing retrograde transport for processing of HJV to the secreted form.

Filipin increases the amount of HJV in cell lysates and at the cell surface, but does not affect the glycosylation status.

Filipin, which binds to cholesterol, has previously been shown to inhibit endocytosis of HJV and other GPI-linked proteins (Chadda et al., 2007; Orlandi and Fishman, 1998; Zhang et al., 2008). Filipin leads to an increase in cellular HJV when protein synthesis is blocked using cycloheximide and also inhibits release of sHJV (Figure 2.6A). Blocking endocytosis of HJV appears to be specific as it was shown previously that filipin does not affect the endocytosis of Tf through the TfR1-mediated dynamin-dependent process (Zhang et al., 2008). Blocking endocytosis of HJV using filipin leads to a mild increase in HJV on the cell surface, but it does not alter the

Endo H sensitivity of HJV, indicating that filipin does not affect trafficking of HJV to the cell surface (Figure 2.6B).

Additionally, cholesterol depletion has been shown to block exocytosis at the plasma membrane by disrupting SNARE cluster formation (Lang et al., 2001). Here we show that filipin inhibits secretion of Tf, consistent with recent reports showing that cholesterol is also required for insulin secretion (Figure 2.6A) (Larsson et al., 2008; Vikman et al., 2009). If HJV were cleaved during the biosynthetic pathway, then an accumulation of cleaved HJV would be expected upon blocking exocytosis. If endocytosis were a prerequisite for cleavage, as would be expected in the proposed retrograde trafficking pathway, then no accumulation of cleaved, 38 kDa HJV, would be expected. Filipin treatment does not lead to an accumulation of the cleaved 38 kDa species of HJV, which supports the retrograde trafficking model.

Inhibition of furin cleavage does not cause a buildup of HJV with complex oligosaccharides in the cell lysates.

Since we hypothesize that HJV undergoes retrograde trafficking to the Golgi prior to being secreted, it is important to determine if HJV obtains complex glycosylation prior to cleavage by furin or other proprotein convertases. To do this we treated cells with furin convertase inhibitor (FCI), which has been shown previously to block the release of sHJV (Lin et al., 2008; Silvestri et al., 2008a) and blocks sHJV release from HJV-HepG2 cells (unpublished data). Cells were treated with FCI and then metabolically labeled for 2 hours (Figure 2.7). Lysates were immunoprecipitated using an anti-HJV antibody and then subjected to Endo H

digestion. No Endo H-resistant HJV was seen in the cell lysates, indicating that blocking furin cleavage does not lead to a build up of complex HJV in the cell lysates. Similar results were also obtained when HJV-HepG2 cells were treated with both FCI and bafilomycin (data not shown). These data suggest that furin cleavage precedes complex glycosylation.

Figures

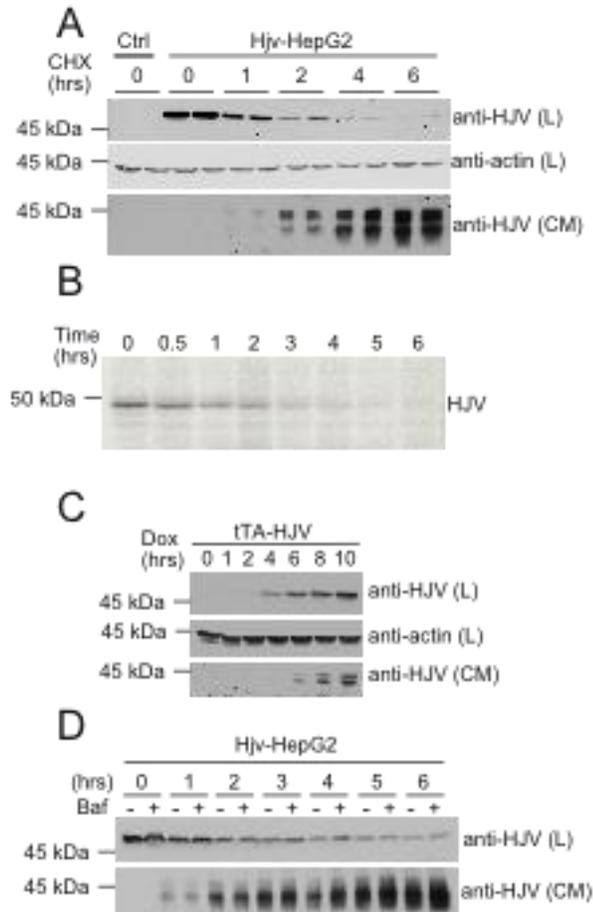


Figure 2.1. Release of cellular HJV.

A. Analysis of cell-associated and secreted HJV after blocking protein synthesis. HJV-HepG2 cells in 12-well plates were incubated in 400 μ l of complete medium with 100 μ g/mL of cycloheximide (CHX) to block protein synthesis. After 0, 1, 2, 4, and 6 hr of incubation, conditioned medium (CM) was collected, and cell lysate (L) was prepared using 100 μ l NET-Triton buffer (150 mM NaCl, 5 mM EDTA, 10 mM Tris (pH 7.4) and 1% Triton X-100) with 1x Protease inhibitors cocktail (Roche Diagnostics, Indianapolis, IN). Each timepoint was performed in duplicate. Western blotting was performed on the total lysates and one-third of conditioned medium using rabbit anti-HJV (0.22 mg/mL) and mouse anti-beta-actin (1:10,000) (lysates only). Control-HepG2 cells (Ctrl) were used as a negative control. HJV is approximately 50 kDa in the cell lysates and 38 kDa in the conditioned medium. β -actin was used as a loading control for the cell lysates. B. Pulse chase analysis of cellular HJV. Cells were metabolically labeled with 35 S-(met/cys) (Perkin Elmer) at 100 μ Ci/mL in MEM medium without met/cys for 30 minutes, washed and then incubated in regular growth medium for 0, 0.5, 1, 2, 3, 4, 5, and 6 hours. Cell lysates were then collected and immunoprecipitated using rabbit anti-HJV 18745 antibody. Immunoprecipitated proteins were washed and separated by SDS-PAGE. Image was

obtained by exposure to x-ray film. C. Analysis of cellular and secreted HJV following induction of HJV synthesis. Expression of HJV in tTA-HJV-HepG2 was induced by addition of 2 $\mu\text{g}/\text{mL}$ doxycycline into the culture medium. The entire cell lysate (L) and one-third of conditioned media (CM) after 0, 1, 2, 4, 6, 8 and 10 hours were subjected to western blots for HJV in cell lysates and medium and β -actin in lysates. Dox: doxycycline treated. D. Contribution of lysosomal degradation to HJV turnover. HJV-HepG2 cells in 12-well plates were incubated in presence of 100 $\mu\text{g}/\text{mL}$ cycloheximide with or without addition of 100 nM bafilomycin A (Baf) for 0, 1, 2, 3, 4, 5 and 6 hours. Proteins from whole-cell lysates (L) and media (CM) precipitated with 6% trichloroacetic acid (TCA) were subjected to immunodetection. Experiments were repeated three times with consistent results.

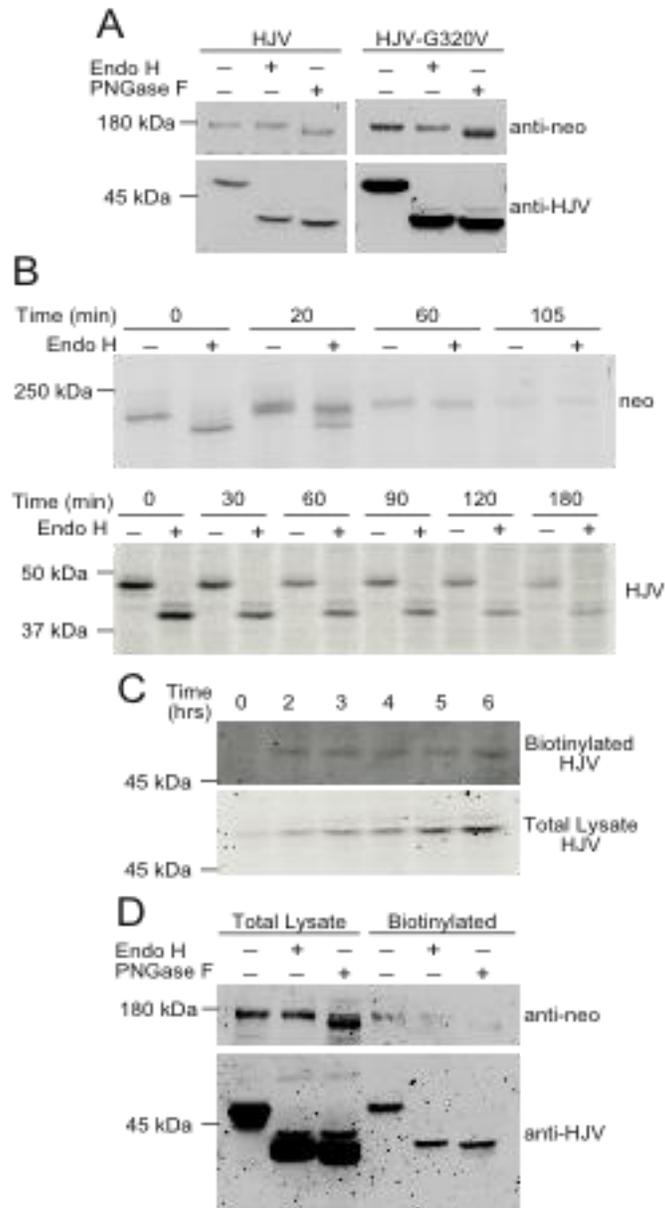


Figure 2.2. Cell-associated HJV has high-mannose oligosaccharides, whereas cellular neogenin has complex oligosaccharides.

A. Endo H and PNGase F sensitivity of cellular HJV and cellular neogenin. Cell lysate was collected from HJV-HepG2 (HJV) cells (transfected with a non-specific siRNA) or HJV-G320V-HepG2 (HJV-G320V) cells. Lysates were subjected to Endo H and PNGase F digestion. Immunoblots were performed using anti-neogenin (0.4 mg/mL Santa Cruz) and anti-HJV antibodies (0.22mg/mL). B. Analysis of Endo H sensitivity of neogenin and HJV by pulse chase (in Neogenin/HJV-HEK293 and HJV-HepG2 cells respectively). Metabolic labeling and immunoprecipitations were performed as described previously (Davies et al., 2003) with the following modifications: HJV-HepG2 (lower panel) or Neogenin/HJV-HEK293 (upper panel) cells in 35 mm dishes were labeled in 1 mL met/cys-free media with 100 μ Ci 35 S-(met/cys) for 30 minutes.

Cells were then washed and incubated in unlabeled medium for the time points indicated. Immunoprecipitations were performed using 2 μ L rabbit anti-HJV antibody, 18745 (generated against residues 1-401 of HJV as described previously (Zhang et al., 2008)), or rabbit anti-neogenin 21567 antibody, which was generated using the neogenin ectodomain as an antigen (purified as described previously (Yang et al., 2008)) to generate a polyclonal antibody in rabbits (Pocono Rabbit Farm & Laboratory, Inc., Canadensis, PA). Immunoprecipitated proteins were subjected to control (mock) or Endo H digestion and separated by SDS-PAGE, followed by soaking of the gel in Amplify (GE Healthcare, Chalfont St. Giles, United Kingdom) and drying of the gels prior to exposure to film. C. Analysis of time taken for HJV to traffic to the cell surface after induction of HJV expression. tTA-HJV-HepG2 cells in 60mm dishes were induced to express HJV by addition of 2 mg/mL doxycycline for 0, 2, 3, 4, 5, and 6 hours. Cell surface proteins were biotinylated at 4°C and pulled down using streptavidin agarose. 100% of the total biotinylated proteins and 15% of the internal (non-biotinylated) proteins were subjected to immunoblotting for HJV using a rabbit anti-HJV 18746 antibody. This experiment was repeated once with similar results. D. Cell surface HJV has high-mannose oligosaccharides. Biotinylation of cell-surface proteins was conducted as described previously (VanSlyke and Musil, 2005). Briefly, HJV-HepG2 cells in a 6-well plate at approximately 80% confluence were biotinylated with 0.25 mg/mL Sulfo-NHS-Biotin (Thermo Fisher Scientific, Waltham, MA) at 4°C for 30 min. Cells were immediately solubilized in NET-Triton/1x protease inhibitors cocktail then biotinylated proteins were isolated using streptavidin agarose beads (Thermo Fisher Scientific). Bound proteins were eluted with NET-Triton/1% β -mercaptoethanol/0.5% SDS and subjected to digestion with Endo H and PNGase F (New England Biolabs, Ipswich, MA), followed by immunodetection of HJV and neogenin. Data are representative of three independent experiments.

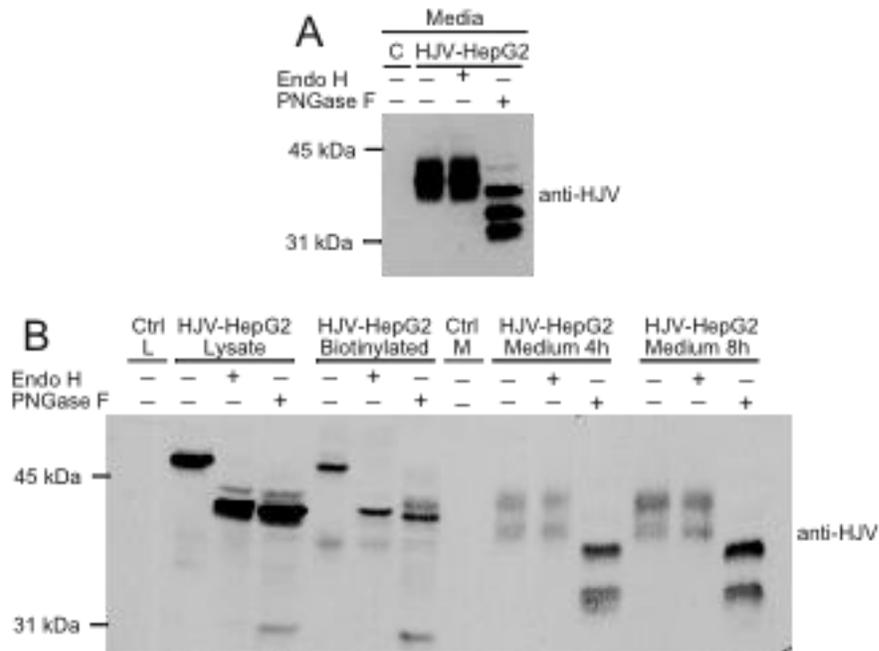


Figure 2.3. Secreted HJV has complex oligosaccharides and is derived from the pool of HJV at the plasma membrane.

A. Secreted HJV has complex oligosaccharides. Conditioned medium was collected from HJV-HepG2 cells and subjected to Endo H and PNGase F digestion, followed by a western blot using a rabbit anti-HJV antibody. Conditioned medium from control-HepG2 cells (C) was included as a negative control. B. Chasing the release of biotinylated cell surface HJV. Cell surface HJV in HJV-HepG2 cells was biotinylated at 4°C, followed by incubation at 37°C for 4 or 8 hours in complete medium. The total biotinylated HJV in the cell lysate (HJV-HepG2 Biotinylated) and the biotinylated HJV released into the medium were isolated using streptavidin agarose beads. The eluates were digested with Endo H and PNGase F. Endo H and PNGase F digestion of one-third of cell lysates are also included. Lysate (Ctrl L) or medium (Ctrl M) from Control-HepG2 cells were used as negative controls. Experiments were repeated three times.

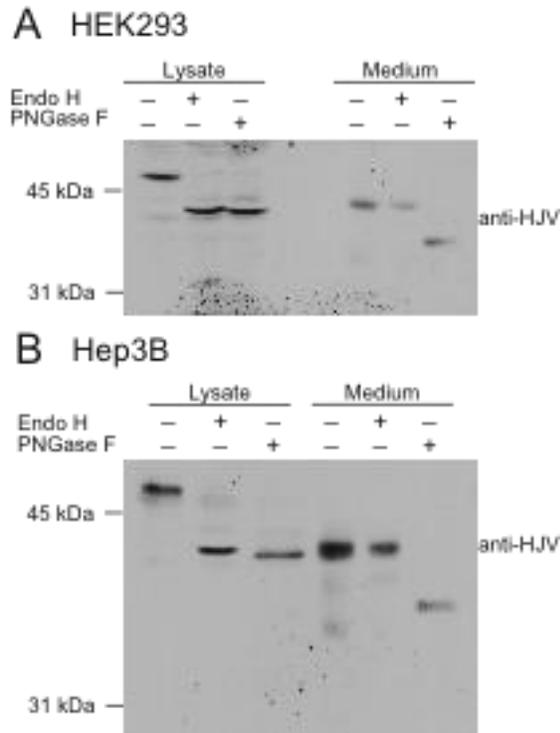


Figure 2.4. The glycosylation patterns of cellular and secreted HJV in HEK293 and Hep3B cells.

A. HEK293 cells were transiently transfected with wild type HFE2-pcDNA3 using Lipofectamine 2000 (Invitrogen, Carlsbad, CA) in 6-well plates and incubated in complete medium. About 48 hours post-transfection, serum-free medium (1 mL) was added. After an additional 24 hours of incubation, conditioned medium was collected and cell lysate was prepared using 300 μ L of NET-Triton buffer with protease inhibitor cocktail. Proteins in the medium (1mL) were precipitated using 6% TCA. Proteins from both the cell lysate (Lysate) and medium were equally divided into three parts and were subjected to Endo H and PNGase F digestion followed by detection of HJV by immunoblot. B. Hep3B cells were transiently transfected with HFE2-pcDNA3 using Lipofectamine 2000. The transfection of HFE2 into Hep3B cells, Endo H and PNGase digestion, and immunodetection were performed as described for HEK293 cells. There was a better separation on the gel for Hep3B cells, which accounts for the apparent increased separation between the control and digested samples in this cell type. The data are representative of three experiments for each cell type.

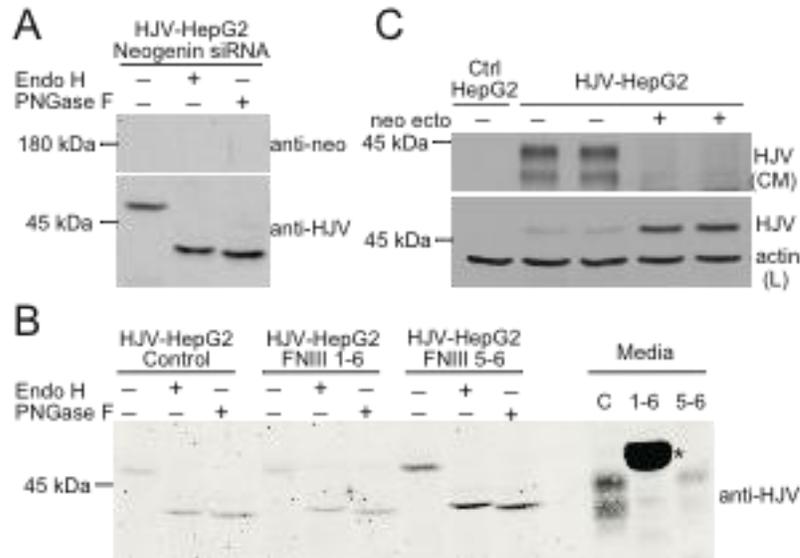


Figure 2.5. Neogenin is necessary for sHJV release but not for the retention of high-mannose oligosaccharides by HJV.

A. Knockdown of neogenin does not alter the glycosylation of cellular HJV. Endogenous neogenin in HJV-HepG2 cells was knocked down using a siRNA specific for neogenin (for the control HJV-HepG2 cells transfected with a non-specific control siRNA see Figure 2A). siRNA (small interfering RNA) specific for human neogenin (25 nM, Dharmacon, Lafayette, CO) or scrambled control siRNA was transfected twice (once on day 1 and once on day 3) using the RNAiMAX transfection reagent (Invitrogen). Seventy-two hours after the second transfection cell lysates were subjected to Endo H and PNGase F digestion. Both neogenin and HJV were detected by immunoblot using anti-neogenin and anti-HJV antibodies, respectively. B. Disruption of the HJV/neogenin interaction inhibits release of HJV but does not perturb the high-mannose glycosylation of HJV. HJV-HepG2 cells were treated with soluble neogenin ectodomain fragments consisting of the FNIII repeats 1-6 (1 μ M) or a smaller fragment of only repeats 5-6 (40 nM) in serum-free medium overnight. Soluble neogenin FNIII 1-6 and FNIII 5-6 as well as the whole neogenin extracellular domain (ectodomain) were generated as previously described (Yang et al., 2008) and were a gift from F. Yang and P.J. Bjorkman at CalTech. Conditioned medium and cell lysates were collected, followed by Endo H and PNGase F digestion and immunodetection of HJV. Untreated HJV-HepG2 cells were used as a control (C). 1-6: neogenin FNIII 1-6 fragment. 5-6: neogenin FNIII 5-6 fragment. A non-specific band resulting from cross-reaction of either the primary or secondary antibodies with the FNIII 1-6 fragment is denoted with an asterisk (*). C. Neogenin ectodomain inhibits HJV release and results in HJV accumulation within cells. HJV-HepG2 cells in 12-well plate were incubated in complete medium with or without addition of soluble neogenin ectodomain at 1 μ M. After 24 hours of incubation, the total cell lysate (L) and 20% of conditioned medium (CM) were subjected to detection of HJV by immunoblot. Actin in cell lysates was used as a loading control. These data are representative of at least two experiments.

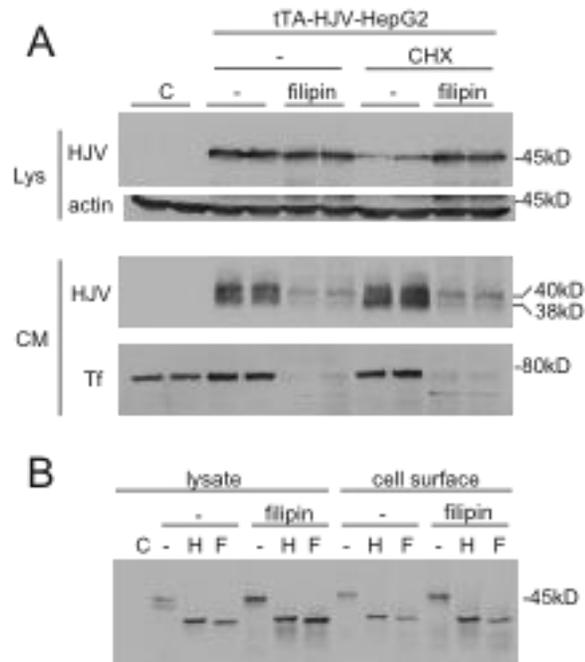


Figure 2.6. Filipin blocks generation of sHJV but does not alter the glycosylation of cell surface HJV.

A. Levels of cellular HJV were measured in tTA-HJV-HepG2 cells in the presence or absence of filipin and cycloheximide (CHX). Cells were grown in 6 well plates with 2 $\mu\text{g}/\text{mL}$ doxycycline to induce HJV expression. Cells were treated for 2 hours in serum-free medium with or without cycloheximide (100 $\mu\text{g}/\text{mL}$) and filipin (10 $\mu\text{g}/\text{mL}$). One half of the cell lysates (Lys) and one fourth of the conditioned medium (CM) were subjected to western analysis with anti-HJV and anti- β -actin or anti-Tf antibodies. Cells transfected with an empty vector (C) were used as a control for antibody specificity. B. Analysis of cellular and cell surface HJV by Endo H and PNGase F digestion in cells treated with filipin. Cells were treated as in A. For the cell lysate, 20% of a 60 mm dish was used. For the cell surface HJV, biotinylated cell surface protein from approximately 2/3 of a 60 mm dish was used for each sample.

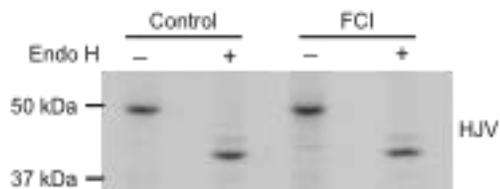


Figure 2.7. Addition of Furin Convertase Inhibitor does not lead to a buildup of Endo H-resistant HJV in the cell lysate.

HJV-HepG2 cells in 35 mm dishes were pretreated with no inhibitor (control) or with furin convertase inhibitor (FCI, 5 μ M Decanoyl-Arg-Val-Lys-Arg-chloromethylketone) for 90 minutes. Cells were then metabolically labeled for two hours in the presence and absence of inhibitor. Cells were washed, lysed and immunoprecipitated using the anti-HJV antibody and subjected to Endo H digestion as described in the methods. This data is representative of two experiments.

Discussion

In this study, we characterized the trafficking of HJV by analyzing the maturation of its Asn-linked oligosaccharides and its turnover. Our results indicate that the trafficking of nascent HJV from the ER to the plasma membrane avoids processing in the Golgi/TGN compartments and does not require its binding partner, neogenin. After reaching the cell surface HJV undergoes retrograde trafficking to the Golgi/TGN where it obtains complex oligosaccharides prior to being released. The majority of HJV that disappeared from cells was detected in the conditioned medium, suggesting that HJV release constitutes the major pathway of cellular HJV turnover.

The release of HJV is physiologically important. Not only has it been shown to be secreted from cell lines either transfected with HJV or endogenously expressing HJV, but it can also be detected in both human and rat serum (Kuninger et al., 2006; Lin et al., 2005; Silvestri et al., 2007; Zhang et al., 2007). In rats, the serum level of HJV increases in response to acute iron deprivation (Zhang et al., 2007). Consistent with a role for HJV in iron homeostasis, sHJV injected into mice decreased BMP signaling and hepcidin levels (Babitt et al., 2007). Both in vitro and in vivo studies demonstrate that cell-associated HJV and sHJV have opposite roles in the regulation of hepatic hepcidin expression. Cell-associated HJV is proposed to act as a co-receptor for BMPs to enhance BMP-signaling and hepcidin expression (Babitt et al., 2006), whereas secreted HJV may compete with cellular HJV for binding to BMPs and thereby suppresses hepcidin expression (Babitt et al., 2007). Importantly, the release of sHJV is negatively regulated by iron-saturated Tf and

non-Tf bound iron (Lin et al., 2005; Silvestri et al., 2007; Zhang et al., 2007). These data support a model in which HJV-mediated regulation of hepcidin expression is modulated by the release of HJV in response to iron loading.

Unlike many transmembrane and GPI-linked proteins, HJV appears to be capable of trafficking to the plasma membrane in the absence of Golgi processing in HepG2 cells as measured by retention of high-mannose oligosaccharides and lack of furin cleavage. Several possible pathways could be responsible for these results. First, HJV may traffic through the Golgi en route to the plasma membrane but be masked by binding to another protein and thus be inaccessible to the Golgi-resident glycosylases and proteolytic processing by furin. For example, proTGF- β is protected from extracellular proprotein convertase cleavage by binding to Emilin1 (Zacchigna et al., 2006). It is also possible that HJV is in a conformation that is inaccessible to glycosylases and then it becomes accessible after it undergoes retrograde trafficking to the Golgi and is cleaved by furin due to a conformational change. Alternately, HJV could bypass the Golgi altogether and traffic directly from the ER or ERGIC (ER Golgi intermediate compartment) to the plasma membrane. Although GPI-linked proteins are known to bud from specialized transport vesicles in the ER and have specific chaperones that mediate trafficking to the plasma membrane, they are generally thought to traffic through the Golgi en route to the plasma membrane (Muniz et al., 2000; Takida et al., 2008). Both GPI-linked ceruloplasmin and 5' nucleotidase obtain complex oligosaccharides in their transit through the biosynthetic pathway (Hellman et al., 2002; Schell et al., 1992).

Acquisition of complex oligosaccharides by HJV therefore appears to be different from these other two GPI-linked proteins.

In HepG2 cells, biotinylated cell surface HJV possesses high mannose oligosaccharides, but sHJV has complex oligosaccharides, indicating that HJV undergoes retrograde trafficking to the Golgi where its oligosaccharides are processed prior to release from cells. Other membrane proteins have been shown to traffic from the plasma membrane back to the trans-Golgi network (TGN), including furin (Molloy et al., 1994) and mannose-6-phosphate receptor, as previously reviewed (Mellman, 1996). TfR1 is capable of undergoing retrograde trafficking as far as the Golgi (Snider and Rogers, 1985; Snider and Rogers, 1986). Whether GPI-linked proteins are able to traffic from the plasma membrane to the Golgi is controversial. One group reported that the GPI-linked proteins, CD59 and a GPI-linked GFP, traffic from the cell surface to the Golgi; however, others reported that GPI-linked GFP traffics from the plasma membrane to recycling endosomes but not to the Golgi (Nichols et al., 2001; Sabharanjak et al., 2002). Retrograde trafficking of HJV prior to generation of sHJV is further supported by previous data showing that cholesterol-dependent endocytosis of HJV is necessary for release (Zhang et al., 2008). In the case of HJV, retrograde trafficking prior to the generation of sHJV may provide an opportunity for regulation of HJV release in response to extracellular factors such as transferrin.

It is possible that HJV could traffic in two separate pathways, one in which it undergoes retrograde trafficking prior to being released, and another in which it is cleaved during biosynthesis. The following evidence supports that retrograde

trafficking is the major, if not the only, pathway for sHJV release. First, depletion of neogenin in HepG2 cells blocks HJV release, but has no effect on HJV trafficking to cell surface (Zhang et al., 2008). This suggests that HJV release does not occur on its way to the cell surface and that HJV trafficking to the plasma membrane is independent of neogenin. Second, addition of soluble neogenin ectodomain (approximately 130 kDa) to the outside of cells blocks HJV processing and results in an accumulation of cellular HJV, suggesting that HJV processing occurs after HJV reaches the cell surface. Third, disruption of the endocytosis of HJV by filipin, a cholesterol-binding agent, blocks HJV release (Maxson et al., 2009; Zhang et al., 2008), but does not block trafficking of HJV to the cell surface or alter the Endo H sensitivity of cell surface HJV. If cleavage in the biosynthetic pathway were a major pathway of release, then a buildup of Endo H-resistant HJV would be expected when release of sHJV was blocked. This was not seen. Fourth, blocking furin cleavage does not lead to a buildup of Endo H-resistant HJV in the cell lysates. Since Endo H-resistance is obtained in the medial Golgi and furin is primarily localized in the TGN and more distal compartments, this suggests that furin-mediated cleavage occurs before complex glycosylation and argues against the cleavage of HJV in the traditional biosynthetic pathway.

On the basis of the published data and the results of this study, we propose a model for HJV trafficking and processing. Nascent HJV traffics from ER to the plasma membrane and avoids modification in the Golgi/TGN in a manner that does not depend on neogenin. Upon reaching the cell surface, HJV interacts with neogenin. It then undergoes cholesterol-dependent endocytosis and retrograde

trafficking to the Golgi/TGN compartments, where HJV is accessible to furin, followed by glycosylases. Soluble HJV is then rapidly released from the cells. Trafficking of HJV to the cell surface prior to generation of sHJV may provide an opportunity for regulation of HJV release by iron-bound transferrin in response to changing iron levels, thus allowing HJV to modulate iron homeostasis. The details of cellular HJV trafficking and the underlying mechanism of iron-regulated HJV release remain to be determined and will be the subject of future work.

Acknowledgments

We would like to thank Fan Yang and Pamela Bjorkman for generously providing us with neogenin ectodomain and neogenin FNIII 1-6 and FNIII 5-6 fragments; Gregory Longmore for generously giving us tTA-HepG2 cells and a tetracycline-inducible pcDNA4 plasmid; and Maja Chloupkova, Kristina Nicholson, Gary Reiness and Juxing Chen for critical reading of this manuscript and helpful comments. This work was supported by National Institutes of Health Grant DK080765 to ASZ. J.M. was partially supported by National Institutes of Health Grant T32 HD049309.

Authorship

Contribution: J.M and A.S.Z performed experiments. J.M, C.A.E, and A.S.Z designed the research, analyzed results, made the figures and wrote the paper.

Conflict-of-interest disclosure: The authors declare no competing financial interests.

CHAPTER 3

The GPI-anchor of hemojuvelin potentiates signaling, but is not required for proteolytic processing by furin.

Julia E. Maxson¹, An-Sheng Zhang¹, Caroline A. Enns¹.

¹Department of Cell and Developmental Biology, Oregon Health & Science
University, Portland, OR 97239

Corresponding Author: Caroline A. Enns, Department of Cell and Developmental
Biology, Oregon Health & Science University, L215, 3181 SW Sam Jackson Park
Road, Portland, OR 97239. Phone: (503) 494-5845. Fax: (503) 494-4253.

Email: ennsca@ohsu.edu

Submitted to FASEB Journal.

Abstract

Mutations in hemojuvelin (HJV) lead to a severe iron overload disease, juvenile hemochromatosis. HJV is a GPI-linked protein that increases expression of the iron regulatory peptide hormone, hepcidin. Hepcidin negatively regulates iron uptake from the intestine and thus is a major regulator of iron homeostasis. HJV functions by potentiating bone morphogenetic protein (BMP) signaling to upregulate hepcidin expression. HJV can also be shed from cells by proteolytic cleavage. In contrast to membrane bound HJV, shed HJV negatively regulates BMP signaling and decreases hepcidin expression, presumably by binding limiting BMPs. The GPI-anchor of HJV directs its internalization through a cholesterol-dependant pathway characteristic of GPI-linked proteins. To investigate the role of the HJV GPI-anchor in cleavage and signaling, we created chimeric proteins with the ectodomain of HJV and the transmembrane and cytoplasmic domains of either low-density lipoprotein receptor (LDLR) or furin in lieu of the GPI-anchor. These chimeric proteins are shed from cells similarly to wild-type HJV. Shedding is furin dependent. In contrast, the chimeras were incapable of increasing hepcidin levels, indicating that the GPI-anchor is not required for cleavage of HJV but it is important for HJV signaling to upregulate hepcidin expression.

Introduction

Hemojuvelin (HJV, gene symbol *HFE2*) is a glycosylphosphatidylinositol (GPI)-linked protein that plays a critical role in iron metabolism (Niederkofler et al., 2004).

Mutations in HJV cause the iron overload disorder, juvenile hemochromatosis (JH) (Papanikolaou et al., 2004). JH patients have severe iron accumulation in their organs, particularly the heart, liver, pancreas and thymus, which can lead to cardiac, liver and endocrine disorders (Papanikolaou et al., 2004). HJV regulates iron metabolism by activating transcription of the iron regulatory peptide hormone, hepcidin (Babitt et al., 2006). Hepcidin is secreted by the liver and decreases iron transport from the intestinal epithelial cells, macrophages and the liver into the blood by down-regulating the iron transporter, ferroportin (Nemeth et al., 2004). HJV therefore negatively modulates iron uptake from the intestine by increasing hepcidin expression.

HJV upregulates hepcidin expression through the bone morphogenetic protein (BMP) signaling pathway (Babitt et al., 2006). HJV is proposed to act as a co-receptor for BMP proteins. Subsequent phosphorylation and activation of the BMP receptor-activated Smad proteins leads to upregulation of hepcidin transcription in the liver, which reduces dietary iron uptake (Babitt et al., 2007). The ability of HJV to activate BMP signaling is decreased by its proteolytic cleavage, which releases it from its GPI-anchor. This soluble form of HJV (sHJV) can act as an inhibitor of BMP signaling by competing with cell-surface HJV for binding to BMPs (Babitt et al.,

2007; Kuninger et al., 2006; Lin et al., 2005; Niederkofler et al., 2004; Zhang et al., 2007). sHJV down-regulates hepcidin expression and increases iron levels in both cell culture studies and when mice are injected with recombinant sHJV, in support of this hypothesis (6). Shedding of HJV is antagonized by iron-bound transferrin (Tf) and high levels of ferric ammonium citrate, which allows cleavage of HJV to be regulated in response to the levels of iron in the blood (Lin et al., 2005; Zhang et al., 2007). Since the cleaved form of HJV has an opposing effect on hepcidin expression, the regulation of HJV cleavage is important in sensing iron levels and the maintenance of iron homeostasis.

HJV is shed from cells by at least two proteases. The furin family of proprotein convertases cleave HJV (Kuninger et al., 2008; Lin et al., 2008; Silvestri et al., 2008a; Zhang et al., 2008). Treatment of cells with furin convertase inhibitor (FCI) blocks HJV shedding in HEK293, Hep3B and other cell lines (Kuninger et al., 2008; Lin et al., 2008; Silvestri et al., 2008a; Zhang et al., 2008). Matriptase-2 has also been implicated in the cleavage of HJV (Silvestri et al., 2008b). Mutations in the matriptase-2 gene (*TMPRSS6*) cause iron deficiency anemia in humans as well as in mouse models (Du et al., 2008; Finberg et al., 2008; Folgueras et al., 2008). High levels of hepcidin expression are detected in *Tmprss6* mutant mice, in keeping with the hypothesis that matriptase-2 decreases hepcidin expression by cleaving HJV and downregulating signaling. Cell culture models over-expressing matriptase-2 demonstrate increased cell surface HJV degradation, complementary to the animal data (Silvestri et al., 2008a).

HJV cleavage involves retrograde trafficking of HJV from the cell surface, where it is cleaved and released from the cell when the vesicle recycles and fuses with the plasma membrane (Maxson et al., 2009). This mechanism is based on the following observations. GPI-linked and other membrane anchored proteins are co-translationally glycosylated in the ER. The high mannose oligosaccharides are processed to complex oligosaccharides in the Golgi. HJV traffics to the cell surface while retaining high-mannose oligosaccharides and avoiding furin cleavage (Maxson et al., 2009). It then undergoes retrograde trafficking to the Golgi where it is modified to complex oligosaccharides, and subsequently secreted (Maxson et al., 2009).

HJV endocytoses through the GPI-associated protein-enriched early endosomal compartments (GEEC) pathway (Zhang et al., 2008). Endocytosis along this pathway is clathrin and dynamin independent, but involves actin, cholesterol and CDC42 (Chadda et al., 2007; Sabharanjak et al., 2002). Treatment of cells with filipin, a cholesterol depleting agent, blocks HJV endocytosis and cleavage of HJV, whereas treatment of cells with dynasore, an inhibitor of clathrin- and caveolin- mediated endocytosis has no effect on HJV shedding (Zhang et al., 2008).

We investigated the role of the GPI-anchor in the shedding of HJV and hepcidin signaling in Hep3B cells, a human hepatoma cell line. In this study we demonstrate that furin is responsible for the shedding of HJV in Hep3B cells. When the GPI-

anchor of HJV was replaced with the transmembrane and cytoplasmic domains of either furin or the low-density lipoprotein receptor (LDLR) shedding still occurred, but the HJV chimeras were unable to upregulate hepcidin expression.

Materials and Methods

Cloning

The HJV/LDLR and HJV furin chimeras were made by overlapping PCR and then ligated into pcDNA3 vector at EcoRI and KpnI sites. The HJV ectodomain was amplified from the pcDNA3-HFE2 vector using the following primers: 5'-ATGGTACCATGGGGGAGCCAGGCC-3' and 5'-GGGCTTCTTCTCGGGGAAGAGATGC-3' for the LDLR construct or 5'-GTGAGGGCAGCAGGGGAAGAGATG-3' for the furin construct. The LDLR transmembrane and cytoplasmic domains were amplified from LDLR pTZ1 (a gift from David Russell at the University of Texas Southwestern Medical Center, Dallas, TX) using the following primers: 5'-GCATCTCTTCCCCGAGAAGAAGCCC-3' and 5'-CTGAATTCTCACGCCACGTCATCCTCC-3'. The furin transmembrane and cytoplasmic domain was amplified from the PCS2-furin vector (given to us by Gary Thomas, Vollum Institute, Portland OR) using the following primers: 5'-CATCTCTTCCCCCTGCTGCCCTCAC-3' and 5'-GCGAATTCTCAGAGGGCGCTCTGGTC-3'.

Cell culture

Hep3B cells were obtained from ATCC (Manassas, VA) and grown in Minimal Eagles Medium (MEM) with 10% fetal bovine serum (FBS), non-essential amino acids, and 1 mM pyruvate in a 5% CO₂ 37°C incubator. Hep3B cells in 6 well plates were transiently transfected using Lipofectamine or Lipofectamine 2000 (Invitrogen, Carlsbad, CA) according to the manufacturer's protocols. tTA-Neogenin HepG2 cells

were generated by subcloning neogenin cDNA into a tetracycline-inducible pcDNA4 vector, which was stably transfected into tTA-HepG2 cells (obtained from Dr. Gregory Longmore at Washington University, St. Louis), and were maintained in MEM with 10% FBS and 800 µg/mL G418. They were transfected with either Fugene HD (Roche) or PolyJet (SignaGen Laboratories, Ijamsville, MD). For collection of conditioned medium, cells were incubated with 1 ml of serum free medium per well of a 6 well plate for 16-24 hours. Cell lysates were prepared by solubilizing cells in 100 µl of NETT (NET-Triton buffer-150 mM NaCl, 5 mM EDTA, 10 mM Tris (pH 7.4) and 1% Triton X-100) with 1x Protease inhibitor cocktail (Roche, Indianapolis, IN).

Immunodetection

Cell lysates and conditioned medium were subjected to reducing sodium dodecyl sulfate-polyacrylamide gel electrophoresis (SDS-PAGE) and then transferred to nitrocellulose membrane. In some cases, conditioned medium was precipitated using 6% trichloroacetic acid (TCA) followed by centrifugation. HJV was detected using affinity purified rabbit anti-HJV antibody (18745 or 18746) generated against residues 1-401 of human HJV (0.22 µg/ml), described previously (Zhang et al., 2005).

Endo H and PNGase F digestion

Cell lysates or conditioned media were digested for 4 hours with Endo H or PNGase F according to the manufacturer's protocol (New England Biolabs, Ipswich, MA).

The control samples were prepared like the Endo H sample, except for the absence of enzyme.

Pulse-chase analysis

Cells in 35 mm (or 60 mm) dishes were metabolically labeled for 30 minutes using ³⁵S- methionine/cysteine (Met/Cys) (Perkin Elmer Life and Analytica Sciences, Waltham, MA) at 100 μ Ci/ml in 1 ml (or 2 ml) of medium lacking Met/Cys, and then washed and incubated in complete growth medium for the indicated time periods. Cells were then lysed in 1 ml NETT with protease inhibitors and immunoprecipitated using 2 μ l rabbit anti-HJV 18745 antibody and protein A Sepharose (Invitrogen, Carlsbad, CA), washed by spinning through NETT buffer with 15% sucrose and then separated by SDS-PAGE. Gels soaked in Amplify (Amersham Biosciences, Pittsburg, PA) were dried and exposed to x-ray film followed by quantitation of the bands using a Phosphorimager (Molecular Dynamics).

Immunofluorescence microscopy

Hep3B cells were plated on poly-L-lysine-coated cover slips (Sigma-Aldrich, St. Louis, MO) and co-transfected with pcDNA3-HFE2 encoding HJV and pcDNA3-furin-flag-HA (given to us by Gary Thomas) using Fugene HD. Cells were permeabilized in PBS with 0.2% Triton X 100 and labeled with rabbit anti-HJV 18745 (1.73 μ g/ml) and mouse anti-flag M2 (9.6 μ g/mL, Sigma-Aldrich F3165), followed by Alexa Fluor 568 goat anti-rabbit IgG (H+L) (4 μ g/ml, Molecular Probes, Invitrogen, Eugene, OR) and Alexa Fluor 488 goat anti-mouse IgG (H+L) (4 μ g/ml, Molecular Probes). Cover

slips were mounted in ProLong Gold Antifade Reagent (Invitrogen) and imaged using an Olympus FV 1000 upright confocal microscope using a 40X Oil objective. Images were processed using ImageJ.

qRTPCR

Analysis of hepcidin and glyceraldehyde phosphate dehydrogenase (GAPDH) mRNA levels were performed as described previously (Zhang et al., 2009).

Results

Substitution of the GPI-anchor of HJV with transmembrane domains

HJV is a GPI-linked protein, and its proteolytic processing regulates its ability to signal to modulate iron metabolism. Based on the endocytosis of HJV through a pathway characteristic of GPI-linked proteins as well as the retrograde trafficking of HJV prior to its cleavage (Maxson et al., 2009), we hypothesized that the GPI-anchor is important for either the secretion of HJV or its role in regulating iron homeostasis. In order to evaluate the effects of the GPI-anchor on secretion of HJV, we engineered two HJV constructs with transmembrane and cytoplasmic domains in lieu of the GPI-anchor signal sequence (Figure 1A). Chimeric proteins were made using overlapping PCR with the ectodomain of HJV and the transmembrane and cytoplasmic domains of either the low-density lipoprotein receptor (LDLR) or the pro-protein convertase, furin. The transmembrane and cytoplasmic domain of LDLR was chosen because it has a motif in its cytoplasmic domain that directs endocytosis through the clathrin and dynamin-mediated pathway (Anderson et al., 1978). The transmembrane and cytoplasmic domains of furin were chosen because furin is proposed to cleave HJV, and is localized primarily in the trans-Golgi network (TGN) and also cycles to and from the plasma membrane (Thomas, 2002).

HJV chimeras are expressed and processed by the cell

To understand the role that the GPI anchor plays in the trafficking and processing of HJV, we first analyzed the expression and post-translational modification of the HJV

chimeras. HJV chimeras were transiently transfected into Hep3B cells, a hepatoma cell line that expresses some hepatocyte-specific genes, but does not express any detectable endogenous HJV protein or matriptase-2 (data not shown). The chimeras were subsequently analyzed by Endo H and PNGase digestion followed by western analysis using a rabbit anti-HJV antibody as described in the methods. Like wild type (WT) HJV, the chimeras are glycosylated, and were sensitive to digestion with Endo H, which cleaves high mannose oligosaccharides, as well as PNGase F, which cleaves both complex and high mannose Asn-linked oligosaccharides (Figure 1B). These results indicate that similar to the WT HJV, the cell-associated chimeras possess only high mannose oligosaccharides. The similar processing of WT HJV and the HJV/LDLR and HJV/furin chimeras made these chimeras a good tool to study the role of the GPI-anchor on HJV secretion.

The processing of the HJV chimeras was then analyzed by pulse-chase studies. Cells were metabolically labeled using ³⁵S Met/Cys for 30 minutes, followed by removal of the radioactive medium and incubation in complete growth medium for 0, 30, 60 minutes or 0, 1.5, 3 and 6 hours. The relatively short half-life of cell-associated WT HJV (approximately 1 hour) could be due to shedding of HJV, in addition to protein turnover (Figure 1C and D). To determine if these chimeras undergo similar proteolytic processing as GPI-HJV, we analyzed the shedding of the transmembrane anchored HJV constructs.

HJV shedding does not require a GPI-anchor

In Hep3B cells, HJV is shed as a single cleavage product (Lin et al., 2005).

Conditioned medium from Hep3B cells transiently transfected with WT HJV or the HJV/furin chimeras was analyzed in triplicate by immunoblot for secreted HJV to address whether shedding of HJV requires a GPI-anchor. Like WT HJV, both of the HJV/furin and HJV/LDLR chimeras were shed, indicating that the GPI-anchor is not required for HJV shedding (Figure 2A). The HJV/furin and HJV/LDLR chimeras were also Endo H-resistant in the conditioned medium, demonstrating that like WT HJV, they obtain complex oligosaccharides prior to being shed. These results indicate that the GPI-anchor is not required for HJV processing and secretion (Figure 2C).

Interestingly, the HJV/furin chimera had reduced shedding relative to WT HJV or the HJV/LDLR chimera. When the ratio of sHJV to HJV in the lysate was quantitated, there was approximately 2 to 3 times more sHJV for WT HJV and the HJV/LDLR chimera than for the HJV/furin chimera (Figure 2B). While a decrease was seen in sHJV, no detectable increase in the amount of HJV in the lysates was observed. These results may be due to the relative levels of cell associated HJV to sHJV. If only a small proportion of the total HJV is shed over the period of collection, then detection of changes in the lysates would not be as sensitive as detection of changes in sHJV. Previous results indicated that HJV is degraded through the lysosomal pathway, in addition to shedding (Maxson et al., 2009)..

The HJV chimeras are cleaved by furin

We initially hypothesized that the HJV/furin chimera would have increased accessibility to furin and consequently cleavage and shedding would be elevated, because the two proteins would be colocalized in the same compartment. Since we observed decreased secretion of the HJV/furin chimera (Figure 2A), we analyzed whether furin was cleaving the chimeric constructs. To determine if the sHJV seen in the media was generated by proprotein convertase cleavage, cells expressing WT HJV or the HJV chimeras were treated with furin convertase inhibitor (FCI), which inhibits furin and other members of the proprotein convertase family. Cell lysates and conditioned media were collected and analyzed by immunoblot. Treatment of cells with FCI inhibited the secretion of WT HJV, HJV/LDLR, and HJV/furin (Figure 3A). Furin siRNA confirmed that furin rather than other proprotein convertases, was responsible for HJV shedding in Hep3B cells (Figure 3B). These results indicated that the secreted forms of the chimeras were generated by furin cleavage and that furin-mediated cleavage is not dependent on GPI-linkage of HJV.

The HJV/furin chimera has similar subcellular localization to furin

Since the HJV/furin chimera has decreased secretion despite being cleaved by furin, we wanted to confirm that the HJV/furin chimera co-localized with furin as we had predicted. Immunofluorescence microscopy was used to assess the subcellular localization of WT HJV and the HJV/furin chimera relative to furin. Hep3B cells were transiently co-transfected with either WT HJV or HJV/furin and a flag-tagged furin construct. Anti-HJV and anti-flag tag antibodies were used to detect HJV

(green) and furin (red) localization in permeabilized cells (Figure 3C). WT HJV had a punctate appearance throughout the cell, and showed little colocalization with furin, which had a perinuclear punctate appearance. The HJV/furin chimera had a punctate staining pattern that overlapped with furin, as would be expected if the transmembrane-cytoplasmic portion of the chimera were directing its trafficking. These results indicate that the HJV/furin chimera and furin have increased colocalization compared with WT HJV and furin and that the reduction in HJV/furin cleavage could not be explained by a lack of colocalization with furin.

Many of the GPI-linked proteins in hepatocytes undergo endocytosis from the basolateral membrane and subsequently traffic to the apical, bile canicular membrane (Schell et al., 1992). Re-uptake is clathrin-independent and either dynamin-dependent or independent and may also depend on flotillin or MAL2 (Ait-Slimane et al., 2009; de Marco et al., 2002). The mechanisms by which flotillin or MAL2 direct this pathway are unclear. In the case of HJV, the protein is cleaved by furin after its clathrin- and dynamin-independent retrograde trafficking, and as a result, it is not trafficked to the apical membrane. Rather, it is secreted into the blood (Kuninger et al., 2008; Lin et al., 2005), which is in contact with the basolateral membrane of hepatocytes. This corresponds with the expression of HJV at the basolateral membrane in both liver hepatocytes (Merle et al., 2007) and in cell culture (Supplemental Figure 1).

The HJV/LDLR chimera processing is independent of the mode of internalization

The HJV/LDLR chimera was designed to internalize through a dynamin- and clathrin- dependent pathway based on the observation that the cytoplasmic domain of LDLR is responsible for clathrin-mediated endocytosis of LDLR (Anderson et al., 1978). Previous studies showed that HJV internalizes through a macropinocytic pathway, which is independent of dynamin and clathrin (Zhang et al., 2008). To distinguish between these two pathways, cells were treated with 80 mM dynasore, an inhibitor of dynamin GTPase activity. Dynamin is necessary for clathrin- and caveolin-mediated endocytosis but not for macropinocytosis. At this concentration clathrin-mediated endocytosis is reduced but macropinocytosis is not (Zhang et al., 2008). While dynasore would be expected to reduce the concentrative pathway of clathrin-mediated endocytosis of the HJV/LDLR chimera, it would not be expected to block the non-concentrative pathway of macropinocytosis. Dynasore reduced the processing of HJV/LDLR but not of WT HJV (Supplemental Figure 2) indicating that the LDLR cytoplasmic domain of the chimera was indeed driving endocytosis.

Signaling of HJV is impaired in the absence of a GPI-anchor

We next wanted to determine whether the GPI-anchor of HJV was important for signaling to upregulate hepcidin expression. GPI-anchors have been proposed to localize proteins to specific membrane domains that may promote signaling through receptor complexes (Brown and London, 2000). To test whether the GPI-anchor of HJV is important for signaling, we used the liver-derived HepG2 cell line, which has

increased hepcidin expression upon transfection of WT HJV (Zhang et al., 2009). The ability of the HJV/furin and HJV/LDLR chimeras to induce hepcidin was analyzed in HepG2 cells expressing these chimeras (Figure 4). While WT HJV induced hepcidin expression, the HJV/furin and HJV/LDLR chimeras did not when compared to an empty vector control (Figure 4A). Expression of these constructs was confirmed by western analysis (Figure 4B). These data indicate that the GPI-anchor of HJV is required for signaling to upregulate hepcidin expression.

Figures

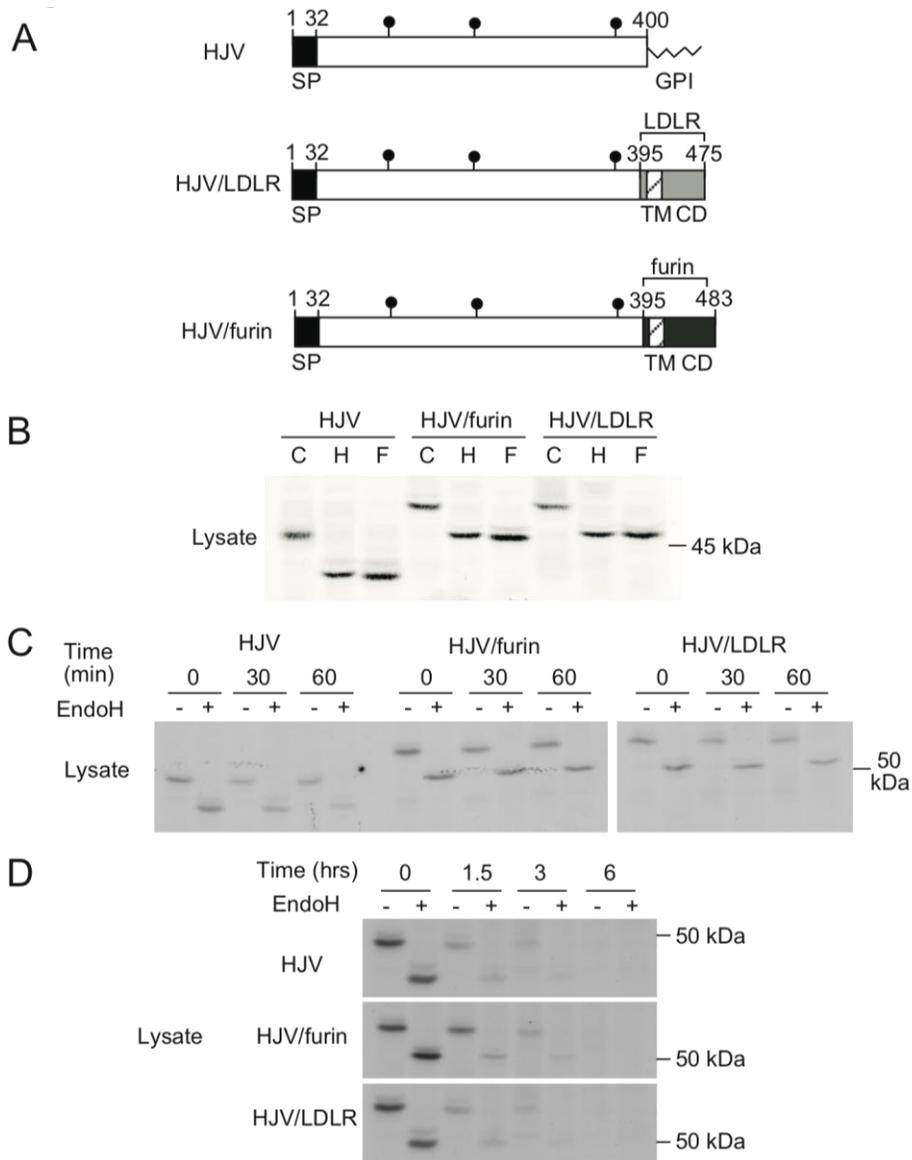


Figure 3.1. HJV constructs with transmembrane domains instead of a GPI-anchor are expressed and processed by the cell.

(A) Fusion constructs of HJV and the transmembrane and cytoplasmic domains of furin (HJV/furin) or LDLR (HJV/LDLR) were made using overlapping PCR as described in the methods section. The GPI-anchor addition sequence of HJV was removed, but the ectodomain of HJV is largely preserved. The three N-linked glycosylation sites of HJV (denoted by black circles) were retained in the chimeras. These sites are predicted based on the canonical motif for N-linked glycosylation of NX(S/T) and have the following amino acid sequences: NCS, NAT and NFT. The endogenous signal peptide on HJV was retained (black). SP, signal peptide; TM,

transmembrane domain; CD, cytoplasmic domain. (B) Immunoblot analysis of HJV chimera oligosaccharides in the cell lysate. Plasmids encoding WT HJV, HJV/Furin or HJV/LDLR chimeras were transfected into Hep3B cells using Lipofectamine 2000. Cell lysates were digested with Endo H (H), PNGaseF (F) or without enzyme (C). HJV was detected using a rabbit anti-HJV antibody as described in the methods. (C) Pulse-chase analysis of HJV chimeras. Chimeras were transfected into Hep3B cells and then subjected to pulse chase analysis with 0, 30 or 60 minute chase periods. (D) Pulse-chase analysis of HJV chimeras as in C except that cells were incubated in unlabeled medium for 0, 1.5, 3 or 6 hours. These experiment were repeated with similar results.

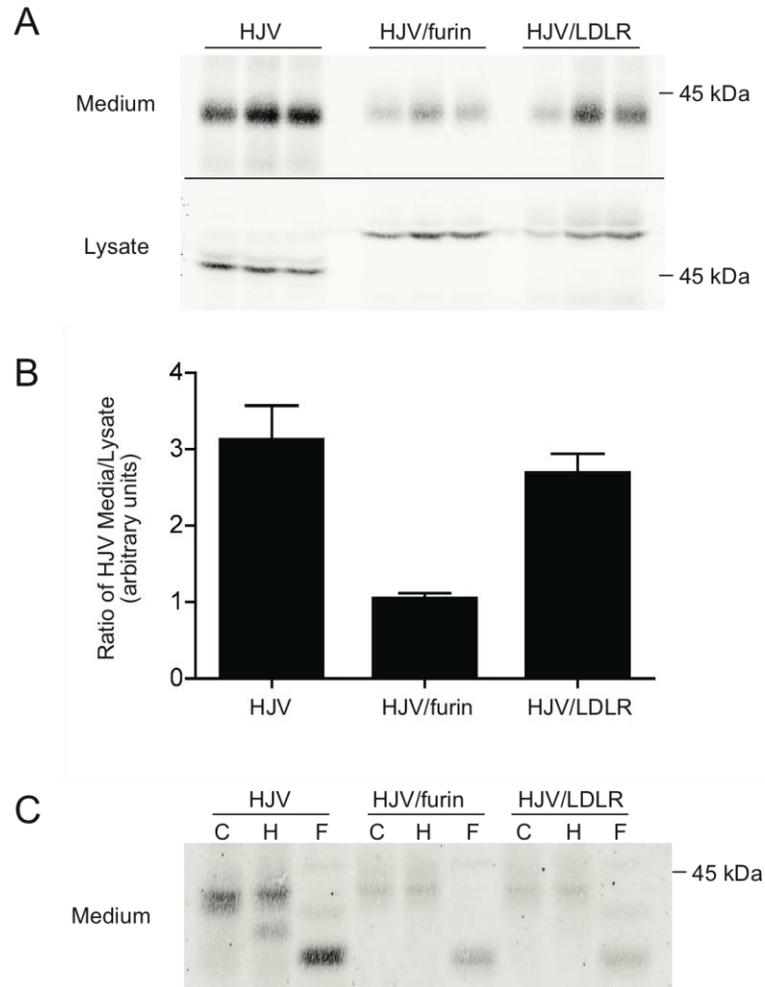


Figure 3.2. HJV secretion does not require a GPI-anchor.

(A) Analysis of the ratio of WT HJV secretion compared with HJV/furin and HJV/LDLR. Hep3B cells in 6 well plates were transfected with WT HJV, HJV/furin and HJV/LDLR chimeras as described in the methods section. Medium was precipitated with TCA and immunoblotting was used to detect HJV in the media and lysate. (B) The ratio of HJV in the cell lysate to the conditioned medium was quantified using the Odyssey Infrared Imager and then compared between constructs. Three wells were analyzed for each construct and the experiment was repeated with similar ratios of HJV in the conditioned medium between the WT HJV and the chimeras. (C) Analysis of the Endo-H sensitivity of secreted HJV generated by cleavage of WT HJV or HJV chimeras. Conditioned medium was TCA precipitated and then incubated without enzyme (C), with Endo H (H) or with PNGase F (F) and then analyzed by SDS-PAGE and immunoblotting.

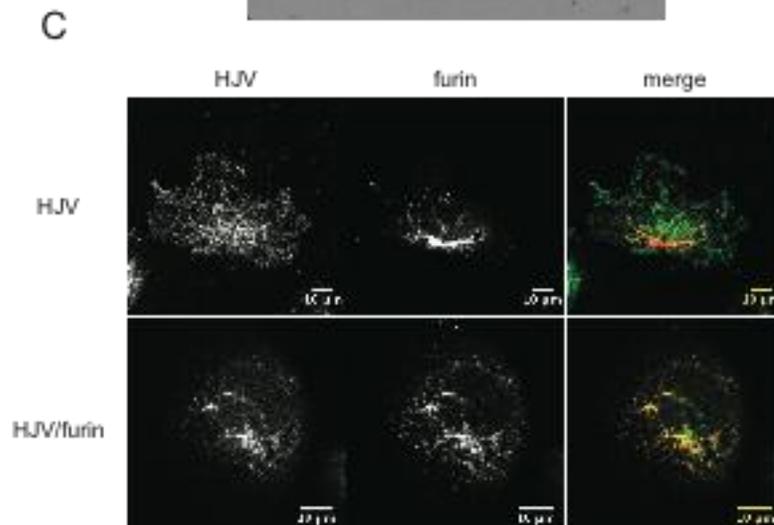
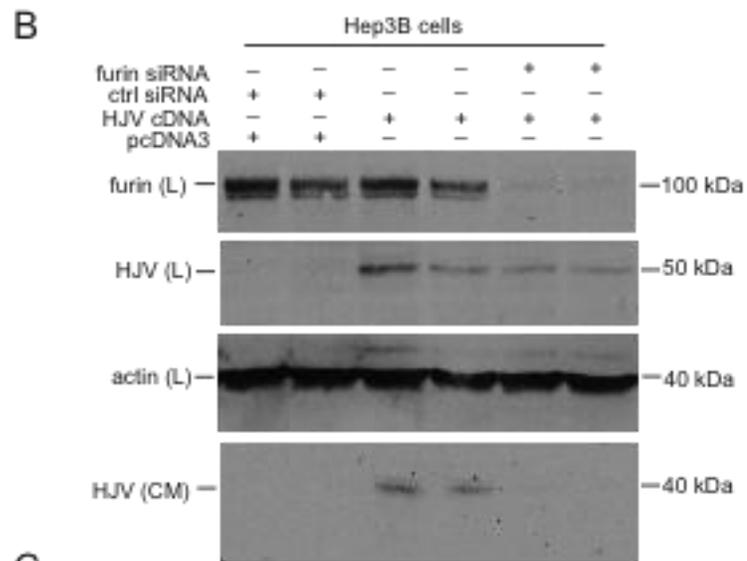
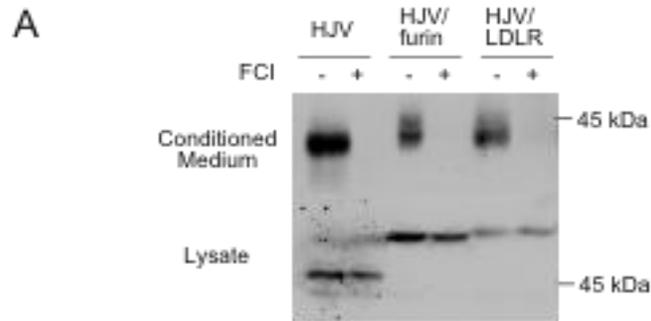


Figure 3.3. Furin-mediated cleavage of HJV chimeras.

(A) Secretion of the HJV chimeras is blocked by addition of a proprotein convertase inhibitor. Hep3B cells transiently transfected with WT HJV, HJV/furin and HJV/LDLR were treated with the proprotein convertase inhibitor, Furin Convertase Inhibitor (FCI). The inhibitor was added when cells were changed to serum free medium and after 20 hours, conditioned medium and cell lysates were analyzed by immunoblotting to detect HJV. Secretion of these constructs was compared between untreated (-) and FCI treated cells (+). Secretion of WT HJV as well as the HJV chimeras was blocked by treatment with FCI, indicating that they are cleaved by a furin family member in these cells. (B) Knockdown of endogenous furin suppresses HJV release in Hep3B cells. SMARTpool siRNA specific for human furin (Thermo-Fisher Scientific, Waltham, MA) was used to knockdown endogenous furin in Hep3B cells. Scrambled control siRNA (Santa Cruz Biotechnology Inc., Santa Cruz, CA) served as a negative control. RNAiMAX reagent (Invitrogen, Carlsbad, CA) was used for the transfection. siRNA transfection was conducted in 12-well plates in complete medium (MEM/10% FCS). About 24-hr after siRNA transfection, HJV was introduced using PolyJet (SignaGen Laboratories). About 48-hr after siRNA transfection, fresh complete medium was replaced. About 72-hr after siRNA transfection, conditioned media were collected and cell lysates were prepared. The total lysate and 20% of CM were subjected to SDS-PAGE. Furin, HJV and β -actin (actin) in the lysate (L) and HJV in the conditioned medium (CM) were detected by immunoblot. (C) The HJV/furin chimera has similar subcellular localization to that of furin. Colocalization of WT HJV and HJV/furin with flag-tagged furin protein were analyzed in Hep3B cells. Hep3B cells were transiently cotransfected with the indicated HJV construct as well as a flag-tagged furin construct. Cells were stained using anti-HJV (green) and anti-flag (red) and imaged by confocal microscopy as described in the methods. While there is some overlap between WT HJV and flag-furin, there is also substantial co-localization between HJV/furin chimera and flag-furin. The HJV and flag-furin localizations are shown in the first two panels and the merged image is shown in the third panel. These are representative staining patterns from two separate experiments with similar results.

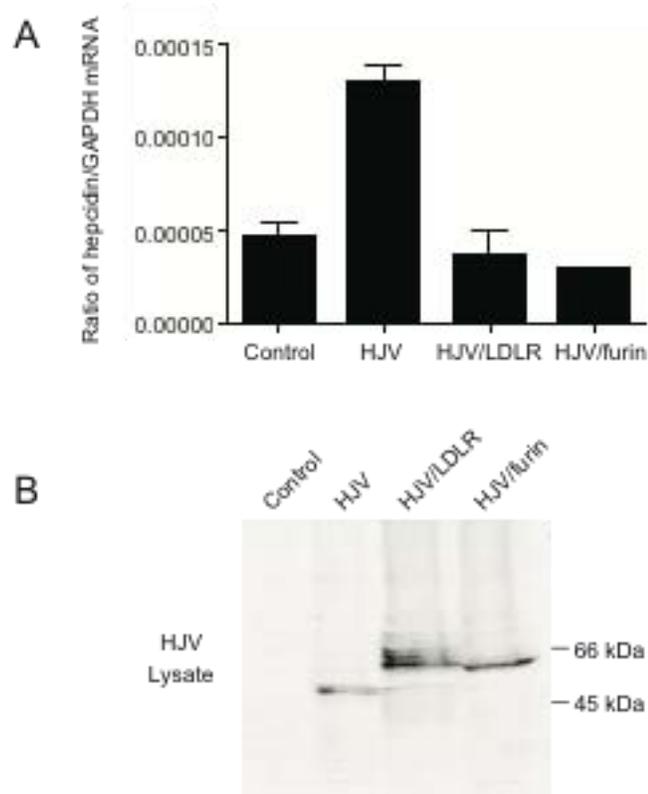


Figure 3.4. The GPI-anchor of HJV potentiates hepcidin expression.

(A) tTA-Neogenin HepG2 cells were transfected with an empty pcDNA3 (control), WT HJV, HJV/furin or HJV/LDLR. Cells were induced to express neogenin using 2 $\mu\text{g}/\text{mL}$ doxycycline in MEM with 2% FBS for 16 hours. Neogenin increases the ability of HJV to activate hepcidin expression (Zhang et al., 2009). Hepcidin and GAPDH levels were then analyzed by qRT-PCR. The ratio of hepcidin to GAPDH levels are presented for each construct. Three biological replicates each with three PCR replicates were performed for each construct. These results are representative of three separate experiments. $p=0.0002$ as analyzed by ANOVA. (B) As a control to show that all of the constructs were expressed in these cells, the tTA-Neogenin HepG2 cells were transfected with the WT HJV, HJV/LDLR or HJV/furin and analyzed by immunoblot using the anti-HJV antibody described in the methods. Untransfected cells serve as a control for antibody specificity. This experiment was performed three times with similar results.

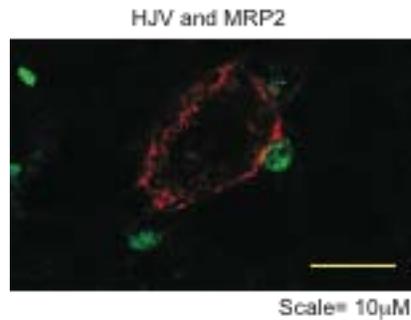


Figure S3.1. GPI-linked HJV is primarily basolaterally localized.

HepG2 cells are a polarized hepatoma-derived cell line that forms apical pockets between cells. Since they are tissue culture cells plated in a monolayer, they cannot form bile canaliculi as hepatocytes do in three dimensions in the liver. The apical marker multi-resistance protein 2 (MRP2-green) stains the apical membrane of these swellings between cells. GPI-HJV (red) was transiently transfected into HepG2 cells using the transfection reagent Fugene HD (Roche). A single transfected cell is shown with untransfected neighbors. HJV appears to localize primarily to the basolateral membrane and has little overlap with the apical marker. Immunofluorescence microscopy was performed on permeabilized cells, essentially as described in the methods, except that mouse anti-MRP2 antibody was used (Clone M2 III-6, 8 μ g/mL, Kamiya Biomedical Company, Seattle, WA) and cells were imaged using a Zeiss LSM710 confocal microscope.

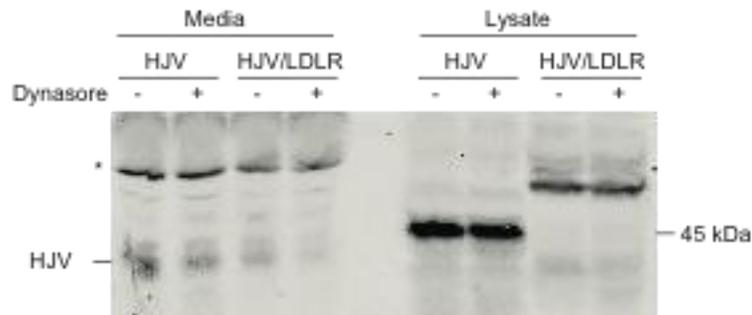


Figure S3.2. Treatment of cells expressing the HJV/LDLR chimera with a dynamin inhibitor reduces secretion of sHJV. Hep3B cells in 6 well plates were transfected with either GPI-HJV or the HJV/LDLR chimera and then treated with MEM media with 2% serum +/- 80 μ M dynasore, which inhibits dynamin/clathrin-mediated endocytosis. After 20 hours, media and lysate were collected. 15% of the media and 100% of the lysate were analyzed by immunoblot as described in the methods. The bands were quantitated using an Odyssey Infrared Imaging System and the ratio of HJV in the media to the lysate was calculated and compared between control and treatment conditions. While the GPI-HJV had approximately the same ratio of media to lysate HJV between control and dynasore treated samples (0.121 and 0.120 arbitrary units respectively) the HJV/LDLR chimera had approximately a 2-fold reduction in secreted HJV upon dynasore treatment (control 0.207 and dynasore 0.104 arbitrary units). Secreted HJV runs below the 45 kDa marker and is marked. A non-specific band is marked by an asterisk (*).

Discussion

We found that while the GPI-anchor of HJV is required for signaling to upregulate hepcidin expression, the processing of HJV appears to be independent of the type of membrane tether. WT HJV and the chimeric forms of HJV with the transmembrane and cytoplasmic domains of either LDLR or furin are initially protected from obtaining complex glycosylation along their biosynthetic pathway and then later get processed to obtain complex oligosaccharides and get cleaved by furin prior to being secreted. Similarly, both WT HJV and the chimeric forms of HJV are processed after endocytosis and retrograde transport. This finding was initially unexpected because GPI-linkage can impart specific trafficking in the endocytic pathway (Brown and London, 2000).

The trafficking of GPI-linked proteins, once they are modified by cleavage of their transmembrane domain and covalent attachment to GPI, has not been studied intensely. Several reports indicate that GPI-linked proteins such as the GPI-linked form of ceruloplasmin pass through the Golgi where its oligosaccharides are converted from high mannose to complex forms on its transit to the plasma membrane (Hellman et al., 2002). The finding that HJV traffics to the plasma membrane without the processing of its oligosaccharides is unusual (Maxson et al., 2009). Hemojuvelin could avoid oligosaccharide processing and cleavage by furin by either trafficking through an alternate pathway devoid of glycosylases, by binding to

another protein, which masks glycosylation and furin cleavage or by being conformationally inaccessible to the oligosaccharide processing and cleavage.

A previous study showed that replacing the GPI-anchor of HJV with a KDEL sequence reduces cleavage of HJV (Silvestri et al., 2008a). The KDEL sequence is an ER retrieval motif that directs soluble ER-resident proteins that have trafficked past the ER to be bound by the KDEL receptor, which is responsible for their retrograde trafficking back to the ER, as reviewed in (Teasdale and Jackson, 1996). A reduction in HJV secretion of the HJV/KDEL construct (Silvestri et al., 2008a) and the primary localization of furin in the TGN (Thomas, 2002) are consistent with a model that furin-mediated cleavage of HJV occurs primarily in a post-ER compartment.

We hypothesize that either the conformation of HJV prevents modification and cleavage in the biosynthetic pathway or that a yet to be identified chaperone protein sterically hinders access of furin and oligosaccharide modification. Once at the cell membrane, HJV undergoes a conformational change due to its release from the chaperone or through association with another protein. Arguing against a chaperone protein that shields HJV from processing during the biosynthetic pathway is the lack of evidence for a chaperone protein in pulse-chase analysis and the fact that soluble forms of HJV are modified and processed during their biosynthesis (Maxson et al., 2009). Arguing in favor of the association with a protein once HJV reaches the plasma membrane or upon endocytosis is the finding that HJV tightly associates with a transmembrane protein, neogenin (Zhang et al., 2005).

Earlier studies showed that neogenin facilitates the cleavage of HJV after it reaches the cell surface, making it a prime candidate for this later possibility (Zhang et al., 2007; Zhang et al., 2008). The role of neogenin in HJV processing and signaling remains controversial. Another group reported that neogenin inhibits HJV secretion in HEK293 cells (Lee et al., 2010). The reason for these differing effects is not yet clear. HJV and neogenin do not appear to co-associate in the biosynthetic pathway (J. Maxson, data not shown).

The data presented here are consistent with the role of retrograde transport in the processing of HJV by furin. The observation that the HJV/furin chimera is not efficiently cleaved by furin, despite their co-localization in the TGN, supports the idea that membrane anchored HJV is not modified in the biosynthetic pathway but rather after it reaches the plasma membrane and re-internalizes. Furin is predominantly located in the TGN and inefficiently traffics to the plasma membrane (Thomas, 2002). At the plasma membrane, it endocytoses and traffics back to the TGN (Molloy et al., 1994). Both furin and the LDLR are internalized by clathrin-mediated endocytosis by the interaction of their cytoplasmic domains with proteins in the clathrin-coated pit. The finding that the shedding of the HJV/LDLR chimera is reduced by inhibition of clathrin-dependent endocytosis further emphasizes the role of retrograde trafficking in cleavage of HJV.

The GPI-anchor of HJV directs HJV through a clathrin-independent, cholesterol-dependent endocytic pathway (Zhang et al., 2008). This study shows that the

processing and cleavage but not signaling of HJV is independent of the type of membrane anchor. In contrast to WT HJV, the chimeric forms of HJV with transmembrane and cytoplasmic domains instead of a GPI-anchor do not upregulate expression of hepcidin in HepG2 cells. The GPI-anchor of HJV could promote signaling by localizing HJV to a specific membrane domain. Alternately, the GPI-anchor of HJV could alter its conformation or flexibility and thus alter its interaction with BMPs and their receptors. The mechanism by which the GPI-anchor of HJV promotes BMP signaling will be the subject of future work.

ACKNOWLEDGEMENTS

We would like to thank Juxing Chen, Junwei Gao, Maria Chloupkova and Kristina DeMaster for reading the manuscript and helpful comments. This work was supported by National Institutes of Health Grant DK080765 to ASZ. JEM was partially supported by National Institutes of Health Grant T32 HD049309, a scholarship from Vertex Pharmaceuticals and an American Heart Associate pre-doctoral fellowship 10PRE3530017. CAE, ASZ and JEM designed the experiments, analyzed the data and wrote the paper. JEM performed the experiments and prepared the figures.

We would like to thank Gary Thomas, Vollum Institute OHSU, for generously providing us with PCS2-furin and pcDNA3-furin-flag-HA plasmids and David Russell, University of Texas Southwestern Medical Center, for giving us the LDLR pTZ1 plasmid. We would also like to thank Stefanie Kaech, Director of the Advanced Light Microscopy Core at The Jungers Center for her training on the Zeiss LSM 710 confocal microscope and also Maya Culberston at OHSU for invaluable microscopy assistance.

CHAPTER 4

Matriptase-2 and proprotein convertase cleaved forms of hemojuvelin have different roles in the down regulation of hepcidin expression

Julia Maxson¹, Juxing Chen¹, Caroline A. Enns¹, and An-Sheng Zhang¹

¹Department of Cell and Developmental Biology, Oregon Health & Science University, Portland, OR 97239 USA

Corresponding Authors:

An-Sheng Zhang, Department of Cell and Developmental Biology L215, 3181 SW

Sam Jackson Park Rd, Portland, OR 97239; fax: (503) 494-4253; e-mail:

zhanga@ohsu.edu

Caroline Enns, Department of Cell and Developmental Biology L215, 3181 SW Sam

Jackson Park Rd, Portland, OR 97239; fax: (503) 494-4253; e-mail:

ennsca@ohsu.edu

Published in Journal of Biological Chemistry, 10 December 2010. Volume 285,

Number 50 Pages 39021-39028.

Abstract

Hemojuvelin (HJV) is an important regulator of iron metabolism. Membrane anchored HJV upregulates expression of the iron regulatory hormone, hepcidin, through the bone morphogenic protein (BMP) signaling pathway by acting as a BMP co-receptor. Membrane HJV can be cleaved by the furin family of proprotein convertases, which releases a soluble form of HJV that suppresses BMP signaling and hepcidin expression by acting as a decoy that competes with membrane HJV for BMP ligands. Recent studies indicate that matriptase-2 binds and degrades HJV, leading to a decrease in cell surface HJV. In the present work, we show that matriptase-2 cleaves HJV at Arg 288, which produces one major soluble form of HJV. This shed form of HJV has decreased ability to bind BMP6 and does not suppress BMP6-induced hepcidin expression. These results suggest that the matriptase-2 and proprotein convertase cleavage products have different roles in the regulation of hepcidin expression.

Introduction

Iron is an essential biological cofactor. The majority of the body's iron is bound by hemoglobin for oxygen transport by red blood cells. While insufficient iron leads to anemia, excessive iron accumulation in the body causes oxidative damage to DNA, proteins, lipids and other biological molecules (De Domenico et al., 2008). Since humans do not have a regulated mechanism for iron excretion, iron homeostasis is maintained by tightly regulating iron absorption from the intestine. Heparin, a liver-derived peptide hormone, acts as a negative regulator of iron absorption (Nemeth et al., 2004).

Hemojuvelin (HJV) is a key player in the induction of hepcidin expression. Loss-of-function mutations in HJV lead to the severe iron overload disorder, juvenile hemochromatosis (JH) (Camaschella, 1998; Papanikolaou et al., 2004). People with homozygous or compound heterozygous mutations in HJV and HJV knockout mice have inappropriately low levels of hepcidin expression resulting in increased iron absorption (Huang et al., 2005; Niederkofler et al., 2005; Papanikolaou et al., 2004). HJV binds to the bone morphogenic proteins (BMPs): BMP2, 4, 5 and 6. Membrane HJV potentiates hepcidin expression by acting as a co-receptor for BMP ligands (Babitt et al., 2006). BMP ligands upregulate hepcidin expression by activating the BMP signaling pathway (Babitt et al., 2006; Babitt et al., 2007; Wang et al., 2005). Recent studies indicate that BMP6, in particular, is important in the regulation of iron metabolism and its expression in the liver is positively regulated by iron levels (Andriopoulos et al., 2009; Kautz et al., 2008; Meynard et al., 2009).

HJV is a GPI-linked membrane protein, expressed in both skeletal muscle and liver. It can be cleaved by proprotein convertases and released as a shed form (sHJV) (Kuninger et al., 2006; Lin et al., 2005; Niederkofler et al., 2004; Silvestri et al., 2008a; Zhang et al., 2007). sHJV generated by proprotein convertase cleavage antagonizes the function of GPI-linked HJV by negatively regulating BMP signaling, thereby decreasing hepcidin expression. Two mechanisms are possible for the downregulation of BMP signaling by sHJV. First, cleavage of hemojuvelin releases HJV, such that sHJV no longer acts as a co-receptor for BMP signaling. Second, sHJV is capable of binding BMPs, thus competing with GPI-HJV (Lin et al., 2005).

Matriptase-2 is a serine protease encoded by the gene *TMPRSS6*. It is mainly expressed in the liver and is a critical regulator of iron homeostasis (Du et al., 2008; Folgueras et al., 2008). Lack of functional matriptase-2, both in humans and in mice, causes inappropriately high hepatic hepcidin expression, which results in iron-deficiency anemia (Du et al., 2008; Folgueras et al., 2008). Matriptase-2 is therefore an important suppressor of hepcidin expression. Recent studies in transfected HeLa cells indicate that matriptase-2 binds and decreases cell surface HJV by cleaving it into a ladder of smaller products (Silvestri et al., 2008b). Since HJV and matriptase-2 are both expressed in liver, matriptase-2 has been proposed to regulate iron homeostasis by modulating the levels of cell surface HJV.

In this study we show that proprotein convertases and matriptase-2 cleave HJV in a site-specific manner and each protease generates one major cleavage product whose sizes are distinct from each other. In contrast to proprotein convertase cleavage, the sHJV product generated by matriptase-2 cleavage has reduced binding

to BMP6 and does not alter BMP6-induced hepcidin expression. These data indicate that the major role of matriptase-2 is to inactivate HJV.

Materials and Methods

Generation of HJV constructs

HJV-p3XFlag-CMV-9 vector with three flag tags at the N-terminus of HJV (Babitt et al., 2006) was kindly provided by Dr. Jodie Babitt at Harvard University. Previously described pcDNA3-HJV (Zhang et al., 2005) was used as a template to generate Arg to Ala mutations and stop codon mutations using the QuikChange XL Site Directed Mutagenesis Kit (Stratagene, Santa Clara, CA) according to the manufacture's protocol. The primers used to generate the constructs are as follows:

Construct Name	Primers
HJV R329A	5'-caagtcagcgactctctgcatcagagcgcaatcgtc-3' 5'-gacgattgcgctctgatgcagagagtcgctgacttg-3'
HJV R332A	5'-ctctctcgatcagaggccaatcgtcggggagc-3' 5'-gctccccgacgattggcctctgatcgagagag-3'
HJV R257A	5'-atcaatggaggtgacgcacctgggggatccag-3' 5'-ctggatccccagggtgctgcacctccattgat-3'
HJV R288A	5'-ctacattggcacaactataatcattgcgagacagctggg-3' 5'-cccagctgtctgcaatgattatagttgtgccaatgtag-3'
HJV Q289X	5'-acaactataatcattcggtagacagctgggcagct-3' 5'-agctgccagctgtctaccgaatgattatagttgt-3'
HJV P258X	5'-gatggttctatcaatggaggtgaccgataggggggatccagttt-3' 5'-aaactggatccccctatcggtcacctccattgataagaaccatc-3'
HJV 336X	5'-cagagcgcaatcgtcggtgagctataaccattgatac-3' 5'-gtatcaatggttatagctcaccgacgattgctgctcg-3'
HJV 345X	5'-ggagctataaccattgatactgccagatagctgtgcaaggaag-3' 5'-cttcctgacagctatctggcagtatcaatggttatagctcc-3'
HJV 386X	5'-gcactggaggatgcccgataattcctgccagacttagag-3' 5'-ctctaagtctggcaggaattatcgggcatcctccagtgc-3'

Cloning of human matriptase-2

The coding sequence of *TMPRSS6* (matriptase-2) cDNA was amplified from a human liver cDNA preparation by PCR using the Expand High Fidelity PCR system (Roche Applied Science), followed by cloning into pGEM-T vector (Promega). The primers

used for *TMPRSS6* cDNA amplification were 5'-TCGGCACCCACTTGCAGTCA-3' (forward) and 5'-GGCAGTTGCCCTGGGCTCTC-3' (reverse). *TMPRSS6* cDNA was subcloned into the pcDNA3 vector (Invitrogen). The vector was verified by DNA sequencing and no mutations were detected.

Cell culture and transfection

Both HepG2 and HEK293 cells were obtained from ATCC. Stably transfected cells were maintained by the addition of 800 µg/mL G418. Fugene HD (Roche, Basel, Switzerland) and Lipofectamine 2000 (Invitrogen, Carlsbad, CA) were used to transfect HepG2 and HEK293 cells, respectively.

Inhibitors

Cells were treated with leupeptin (Sigma, St. Louis, MO) and the furin convertase inhibitor (FCI), decanoyl-Arg-Val-Lys-Arg-chloromethyl ketone (Alexis, San Diego, CA). The stock solution of leupeptin (10 mM) was solubilized in water and FCI (5 mM) was dissolved in DMSO. The final concentrations of the inhibitors are denoted in the figure legends.

sHJV/BMP6 binding assay

sHJV/PC and sHJV/M2 were filter-concentrated from the serum-free conditioned medium, collected from HEK293 cells stably expressing flag-tagged HJV (HEK293-fHJV) and HEK293-fHJV cells transiently transfected with pcDNA3-*TMPRSS6*, respectively. sHJV concentrations were estimated by western blot using

baculovirus-generated sHJV as a standard. BMP6 was purchased from R & D Systems (Minneapolis, MN). sHJV/BMP6 binding assays were performed as previously described (Andriopoulos et al., 2009), except that an anti-FLAG-M2 Affinity Gel (Sigma) was used to pulldown sHJV.

Immunoblot analysis

Immunoblot analysis on cell lysates, conditioned medium and binding eluate were performed as described previously (Maxson et al., 2009) using an affinity-purified rabbit anti-HJV antibody generated against residues 1-401 of human HJV (0.22 µg/mL) (Zhang et al., 2005), a mouse anti-β-actin antibody (1:10,000; Chemicon International, Billerica, MA), a rabbit anti-matriptase-2 antibody (1 µg/mL), a goat anti-BMP6 antibody (1:1000; Santa Cruz Biotechnology, Santa Cruz, CA), and the corresponding horseradish peroxidase-conjugated (1:5000) or Alexa 680 conjugated secondary antibodies (1:10,000) (Chemicon International, Millipore, Billerica, MA). Immunoblots were visualized by chemiluminescence (Pierce supersignal, Thermo Fisher Scientific Inc., Waltham, MA) or using an Odyssey infrared imaging system (LI-COR Biosciences, Lincoln, NE).

Generation of the anti-matriptase-2 antibody

Rabbit anti-matriptase-2 antibody was generated by the injection of purified human matriptase-2 fragment into rabbits at Pocono Rabbit Farm & Laboratory Inc. (Canadensis, PA). Purified human matriptase-2 fragment was prepared using baculovirus. Briefly, the DNA encoding the human matriptase-2 residues K70-D558

was PCR-amplified and cloned into pAcGP67A vector, a baculovirus transfer vector with gp67 secretion leader. 6x His-tag was introduced in front of the N-terminus. Supernatants from baculovirus-infected high five cells were harvested and buffer exchanged into 20 mM Tris, 300 mM NaCl and then loaded to a Ni-NTA column (Qiagen) with the addition of imidazole at a final concentration of 10 mM. Nickel column eluates were further purified over Superdex 200 10/30 size exclusion column (GE Healthcare) using 20 mM Tris, pH 7.4, 150 mM NaCl, and 5 mM EDTA as a running buffer. Protein purity was visualized using SDS/PAGE before sent for antibody production. Rabbit anti-matriptase-2 IgG was purified with protein A-sepharose beads (Invitrogen).

siRNA knockdown of matriptase-2

SMARTpool siRNA specific for human *TMPRSS6* (Dharmacon, Thermo Fisher Scientific Inc., Waltham, MA) was used to knock down the matriptase-2 in HepG2 cells that stably express exogenous *TMPRSS6*, as previously described (Zhang et al., 2007). RNAiMAX reagent (Invitrogen, Carlsbad, CA) was used for the transfection. The negative control siRNA was previously described (Zhang et al., 2007).

RT-PCR analysis

qRT-PCR was performed as described previously (Zhang et al., 2004). Primers used to measure rat *TMPRSS6* (matriptase-2) are forward 5'-agaaggtggatgtgcaactgac-3' and reverse 5'-cttgcccttgcgataacca-3'. Primers used to measure human *TMPRSS6* are

forward 5'-ctgtgcagcgaggctctatcg-3' and reverse 5'-agtcaccctgacaggcatcct-3'. Rat GAPDH primers (Zhang et al., 2004) and human GAPDH primers (Zhang et al., 2009) are the same as previously reported.

Immunofluorescence microscopy

HepG2 cells were plated on #1.5 glass cover slips (Warner Instruments, Hamden, CT) and transfected with the indicated HJV plasmids using Fugene HD (Roche). Cells were stained using rabbit anti-HJV (1.73 µg/mL), and mouse anti-KDEL 10C3 (5 µg/mL, Stressgen, Victoria, BC), Alexa Fluor 568 goat anti-rabbit IgG (H+L) (4 µg/mL, Molecular Probes, Invitrogen, Eugene, OR), and Alexa Fluor 488 goat anti-mouse IgG (H+L) (4 µg/mL, Molecular Probes). Cells were imaged using an 63X oil objective on a LSM 710 microscope (Carl Zeiss).

Flow cytometry

HEK293 cells stably expressing WT, R257A or R288 HJV were grown in 100 mm dishes (a 100 mm dish is sufficient for 6 samples). Cells were detached by incubating in Cell Dissociation Buffer (Invitrogen). For surface HJV detection, cells were incubated in affinity purified Rb anti-HJV 18745 antibody (4 µg/ml) in FACS specific Buffer (FSB-Hanks w/o calcium or magnesium, 10 mM HEPES, pH 7.4, 1% FBS) for 1.5 hours at 4°C, washed and then incubated in Alexa Fluor 488 Gt anti-Rb IgG (3.3 µg/ml) (Invitrogen) for 30 minutes at 4°C. For detection of total HJV, cells were fixed in phosphate buffered saline (PBS) with 4% paraformaldehyde, washed,

permeabilized in PBS with 0.1% Triton X-100, washed and incubated in Rb anti-HJV 18745 antibody (4 $\mu\text{g/ml}$) in FSB for 30 min at 37°C. Cells were washed and then incubated in Alexa Fluor 488 Gt anti-Rb IgG (3.3 $\mu\text{g/ml}$) for 30 min at 4°C. Three samples were analyzed for cell surface and total HJV expression along with no antibody and non-specific IgG controls for each cell line. Flow cytometry was performed using a FACSCalibur flow cytometer (Becton Dickinson, Franklin Lakes, NJ) at the Oregon Stem Cell Center Flow Cytometry Core, Oregon Health & Science University.

Results

Cleavage of HJV by matriptase-2 generates one major form of soluble HJV in HEK293 cells.

Recent studies showed that membrane HJV can be cleaved by both the furin family of proprotein convertase and matriptase-2, and that the cleaved forms are shed from cells (Kuninger et al., 2008; Lin et al., 2008; Silvestri et al., 2008a; Silvestri et al., 2008b). We therefore wanted to characterize the differences between matriptase-2 and proprotein convertase cleavage of HJV. The size of sHJV generated by matriptase-2 cleavage was compared to that produced by proprotein convertase cleavage. HEK293 cells stably expressing HJV (HEK293-HJV) were transiently transfected with either empty vector or a plasmid containing matriptase-2 cDNA (pcDNA3-*TMPRSS6*). Similar to a previous report (Lin et al., 2008), the sHJV that was shed by the empty vector-transfected HEK293-HJV cells, migrated at approximately 40 kDa in SDS-PAGE, and its secretion was blocked in the presence of decanoyl-Arg-Val-Lys-Arg-chloromethylketone, a furin convertase inhibitor (FCI), which inhibits proprotein convertases (Figure 4.1). The inhibition of the 40 kDa sHJV by FCI suggests that it is the product of proprotein convertase cleavage. In matriptase-2 transfected HEK293-HJV cells (HEK293-HJV/M2), however, we detected the major form of sHJV in the conditioned medium (CM) migrating at approximately 36 kDa (Figure 4.1).

The secretion of the 36 kDa sHJV was not inhibited by FCI, but it was blocked by leupeptin, a serine-cysteine protease inhibitor (Figure 4.1). These results are consistent with generation of this cleavage product by matriptase-2, a serine

protease (Velasco et al., 2002). Notably, a faint second band lower than the major matriptase-2 cleavage product was detected, which could be the result of heterogenous cleavage. It is not the result of heterogeneous N-linked glycosylation of HJV (Maxson et al., 2009). Interestingly, we found that the blockage of matriptase-2-cleaved sHJV by leupeptin was correlated with the appearance of the proprotein convertase-cleaved sHJV in the CM (Figure 4.1). These results suggest both that the cleavage site for matriptase-2 is different from the cleavage site for proprotein convertases, and that in the presence of excess matriptase-2, cleavage by a proprotein convertase is overridden by the processing by matriptase-2.

Endogenously expressed matriptase-2 in HepG2 cells is able to cleave HJV.

We wanted to test whether the cleavage products identified in the medium of HepG2 cells are produced by proprotein convertases and matriptase-2. HepG2 cells were used because they are human hepatoma cell line and the liver is the major site of matriptase-2 expression in the body. Two different species of sHJV were previously detected in the CM from HepG2 cells that stably express HJV (HepG2-HJV) (Zhang et al., 2007). Furin is a proprotein convertase that has been implicated in HJV cleavage and is ubiquitously expressed in tissues, including the liver (Thomas, 2002). We first examined the relative abundance of matriptase-2 mRNA versus furin mRNA in HepG2 cells and compared with those in HEK293 cells, rat liver, rat muscle, rat hepatocytes, and human liver. The level of matriptase-2 mRNA was slightly higher than that of furin in HepG2 cells (Figure 4.2A). Their ratio was similar to those detected in rat liver, rat hepatocytes and human livers, but were much higher than

in HEK293 cells and rat muscle. These results indicate that HepG2 cells endogenously express both furin and matriptase-2 and that HEK393 cells do not express appreciable amounts of matriptase-2 mRNA.

The protease inhibitors, FCI and leupeptin, were also used to distinguish between the two protease activities. FCI blocked the release of the larger sHJV form, migrating at 40 kDa, whereas leupeptin blocked the 36 kDa form of sHJV (Figure 4.2B). Cell surface biotinylation studies indicated that the cleavage of HJV was blocked by leupeptin after HJV has trafficked to the cell surface (Figure S4.1). In the presence of both FCI and leupeptin, both forms of sHJV were no longer detectable in the medium, suggesting the lack of involvement of other classes of proteases.

To further verify that the smaller form of sHJV is indeed derived from matriptase-2 cleavage, we generated a HepG2 cell line that was stably transfected with matriptase-2 to increase the processing of HJV (HepG2-M2) (Figure 4.2C). Transient introduction of HJV into HepG2-M2 cells increased the relative amount of the 36 kDa band and decreased the 40 kDa band. Formation of the 36 kDa band was blocked by leupeptin, but not FCI (Figure 4.2C; lower panel). Knockdown of matriptase-2 by siRNA also reduces the lower molecular weight cleavage product (Figure 4.2D). Interestingly, when HJV is expressed, more matriptase-2 protein is detected, however the underlying mechanism is not known (Figure 4.2C). Together, these results support that endogenously and exogenously expressed matriptase-2 in HepG2 cells is able to cleave HJV that is released from cells and migrates as a 36 kDa band.

Proprotein convertase-mediated cleavage of HJV is blocked in the R332A HJV mutant.

Treatment of cells with FCI blocks shedding of the 40 kDa (upper band) of HJV from HepG2 cells (Figure 4.2) and the single, 40 kDa band of HJV from HEK293 cells (Figure 4.1). To confirm that the 40 kDa band is generated by cleavage at the canonical proprotein convertase cleavage-site cluster, mutations were made in the critical Arg residues in this motif (Figure 4.3A). The proprotein convertase cleavage cluster in HJV has three overlapping RXXR motifs. Mutation of Arg 329 should disrupt the first two motifs while mutation of Arg 332 should disrupt the second two motifs. The cleavage and secretion of these HJVs were assessed in HEK293 cells (Figure 4.3B). While all of the HJVs are detected in the cell lysates, there is reduced secretion of R329A HJV and no detectable secretion of R332A HJV. When these constructs were transfected into HepG2 cells, the R329A mutation reduced shedding of the 40 kDa form into the medium (Figure 4.3C). The R332A mutation also selectively and substantially reduces shedding. Mass-spectrometry analysis confirmed that the second and third sites are both cleaved by proprotein convertases (Figure S4.2). Thus, the single endogenous HJV cleavage product in HEK293 cells is produced by cleavage in the canonical proprotein convertases cleavage-site cluster.

Immunofluorescence microscopy was employed to determine whether the R332A mutation in HJV blocks proprotein convertase-mediated cleavage of HJV by causing misfolding and endoplasmic reticulum (ER)-retention of the protein (Figure 4.3D). WT-, R329A- and R332A-HJV constructs were transiently transfected into

HepG2 cells, which were subsequently detected with anti-HJV and anti-KDEL antibodies. The anti-KDEL antibody recognizes proteins with the KDEL ER-retrieval sequence, and serves as a marker for the ER. Like WT HJV, the R329A- and R332A-HJVs have a punctate appearance (red) in contrast with the lacy morphology of the ER (green). Immunofluorescent microscopy indicates both cell surface and intracellular staining of all these forms of HJV. In addition, little co-localization of HJV with the ER is detected. Therefore, the reduction in cleavage of R329A HJV and the block in cleavage of R332A HJV are not caused by the inability of these forms of HJV to fold and traffic past the ER.

The R288A mutation in HJV specifically blocks the cleavage of HJV by matriptase-2.

Previous studies indicated that matriptase-2 cleaves its substrates at the carboxy side of Arg residues (Velasco et al., 2002). Based on our observations that sHJV generated by matriptase-2 cleavage is smaller than that cleaved by proprotein convertases, we reasoned that the major cleavage site by matriptase-2 lies N-terminal to the proprotein convertase cleavage site. From the molecular weight of the cleaved product and the preference of matriptase-2 to cleave after Arg, we predicted that Arg 257 or Arg 288 could be the sites of matriptase-2 cleavage.

HEK293 cells stably expressing HJV, R257A HJV (R257A), or R288A HJV (R288A) were transiently transfected with either pcDNA3-*TMPRSS6* or pcDNA3 empty vector (C) to determine which mutation blocks matriptase-2 cleavage. When matriptase-2 (M2) was introduced into HEK293-R257A and R288A HJV cells, however, the 36 kDa

form of the sHJV was only detected in R257A HJV, but not in R288A HJV (Figure 4.4A). Furthermore, leupeptin did not block the secretion of R288A HJV. As expected, introduction of matriptase-2 into HEK293-HJV cells shifted the molecular mass of sHJV from 40 kDa to 36 kDa (Figure 4.4A). These results suggest that R288 of HJV is likely the matriptase-2 cleavage site. Similar results were obtained when R288A HJV was introduced into HepG2-M2 cells (Figure S4.3). Efforts to verify the cleavage site by mass spectrometry were unsuccessful (Figure S4.2). Although we obtained 83% coverage of the peptides of sHJV isolated from the medium, peptides in the region of matriptase-2 cleavage were not detected by mass-spectrometry using arginase, aspartyl or trypsin-generated fragments (Figure S4.2). The lack of coverage of this area could possibly be due to posttranslational modification, heterogeneous matriptase-2 cleavage or exoprotease digestion, which precludes confirmation of the matriptase-2 cleavage sites by mass-spectrometry. Notably, a faint second band lower than the major matriptase-2 cleavage product can be detected. It could be the result of heterogenous cleavage by matriptase-2.

Matriptase-2 is expressed at the cell surface (Velasco et al., 2002). Misfolding of the R288A HJV and lack of trafficking to the cell surface could be a possible explanation for the lack of cleavage by matriptase-2. To test this possibility, flow cytometry was performed to determine the ratio of cell surface to total HJV in HEK293 cells that stably express wild type, R257A or R288A HJV. All three forms of HJV were detected on the cell surface (Figure 4.4B). The average amount of HJV on the cell surface relative to total HJV was 49% for WT HJV, 48% for R257A HJV and 38% for R288A HJV. The differences between the different forms of HJV are not

statistically significant by ANOVA analysis. These results show that the R288A HJV reaches the cell surface. Therefore, the lack of R288A HJV cleavage by matriptase-2 does not result from sequestration of this mutated protein in the ER.

Truncation of HJV after Arg 257 or Arg 288 results in ER retention of HJV.

To confirm that Arg 288 is the site of HJV cleavage by matriptase-2, we created truncations that could be compared to the size of shed HJV generated by matriptase-2 cleavage. These truncated forms of HJV were created by placing stop codons (X) after the candidate Arg residues at positions 258 and 289. When these truncated forms of HJV were expressed in HEK293 cells, they were detected in the cell lysate, but did not appear to be secreted (Figure 4.5A). In contrast, HJV truncated at the proprotein convertase cleavage motif cluster is secreted (Figure S4.4). The glycosylation differences of the P258X HJV in the lysate and the shed HJV produced by matriptase-2 cleavage in the medium precluded comparison of the sizes of these two forms of HJV.

Immunofluorescence microscopy was performed to compare the subcellular localization of the P258X- and Q289X- HJV to the anti-KDEL ER marker. Both forms of HJV extensively co-localized with the ER (Figure 4.5B). Additionally, in contrast to WT HJV, very little punctate staining was evident. These results indicate that P258X- and Q289X- HJVs are not shed because they are retained in the ER, possibly due to misfolding. Furthermore, these data suggest that the region between the Arg 288 and the proprotein convertase cleavage cluster is important for folding and secretion of HJV. Together these results indicate that endogenous matriptase-2 cleaves HJV in a

site-specific manner, which would result in a reduction in membrane HJV available for BMP signaling.

sHJV generated by matriptase-2 has reduced binding to BMP6 and does not suppress BMP6-induced hepcidin expression.

sHJV generated by proprotein convertase cleavage (sHJV/PC) binds to BMP6 and inhibits BMP6-induced hepcidin expression (Andriopoulos et al., 2009). To determine the potential role of sHJV generated by matriptase-2 cleavage (sHJV/M2) in the regulation of hepcidin expression, we tested its ability to bind BMP6. Concentrated sHJV/M2 with a flag tag at the N-terminus was incubated with BMP6, followed by pulldown of HJV. sHJV/PC with a flag tag at the N-terminus was included as a positive control. While the anti-flag bead pulled down both sHJV/PC and BMP6 in the positive control, they pulled down less BMP6 with sHJV/M2 (Figure 4.6A). These observations indicate that sHJV/M2 has reduced binding to BMP6.

We also compared the effects of concentrated sHJV/M2 and sHJV/PC (Figure 4.6B) on BMP6-induced hepcidin expression in HepG2 cells (Figure 4.6C). In agreement with the results of BMP6 binding assay, sHJV/PC, but not sHJV/M2, suppressed the induction of hepcidin expression by BMP6 (Figure 4.6C). While matriptase-2 has been shown previously to reduce hepcidin expression by decreasing the amount of cell surface HJV available for signaling (Silvestri et al., 2008b), these results suggest that sHJV/M2 lacks the additional ability to reduce BMP signaling by competing with membrane-bound HJV for binding to BMPs.

Figures

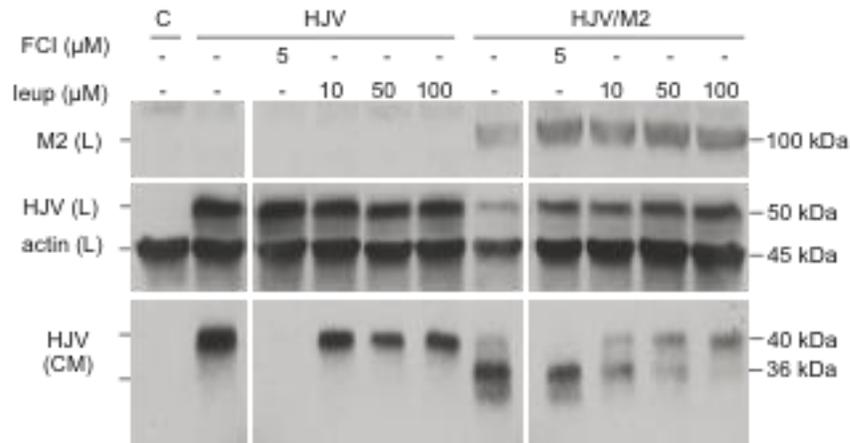
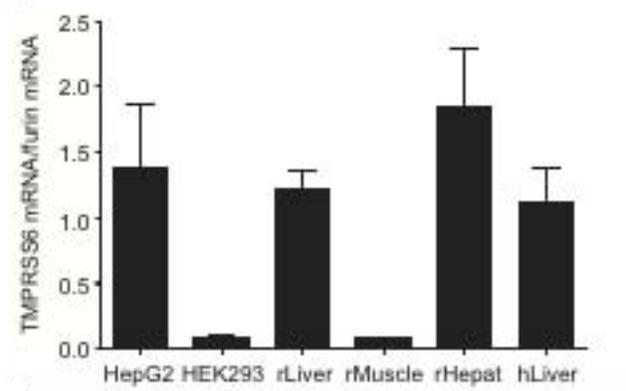


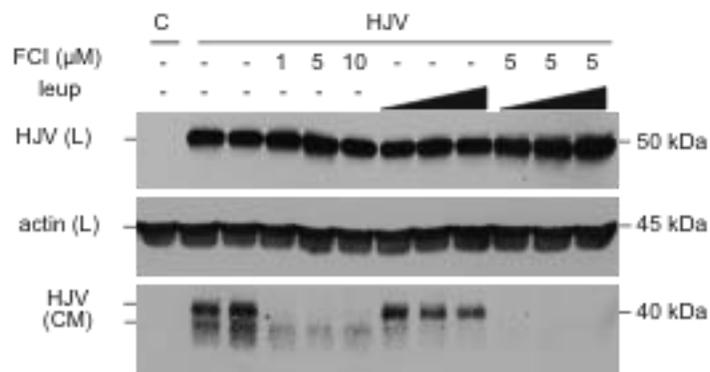
Figure 4.1. Cleavage of HJV by matriptase-2 generates one major isoform of soluble HJV in HEK293 cells.

HEK293 cells stably expressing HJV were subcultured into 12-well plates in DMEM/10% FBS on day 1. On day 2, cells were transfected with either pcDNA3 empty vector (HJV) or pcDNA3-*TMPRSS6* (HJV/M2) using Lipofectamine 2000. At about 24 hr after transfection (day 3), culture medium was changed to 1 ml DMEM/2% FBS per well with or without furin convertase inhibitor (FCI, 5 μM), or leupeptin (Leup; 10, 50 or 100 μM). After 24 hr of incubation (day 4), conditioned medium (CM) was collected and cell lysate was prepared. The total lysate and 12% of CM were subjected to SDS-PAGE, followed by immunodetection of matriptase-2 (M2), HJV and β-actin in the lysate (L) and HJV in CM. HEK293 cells stably transfected with pcDNA3 empty vector (C) were included as a negative control for HJV. The samples were run, transferred and probed with antibodies on a single blot for the two panels. The upper portion of the gel was probed with anti-matriptase-2 and the middle with anti-HJV followed by anti-actin. The molecular masses of the sHJV are denoted to the right of the immunoblot and were calculated by interpolation between the 45 kDa and 31 kDa markers. Similarly the 50 kDa size of cell-associated HJV was calculated by interpolation between the 45 kDa and 66 kDa markers and the size of size of matriptase-2 by interpolation between the 116 kDa and 97 kDa markers. Immunoblots were imaged using chemiluminescence. The images in each row come from the same blot. The experiments were performed three times with consistent results.

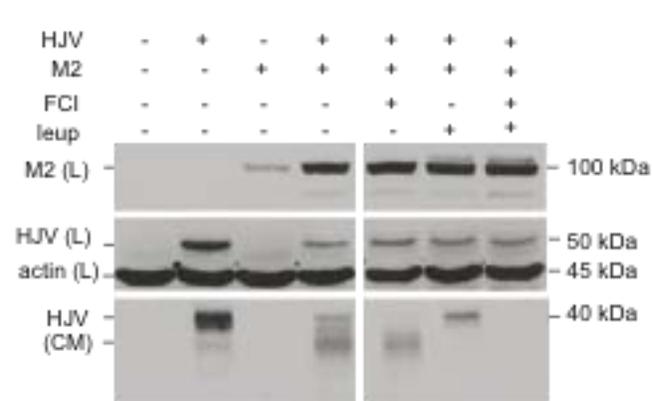
A.



B.



C.



D.

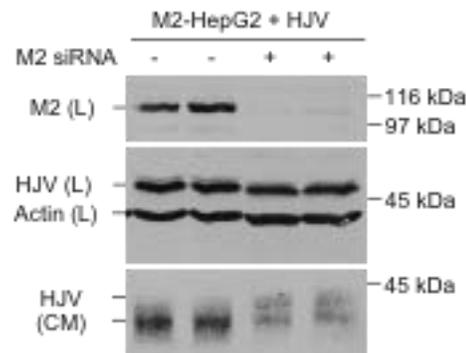


Figure 4.2. The endogenously expressed matriptase-2 in HepG2 cells is able to cleave HJV.

A. qRT-PCR analysis of *TMPRSS6* (matriptase-2) and furin mRNA in HepG2 cells, HEK293 cells, rat liver, rat skeletal muscle (gastrocnemius), rat hepatocytes, and human liver. The relative amounts of *TMPRSS6* mRNA versus furin mRNA in each specific cell type or tissues (mean & standard deviation) are presented. Results are from three individual cDNA preparations of HepG2 and HEK293 cells, and five samples of rat liver (rLiver), rat muscle (rMuscle), rat hepatocytes (rHepat), and human liver (hLiver). B. Secretion of the two isoforms of soluble HJV from HepG2-HJV cells is inhibited by either FCI or leupeptin. HepG2 cells stably expressing HJV (HepG2-HJV) were subcultured into a 12-well plate in MEM/10% FBS. About 48 hrs after subculture, culture medium was changed to MEM/2% FBS with or without FCI (1, 5 and 10 μ M) or leupeptin (leup; 10, 50 or 100 μ M). Conditioned medium and cell lysates were prepared and immunoblotting was performed as in Figure 4.1. HepG2 cells stably transfected with pcDNA3 empty vector (C) were included as a negative control for HJV. C. Increased expression of matriptase-2 in HepG2 cells suppressed the secretion of HJV that is cleaved by proprotein convertases. HepG2 cells stably transfected with pcDNA3 empty vector or pcDNA3-*TMPRSS6* (matriptase-2) were subcultured into 12-well plates and transfected with either pcDNA3 empty vector or pcDNA3-HJV (HJV) as in Figure 4.1. Conditioned medium and cell lysate were collected with or without FCI (5 μ M) or leupeptin (Leup; 100 μ M) treatment. Immunodetection was performed as in Figure 4.1. HepG2 cells stably transfected with pcDNA3 empty vector (C) were included as a negative control for HJV. Immunoblots were imaged using chemiluminescence. These experiments were performed at least three times with consistent results. D. Knockdown of matriptase-2 reduces HJV cleavage. Transfection of matriptase-2 or control siRNAs was conducted in 12-well plates in complete medium. After about 24-hrs, HJV was introduced using FuGene HD transfection reagent (Roche). Conditioned medium was collected and cell lysate were prepared for immunodetection after about 72-hrs of siRNA transfection. siRNA knockdown greatly reduces the levels of matriptase-2. Matriptase-2 siRNA transfection reduces the amount of the 36 kDa HJV cleavage product and also leads to a slight increase in the 40 kDa furin cleavage product. Standard molecular weight markers are marked on the right side of the blot.

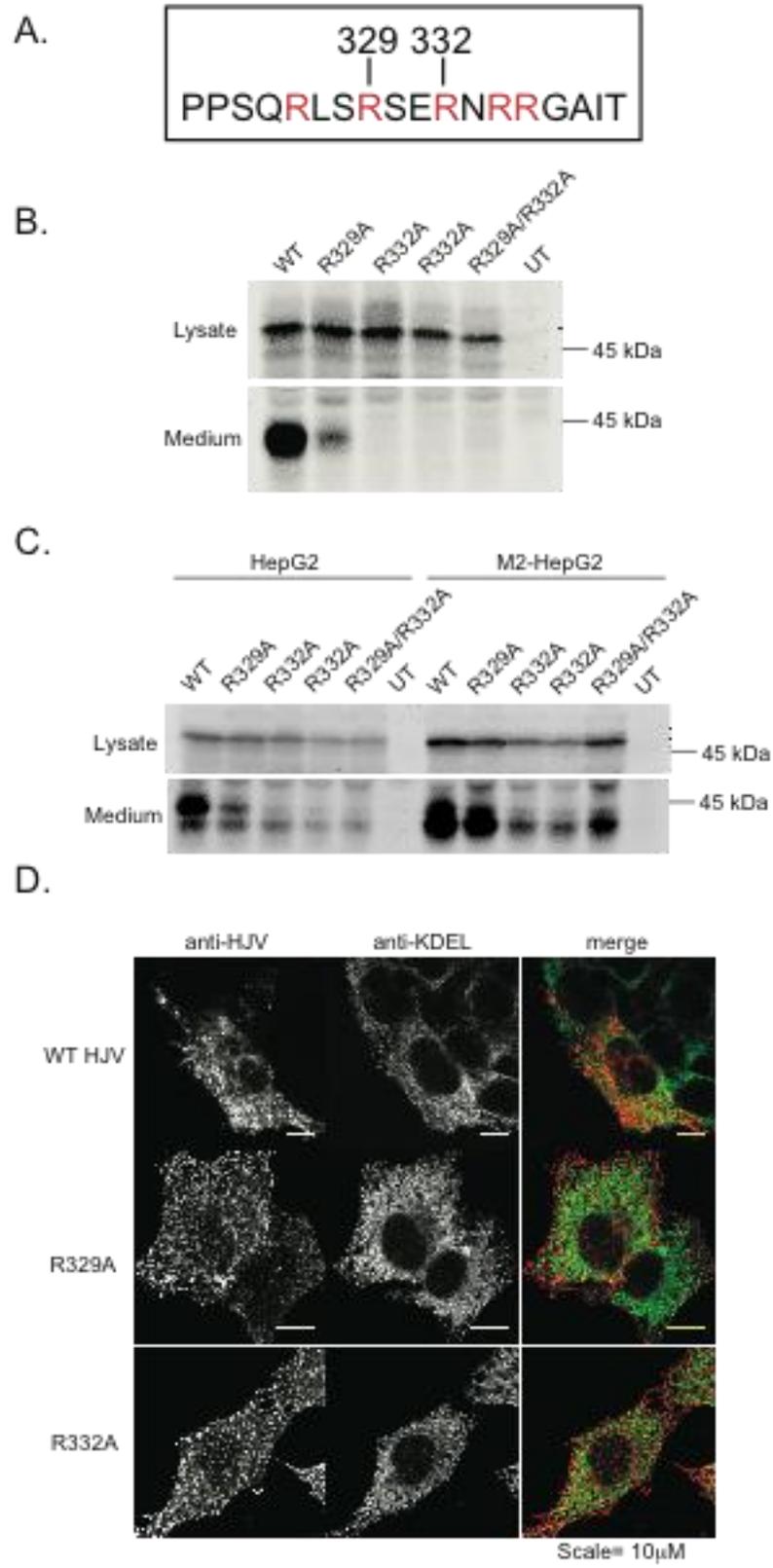


Figure 4.3. Proprotein convertase-mediated cleavage of HJV is blocked by mutation of Arg 332.

A. Schematic of the proprotein convertase cleavage motifs in human HJV. The arginines that were mutated to alanines are labeled. B. HJV cleavage is blocked by the R332A mutation in HEK293 cells. These constructs were transiently transfected into HEK293 cells, and the presence of shed HJV in the media was assessed by immunoblot analysis. Fluorescent secondary antibodies were used to visualize HJV. While the R329A mutation reduces HJV cleavage, the R332A mutation completely abolishes proprotein convertase-mediated cleavage of HJV in HEK293 cells. Two separate R332A HJV transfections are shown. This experiment was repeated with consistent results. Immunoblots were imaged using chemiluminescence. C. The R332A mutation blocks the upper, proprotein convertase-generated cleavage product in HepG2 cells. Mutated HJV constructs were transfected into HepG2 cells or HepG2 cells stably expressing matriptase-2 (M2-HepG2) and HJV were analyzed in the media and lysate as in B. UT, untransfected. This experiment was repeated with consistent results. D. The R329A and R332A forms of HJV are not ER retained. WT, R329A and R332A HJV-pcDNA3 constructs were transiently transfected into HepG2 cells. Cells were stained with rabbit anti-HJV (red) and mouse anti-KDEL (green) antibodies and corresponding fluorescent secondary antibodies, and imaged by confocal microscopy. A single section is shown for each image and the merged image is shown in the third panel. The scale bar is shown in the bottom right hand corner. The images shown are representative of several captured images for each form of HJV.

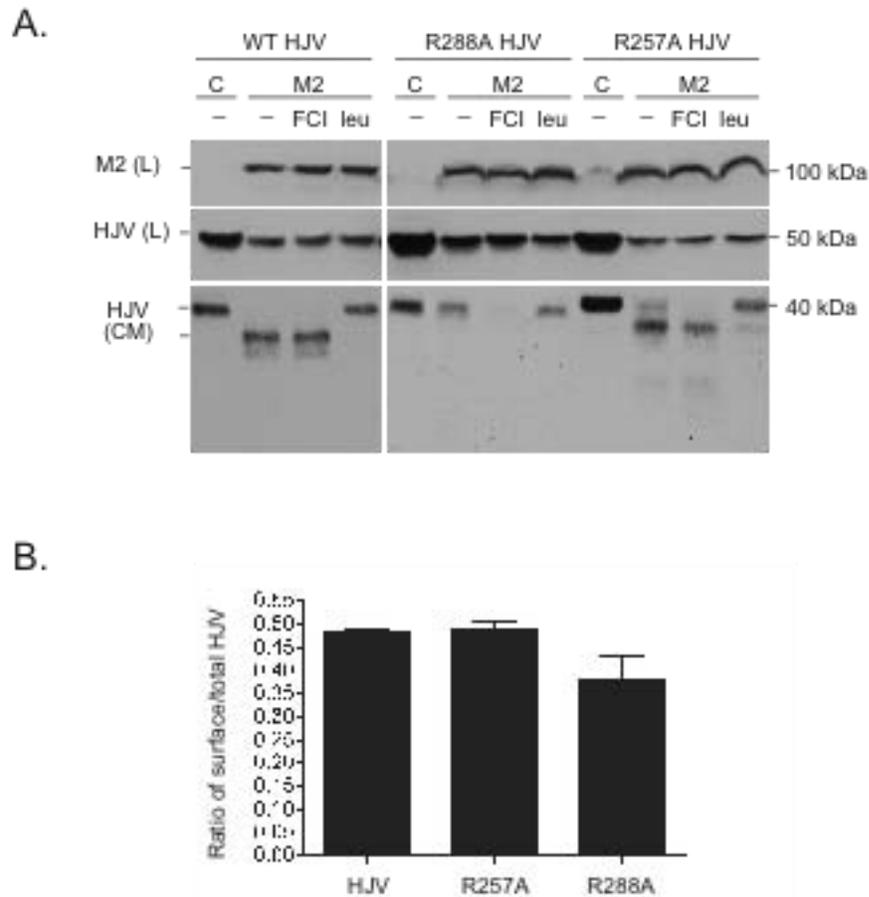


Figure 4.4. Matriptase-2-mediated cleavage of HJV is blocked by mutation of Arg 288.

A. HEK293 cells. HEK293 cells stably expressing HJV, R257A HJV, or R288A HJV were transfected with either pcDNA3 empty vector (C) or pcDNA3-*TMPRSS6* (M2). Conditioned medium and cell lysate were collected after incubation with 5 μ M FCI or 100 μ M leupeptin (Leup) for 24 hours. Immunoblot analysis was performed as in Figure 4.1. This experiment was done three times with consistent results. B. R288A HJV reaches the cells surface. Flow cytometry was performed on HEK293 cells stably expressing WT, R257A and R288A HJV as described in Experimental Procedures. The ratio of cell surface to total HJV was calculated and the experiment was performed in triplicate. All three of these forms of HJV are detected on the cell-surface to similar extents.

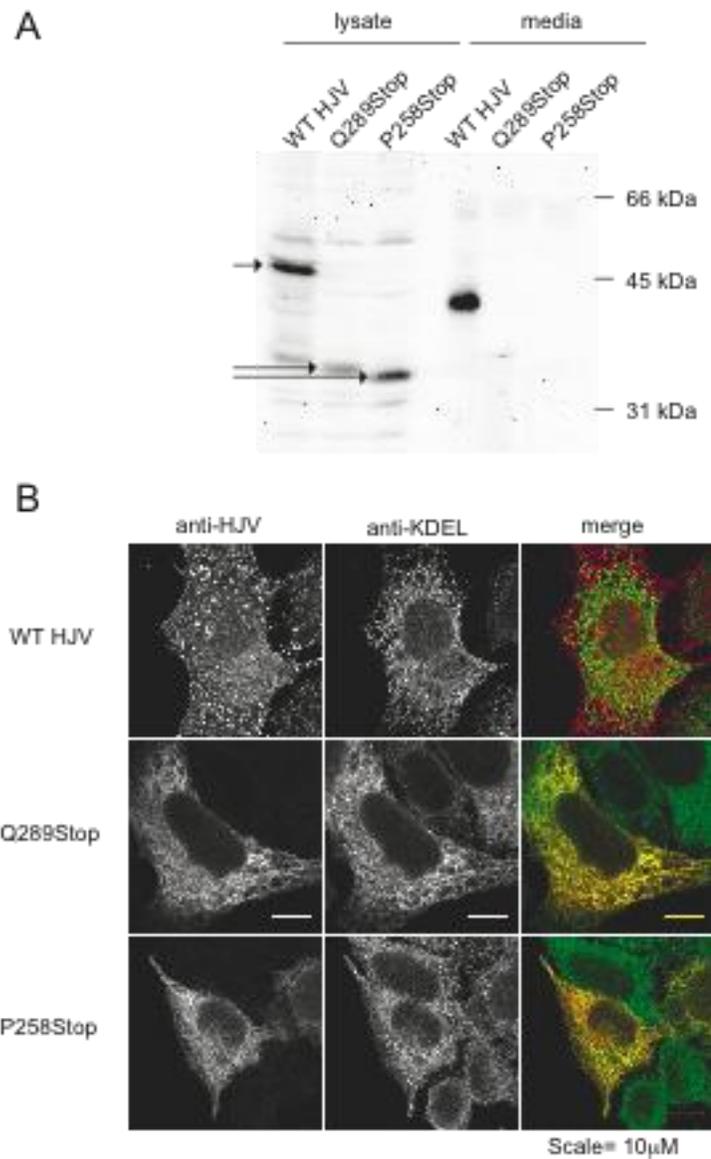


Figure 4.5. Truncation of HJV after Arg 257 or Arg 288 results in ER retention of HJV.

A. The P258X- and Q289X-HJV are not secreted. Site directed mutagenesis was used to put a stop codon at positions 258 or 289 in HJV. These constructs were transfected into HEK293 cells and the presence of HJV was analyzed in the media and the lysate by immunoblot. Fluorescent secondary antibodies were used to visualize the bands. Arrows mark the HJV detected in the lysate. This experiment was repeated with similar results. B. The P258X- and Q289X-HJVs are retained in the ER. The constructs were transfected into HepG2 cells and then stained using rabbit anti-HJV (red) and mouse anti-KDEL (green) antibodies and corresponding fluorescent secondary antibodies, and imaged by confocal microscopy. A single section is shown for each image and the merged image is shown in the third panel.

The scale bar is shown in the bottom right hand corner. The images shown are representative of several captured images for each form of HJV.

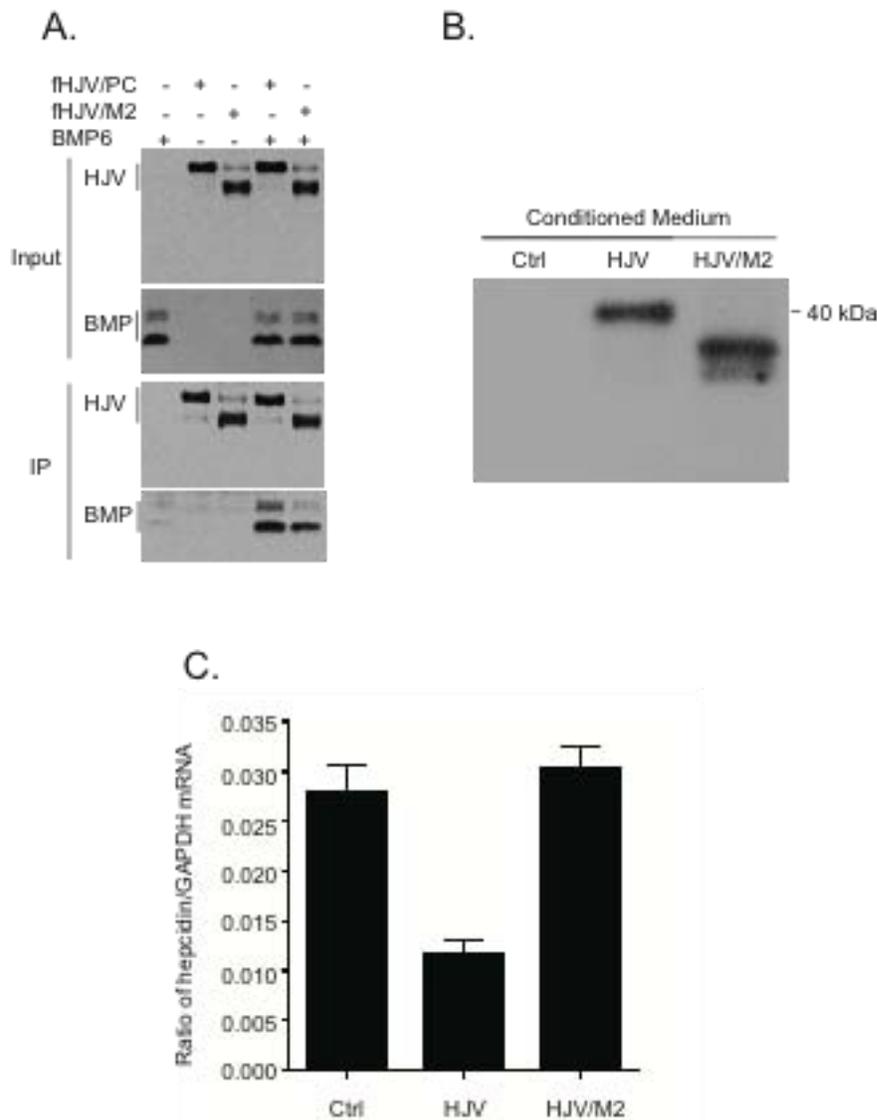


Figure 4.6. sHJV generated by proprotein convertase cleavage suppresses BMP6-induced hepcidin expression, but sHJV produced by matriptase-2 does not.

A. sHJV/BMP6 binding assay. BMP6 (500 ng) alone, fHJV/PC (500 ng) alone, fHJV/M2 (500 ng) alone, or BMP6 (500 ng) in combination with fHJV/PC (500 ng) or fHJV/M2 (500 ng) were incubated at 4°C overnight in 250 µl of 50 mM Tris-HCl, 150 mM NaCl, 0.2% Tween-20, pH 7.4. sHJV was pulled down with an anti-flag-M2 Affinity Gel (Sigma). sHJV and BMP6 in 2% of input, sHJV in 10% of eluate, and BMP6 in 90% of eluate were immunodetected using the corresponding antibodies. This experiment was performed three times with consistent results. B. Immunoblot analysis of sHJV in the concentrated conditioned medium from HEK293, HEK293-HJV and HEK293-HJV/matriptase-2 cells. 10 µl of the media described in C was subjected to SDS-PAGE, followed by immunodetection of HJV using

chemiluminescence. C. sHJV produced by matriptase-2 does not suppress BMP6-induced hepcidin expression in HepG2 cells. HepG2 cells were subcultured into 12-well plates. After 48 hours of culture, medium was switched to MEM/1% FBS and incubated for 6 hr to serum-starve the cells. The medium was then changed to MEM/1% FBS with 10% concentrated conditioned medium in volume from HEK293 (C), HEK293-HJV (HJV) and HEK293-HJV/matriptase-2 cells (HJV/M2), respectively, as well as 2.5 ng/ml BMP6. The estimated final concentrations of sHJV in HJV and HJV/M2 groups were about 2 µg/ml. After 18 hr of incubation, total RNA was isolated and cDNA was prepared for qRT-PCR analysis of hepcidin and GAPDH mRNA. The hepcidin mRNA levels are expressed as the amount relative to that of GAPDH in each specific sample. The results are from three separate experiments and the mean values and the standard deviation (SD) are presented.

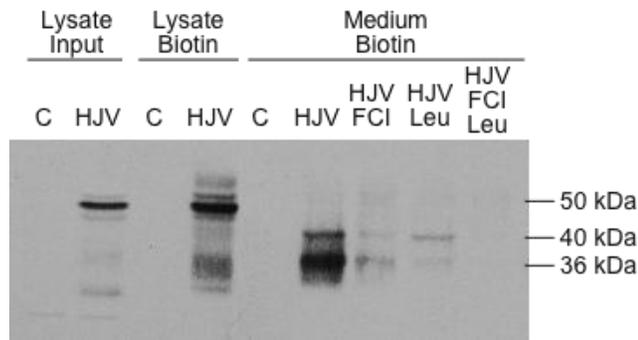
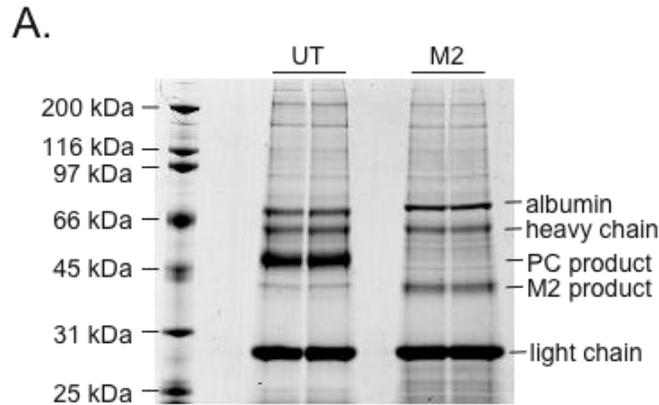


Figure S4.1: Leupeptin and furin convertase inhibitor block cell surface HJV from being secreted into the medium. Secretion of cell surface HJV was analyzed by biotinylation as described previously (Maxson et al., 2009). Briefly, cell surface proteins in both HJV-HepG2 (HJV) cells and pcDNA3-HepG2 cells (C) were biotinylated at 4°C. One set of cells was used to prepare cell lysates immediately after biotinylation for the detection of total biotinylated cell surface HJV (Lysate Biotin). The other set of cells were incubated at 37°C CO₂ incubator for 5 hours in the presence of furin convertase inhibitor (FCI, 5 μM), leupeptin (Leu, 100 μM), or both. The conditioned medium (CM) was then collected. The biotinylated proteins in both the cell lysates and the CM (Medium Biotin) were isolated using streptavidin agarose. The eluted proteins were separated by SDS-PAGE, transferred to nitrocellulose and immunodetected with anti-HJV and anti-rabbit horse-radish peroxidase. One tenth of the total lysate was run as a control (Lysate Input). FCI blocked secretion of the upper HJV band and to a lesser extent the lower HJV band from the cell surface while leupeptin reduced secretion of the lower band from the cell surface. The combination of the two inhibitors blocked the secretion of both bands. Thus, the cleavage of HJV on the cell surface is inhibited by either FCI or leupeptin. Calculated molecular weights based on standard molecular weight markers are shown. This immunoblot is representative of three separate experiments.



B.

MSALLILALVGAAVADYKDHDGGDYKDHDIDYKDDDDKLAAAHSQCKILRCNAEYVSSTLSL
RGGSSGALRGGGGGRGGVGSGLCRALRSYALCTRRTARTCRGDLAFHSAVHGIEDLMI
QHCSRQGPTAPPPRGPALPGAGSGLPAPDPCDYEGRFSRLHGRPPGFLHCASFGDPHVRS
FHHHFHTCRVQGAWPLLDNDFLFVQATSSPMALGANNATATRKLTIIFKNMQECIDQKVYQ
AEVDNLPVAFEDGSINGGDRPGSSLSIQTANPGNHVEIQAAYIGTTIIRQTAGQLSFSIKVAE
DVAMAFSAEQDLQLCVGGCPPSQRLSRSENR

Figure S4.2. Mass spectrometry analysis of sHJV. A. Flag-tagged human HJV in the p3XFlag-CMV-9 vector was stably transfected into HEK293 cells. Cells were either untransfected (UT) or transiently transfected with matriptase-2 (M2). The latter was treated with 5 μ M FCI. These cells secrete HJV in sufficient quantities to purify it for mass-spectroscopy using anti-flag affinity gel (Sigma). The immunoprecipitated protein was separated by SDS-PAGE and stained with Coomassie Blue-R250. Standard molecular weight markers are in the left lane and their molecular masses are denoted to the left of the blot. (A). HJV-HEK293 cells secrete a single form of HJV corresponding to the proprotein convertase cleavage product. When cells are transfected with matriptase-2 and treated with furin convertase inhibitor (FCI) they secrete a single, lower molecular weight product (matriptase-2 cleavage product). B. The proprotein convertase-cleaved product from untransfected flag-HJV HEK293 cells was excised from the gel above (A) and subjected to in-gel digestion with the proteases AspN, GluC or trypsin. The digested fragments were subjected to Tandem MS/MS Electrospray Ionization Mass-Spectrometry analysis. The regions of coverage from all digests combined are shown in yellow in (B). The combined coverage of flag-HJV not including the signal peptide (underlined) is 83%. We would not expect to get 100% coverage because some peptides produced by the digestion will be either too small or large to analyze, or contain N-linked glycosylation (blue) or other post-translational modifications that prevent their identification. There is no coverage in the region N-terminal to Arg 288 (red) with any of the three protease digestions. Therefore, mass-spectrometry cannot be used to confirm matriptase-2 cleavage at Arg 288.

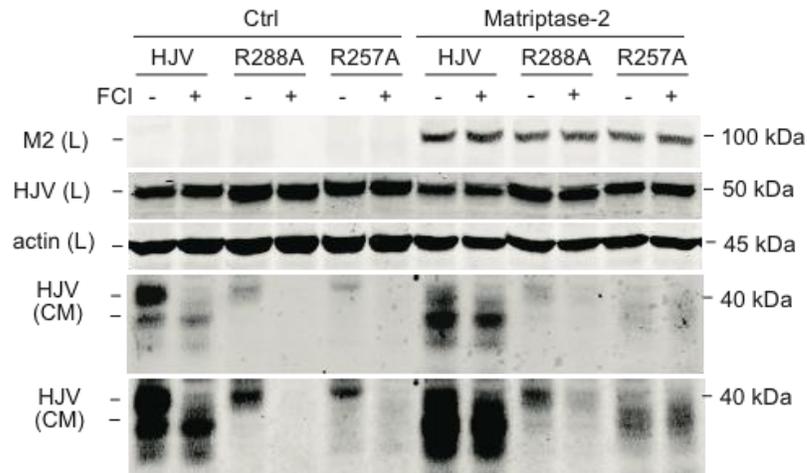


Figure S4.3. Mutation of Arg 288 reduces matriptase-2 mediated cleavage of HJV. HepG2 cells stably transfected with empty vector (ctrl) or matriptase-2 were subcultured into 12-well plates in MEM/10% FBS on day 1. On day 2, cells were transfected with pcDNA3-HJV (HJV), R257A HJV (R257A), or R288A HJV (R288A), using Lipofectamine 2000 reagent. About 24 hr after transfection (day 3), culture medium was changed to MEM/2% FBS with or without 5 μ M FCI. After 24 hr of incubation (day 4), conditioned medium (CM) was collected and cell lysate was prepared. The total lysate and 12% of CM and were subjected to SDS-PAGE, followed by immunodetection of matriptase-2 (M2), HJV and β -actin in the lysate (L) and HJV in CM. Calculated molecular masses are denoted to the right of the immunoblot. Chemiluminescence was used to visualize the bands.

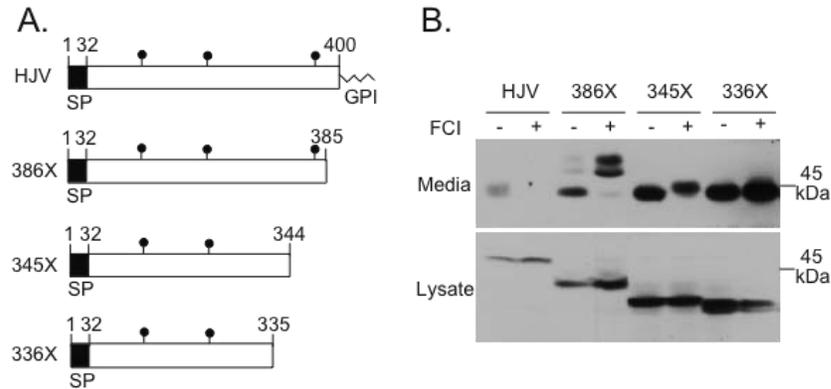


Figure S4.4: Truncation of HJV after the proprotein convertase cluster confirms the site of HJV cleavage. To confirm the mapping of the proprotein convertase cleavage motif by site directed mutagenesis we created truncated HJV constructs to compare to the size of HJV cleaved by furin (A). The 336X construct has a stop codon inserted after the cluster of three RXXR proprotein convertase cleavage motifs. The truncated constructs were all secreted by HEK293 cells (B). Upon addition of a FCI, GPI-anchored HJV was not secreted. The soluble products of the 386X and 345X constructs had a higher molecular weight in the presence of FCI, indicating that without the inhibitor they are further processed to a shorter form by proprotein convertases. In the presence of FCI, the 386X construct had two bands. This could arise from heterogeneity in glycosylation at N372, which not present in the smaller truncation mutants. The size of the HJV 336X construct does not shift detectably in the presence of FCI, indicating that the site of proprotein convertase is N-terminal to or very close to residue 336. The migration of actin (45 kDa) is marked to the right of the immunoblot.

Discussion

In the present study we show that matriptase-2 cleaves GPI-linked HJV in a site-specific manner and generates one major HJV cleavage product. Site-directed mutagenesis of HJV Arg 288 to Ala abolished cleavage by matriptase-2, indicating Arg 288 as the likely cleavage site. These results are in contrast to a previous study by Silvestri et al. showing that expression of matriptase-2 produces a ladder of cleaved HJV products in the conditioned medium (Silvestri et al., 2008b). This discrepancy might be due to the different cell types used or to the levels of matriptase-2 expressed.

We also show that expression of HJV increases the levels of matriptase-2. Matriptase-2 binds HJV (Silvestri et al., 2008b). Formation of a complex between HJV and matriptase-2 could stabilize matriptase-2 and reduce its degradation. The physiological implications of this observation are not known and need to be examined.

The proprotein convertase cleavage site in HJV does not overlap with that of matriptase-2. In addition to the different sizes of the two cleaved products, we found that the R332A mutation in HJV blocks proprotein convertase-mediated cleavage but not matriptase-2 cleavage. HJV has an overlapping cluster of three RXXR motifs, all of which are consensus sequences for proprotein convertase cleavage (Thomas, 2002). The R329A mutation in HJV, which is predicted to disrupt the first and second cleavage motifs, reduces proprotein convertase-mediated HJV cleavage, but does not abolish it, indicating that the third site is likely utilized to some extent. This also indicates that at least one of the first two sites is utilized. The R332A HJV mutation,

which is expected to abolish cleavage at the second and third site, diminishes proprotein convertase-mediated secretion. Therefore, the second and third sites are both capable of being cleaved by proprotein convertases. The third site has been shown previously to contribute to proprotein convertase-mediated cleavage of HJV by mutational analysis (Silvestri et al., 2008a) and by N-terminal protein sequencing of the proprotein convertase products of a HJV-alkaline phosphatase fusion construct (Lin et al., 2008). These data extend our understanding of the ability of proprotein convertases to cleave HJV at multiple consensus motifs.

Notably, the matriptase-2 HJV cleavage product decreases when proprotein convertase cleavage is inhibited by FCI or mutation of the R332A cleavage site. The degree to which blocking proprotein convertase-mediated cleavage of HJV reduces matriptase-2 cleavage is somewhat variable from experiment to experiment. Several possibilities could explain this effect. Proprotein convertase-mediated cleavage could promote subsequent matriptase-2 cleavage. Alternately, matriptase-2 cleavage could occur with or without prior proprotein convertase cleavage. In the absence of cleavage by proprotein convertases, matriptase-2 cleavage may occur at multiple sites and results in smaller cleavage products that are not detected by immunoblot analysis. Further experiments are needed to examine the order of HJV cleavage by both proprotein convertases and matriptase-2 with respect to HJV trafficking and regulation by iron.

The liver is the major organ that expresses both HJV and matriptase-2, and we found that HepG2 cells endogenously express matriptase-2 mRNA. Importantly, the ratio of matriptase-2 mRNA to that of one proprotein convertase, furin, in HepG2

cells is similar to the ratios in the liver, and in isolated primary hepatocytes. HepG2 cells are therefore a good model cell line to study the cleavage of HJV by matriptase-2.

Previous studies detected two major soluble HJV products in the conditioned medium of HepG2 cells that express HJV (Maxson et al., 2009; Zhang et al., 2007; Zhang et al., 2008). Here we show that they are the cleavage products of matriptase-2 and proprotein convertases. Expression of the proprotein convertase, furin, is ubiquitously detected in all tissues as well as in HepG2 cells. Other proprotein convertases are also expressed in the liver (Seidah et al., 2008). Our experiments do not differentiate between the different possible proprotein convertases that could be involved in HJV processing.

The role of sHJV generated by matriptase-2 cleavage in the regulation of BMP6-induced hepcidin expression was analyzed. The sHJV generated by proprotein convertase cleavage binds to BMPs, which may sequester BMPs away from membrane anchored HJV and BMP receptors to reduce signaling (Babitt et al., 2007; Lin et al., 2005; Lin et al., 2007; Yang et al., 2008). Here we show that in contrast to the proprotein convertase cleavage product, the smaller matriptase-2-generated sHJV has reduced binding to BMP6 and was unable to antagonize BMP6-induced hepcidin transcript levels in HepG2 cells. Previous studies have shown that cellular HJV is essential for the induction of hepcidin expression (Babitt et al., 2006; Huang et al., 2005; Lin et al., 2005; Niederkofler et al., 2005; Papanikolaou et al., 2004), and that matriptase-2 reduces the amount of cell surface HJV and suppresses HJV-induced hepcidin expression (Silvestri et al., 2008b). These results, in conjunction

with our data, support a model in which matriptase-2 suppresses hepcidin expression by cleaving cellular HJV to produce a form of HJV with reduced affinity for BMPs. This study shows that endogenously expressed matriptase-2 cleaves HJV in a site-specific manner, strengthening the link between matriptase-2 and the regulation of hepcidin expression.

Acknowledgements

We thank Jodie Babitt (Harvard, Boston Massachusetts) for generously giving us HJV-p3XFlag-CMV-9 vector, Fan Yang (Caltech, Pasadena California) for providing us with the purified protein used to generate the rabbit anti-matriptase-2 antibody, Stefanie Kaech Petrie in the Advanced Light Microscopy Core at the Jungers Center for Neurosciences Research at OHSU for microscopy assistance, Larry David at the mass-spectrometry core at OHSU for providing mass-spectrometry analysis, the Oregon Stem Cell Flow Cytometry Core for flow cytometry resources, and Junwei Gao, Kristina DeMaster, and Maria Chloupkova for critical reading of this manuscript and helpful comments. This work was supported by National Institutes of Health Grants DK080765 to ASZ and DK72166 to CAE. JEM was partially supported by a National Institutes of Health Grant T32 HD049309, by a scholarship from Vertex Pharmaceuticals, and by an American Heart Association pre-doctoral fellowship 10PRE3530017.

CHAPTER 5
CONCLUSIONS AND FUTURE DIRECTIONS

HJV undergoes retrograde trafficking to the Golgi prior to being cleaved by furin and secreted.

While HJV is clearly a critical regulator of iron homeostasis, little was previously known about its trafficking and processing. HJV is cleaved by the furin family of proprotein convertases, and this cleavage produces a soluble form of HJV that antagonizes BMP signaling to reduce hepcidin expression. Chapter 2 of this thesis investigates the maturation and cleavage of HJV and uncovers an interesting mechanism of HJV trafficking. HJV has a relatively short half-life of approximately one hour (Figure 2.1). The disappearance of HJV from the lysate correlates with the appearance of shed HJV in the medium (Figure 2.1). To follow the progression of HJV through the secretory pathway, we analyzed the N-linked glycosylation of HJV. N-linked glycosylation is added co-translationally in the ER. Initially this glycosylation is a high-mannose form. As the proteins traffic through the Golgi, the high mannose oligosaccharides are modified to a complex form (Figure 5.1). We analyzed the N-linked glycosylation of HJV by digesting it with Endo H, an enzyme that cleaves high-mannose but not complex oligosaccharides. HJV retains high-mannose oligosaccharides in the cell for at least three hours (Figure 2.2). Since this interval is within the time period when a protein could reach the cell surface, we analyzed HJV on the cell surface, and have shown that HJV retains high-mannose oligosaccharides. Surprisingly, despite the fact that HJV retains high-mannose oligosaccharides in the cell lysate, it has complex oligosaccharides when secreted (Figure 2.3). Furthermore, we have shown that Endo H-sensitive HJV on the cell surface can subsequently be secreted as an Endo H-resistant form (Figure 2.3),

leading us to propose the following model for the trafficking and shedding of HJV (Figure 5.2). HJV traffics to the cell surface in a conformation that is unable to obtain complex oligosaccharides or be cleaved by furin. On the cell surface, it is capable of participating in BMP signaling. HJV then undergoes retrograde trafficking to the Golgi, where it undergoes oligosaccharide processing and cleavage by furin, prior to being secreted. Trafficking of HJV to the cell surface prior to being cleaved would not only allow HJV to act as a BMP co-receptor on the cell surface, but may also provide an avenue for regulation of HJV cleavage by iron-bound Tf. The mechanism by which Tf regulates HJV secretion is still unclear and is an important avenue of future research.

The role of the GPI-anchor of HJV in the processing and signaling of HJV.

HJV endocytoses through a clathrin- and dynamin-independent pathway characteristic of GPI-linked proteins. Since HJV endocytoses prior to being cleaved and shed, we reasoned that the GPI-anchor of HJV might affect its secretion. In Chapter 3, I analyzed the role of the GPI-anchor of HJV in its trafficking and cleavage by creating chimeric HJV constructs with the transmembrane and cytoplasmic domains of furin or LDLR (Figure 3.1). I have shown that the transmembrane domain of HJV is not required for proper glycosylation of HJV or for cleavage. Interestingly, there was a reduction of HJV secretion when HJV has a furin transmembrane domain instead of a GPI-anchor (Figure 3.2). This chimeric construct has similar subcellular localization to furin, as shown by immunofluorescence microscopy. Furin is primarily localized to the TGN, but also

cycles to the cell surface. It is possible that the HJV/furin chimera therefore has reduced trafficking to the cell surface, and since HJV undergoes retrograde trafficking from the cell surface to the Golgi prior to being secreted, this would reduce its secretion (Figure 5.3). While GPI linkage of HJV is not required for secretion, it is important for signaling of HJV (Figure 3.4). The chimeric forms of HJV are not able to upregulate hepcidin expression as is seen for GPI-HJV. The mechanism by which the GPI linkage of HJV potentiates signaling is not known and will be the subject of future research. The GPI anchor possibly increases the proximity of HJV to BMP co-receptors by localizing it to a specific membrane domain. Alternately, the GPI anchor could alter the conformation or flexibility of HJV and therefore increase HJV's ability to potentiate signaling. Although HJV has been shown to bind to BMP ligands, the exact mechanism by which HJV potentiates BMP signaling is not known. BMP receptors are capable of binding to BMP ligands and signaling to upregulate hepcidin expression in the absence of HJV. Binding of HJV to BMP ligands could increase the proximity of BMP ligands to their receptors, thereby increasing the effective concentration of BMPs and enhancing signaling. Elucidating the mechanism by which HJV potentiates BMP signaling will be an important next step in understanding the regulation of iron metabolism by HJV.

Site-specific cleavage of HJV by matriptase-2

HJV is capable of being cleaved by furin family members, as well as by matriptase-2 (Lin et al., 2008; Silvestri et al., 2008a; Silvestri et al., 2008b). I have shown that HJV is cleaved by matriptase-2 to produce a product that is smaller than that produced

by furin cleavage, and I have identified the predominant site of cleavage to be Arg 288 (Figure 4.4). HEK293 cells do not express detectable amounts of matriptase-2, consistent with detection of only the furin cleavage product of HJV in the medium (Figure 4.1). Interesting, while the furin cleavage product is capable of reducing hepcidin expression when added back to cells, the matriptase-2 cleavage product does not alter hepcidin production. This result may be caused by reduced binding of the matriptase-2 cleavage product to BMP ligands or by a lack of interaction of HJV with BMP receptors (Figure 4.6). This observation leads me to propose a model in which the furin derived cleavage product reduces hepcidin expression by binding to available BMPs and blocking their interaction with membrane-anchored HJV. In contrast, the cleavage of HJV by matriptase-2 reduces the amount of cell surface HJV available for signaling (Figure 5.4).

I have shown that the second and third furin motifs in HJV are utilized. Mutation of Arg 332 abolishes furin-mediated cleavage of HJV (Figure 4.3). Additionally, I have shown that Arg 288 is the predominant site of matriptase-2 cleavage (Figure 4.4). Mapping of these sites will allow our group to test the importance of these cleavages *in vivo*. HJV is primarily expressed in liver and muscle. While furin is expressed in both liver and muscle, expression of matriptase-2 is restricted to the liver. Since furin and matriptase-2 have different expression patterns *in vivo*, they may be regulated differently to limit BMP6 signaling under normal conditions and also to regulate HJV cleavage in response to changes in iron status.

I hypothesize that in response to low iron, HJV is cleaved by furin in the muscle to provide a source of sHJV in the blood that travels to the liver, actin to down-regulate hepcidin expression in the liver. To test this model, WT HJV or HJV with a mutation that blocks furin cleavage under a muscle-specific promoter in an AAV 2/8 vector will be injected into WT mice. I have cloned flag-tagged mouse HJV into a pAAV2/8-MHCK-pA viral vector that has a muscle-specific MHCK7 regulatory cassette (hybrid α -myosin heavy chain enhancer/MCK promoter-enhancer) (Sun et al., 2005). Additionally, I have made another construct with a mutation in the furin cleavage site. To determine if serum sHJV can be derived from muscle HJV, an immunoblot analysis will be performed on the serum using the anti-flag antibody. To analyze the contribution of muscle HJV to the regulation of hepcidin expression, mRNA levels in the isolated liver tissues will be measured using qRT-PCR. If muscle serves as a source of sHJV to down-regulate hepcidin expression in the liver, then it would be expected that an increase in muscle HJV expression would down-regulate hepcidin expression in the liver, thereby increasing serum Tf saturation. If the secreted form of muscle HJV is required for this effect, then disruption of furin cleavage would be expected to abolish its signaling, because matriptase-2 is not expressed in the muscle.

Matriptase-2 and furin are both expressed in the liver and may both contribute to cleavage of HJV *in vivo*. To test the relative importance of the HJV cleavage sites in the down-regulation of hepcidin expression *in vivo*, HJV knockout mice will be injected with either AAV 2/8 virus expressing WT HJV or HJV with mutations in either the furin or matriptase-2 cleavage sites under the control of the

liver-specific promoter. The hepatocyte-specific AAV-HJV virus fully restores expression of hepcidin in the liver of HJV KO mice (Zhang et al., 2010). If matriptase-2 and furin cleavage are both important for negatively regulating the levels of hepcidin in the liver, then the AAV-R332A-HJV and AAV-M2 site mutant-HJV viruses should produce a greater induction of hepcidin expression than AAV-HJV, eventually leading to anemia as in the matriptase-2 mutant mouse. These studies will provide insight into the importance of these proteases in iron homeostasis by regulating HJV cleavage. Importantly these studies will determine whether the role of HJV in cardiac and skeletal muscle is to provide a source of soluble HJV to down regulate hepcidin expression in response to low iron.

This thesis provides insight into the signaling, trafficking and processing of HJV. The critical questions that need to be addressed in the future are the role of Tf and neogenin in the regulation of HJV cleavage, the mechanism by which HJV potentiates BMP signaling, and the relative contribution of furin and matriptase-2 to the cleavage of liver and muscle derived HJV *in vivo*.

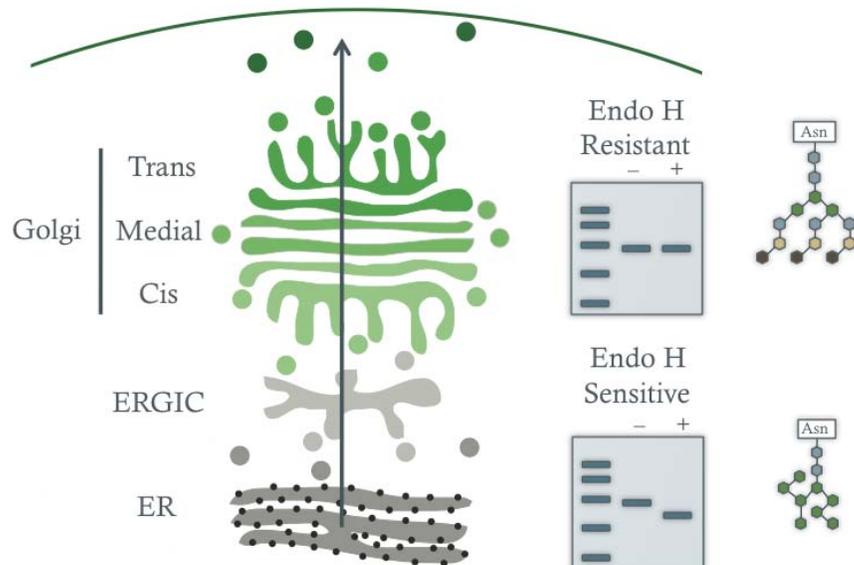


Figure 5.1. Glycosylation of proteins in the secretory pathway.

Membrane-anchored proteins are initially in a high mannose form that is Endo H sensitive in the ER. The shift in molecular weight when the high mannose N-linked oligosaccharides are removed by Endo H can be visualized by western analysis. As these proteins progress through the Golgi, high mannose oligosaccharides are removed and complex oligosaccharides are added, which are resistant to Endo H. Analysis by Endo H digestion can therefore be used to follow the progression of proteins through the secretory pathway.

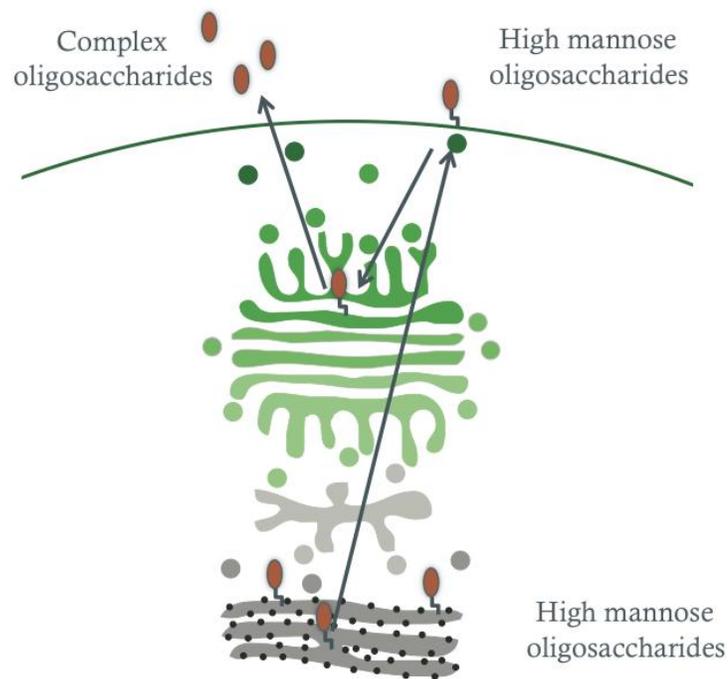


Figure 5.2. HJV undergoes retrograde trafficking to the Golgi prior to being secreted.

HJV initially has high mannose oligosaccharides in the ER. Unlike many other membrane anchored-proteins, it traffics to the cell surface while maintaining high mannose oligosaccharides. It then undergoes retrograde trafficking to the Golgi where it can be cleaved by furin and obtain complex oligosaccharides prior to being secreted.

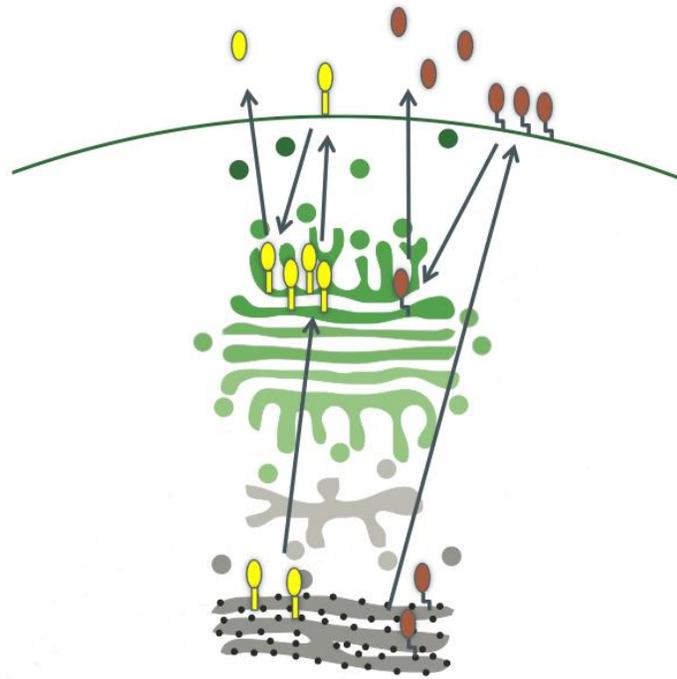


Figure 5.3. Model of trafficking and secretion of the HJV/furin chimera. The HJV/furin chimera (yellow) has reduced secretion when compared to GPI-HJV (brown). Like furin, the HJV/furin chimera is primarily localized to the TGN, but a small portion also cycles to the cell surface. Since trafficking to the cell surface precedes cleavage, there is reduced secretion of the HJV/furin chimera compared to GPI-HJV despite increased co-localization with furin.

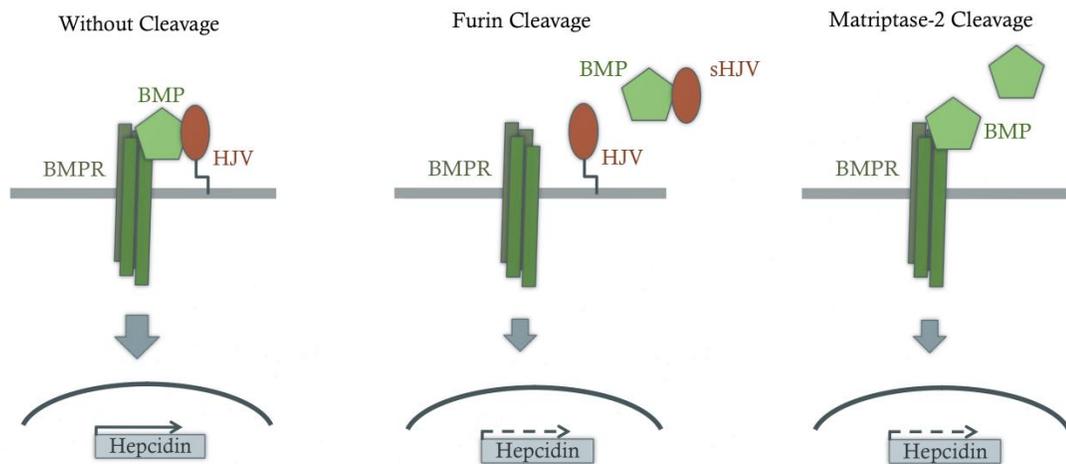


Figure 5.4. Model of inhibition of BMP signaling by furin and matriptase-2 cleavage of HJV.

Cleavage of HJV by furin (middle panel) creates a soluble form of HJV (sHJV) that is capable of binding to BMPs and reducing their interaction with membrane HJV and the BMP receptor complex. In contrast, cleavage of HJV by matriptase-2 (right panel) reduces the amount of membrane HJV available to participate in BMP signaling.

APPENDIX A

The cytoplasmic domain of neogenin promotes hemojuvelin secretion

RATIONALE

Previous studies indicated that HJV binds to neogenin, a transmembrane protein. The role of neogenin in iron homeostasis remains controversial. Our previous studies indicated that neogenin facilitates the cleavage and shedding of HJV. However, a recent paper showed that transient transfection of neogenin and HJV decreases HJV shedding, and increases the stability of the membrane-associated HJV (Lee et al., 2010). We therefore wanted to reexamine the role of neogenin in HJV shedding. HJV is a GPI-linked protein that undergoes endocytosis prior to cleavage and shedding (Maxson et al., 2009). Neogenin is a single pass transmembrane protein with a large cytoplasmic domain. We therefore wondered if the cytoplasmic domain of neogenin might direct trafficking and cleavage of HJV.

METHODS

HJV and neogenin containing pCDNA3 vectors were used as described previously (Zhang et al., 2005). A truncated neogenin construct was made by placing a stop codon in the cytoplasmic domain proximal to the transmembrane domain at amino acid Q1135 using the QuikChange Site Directed Mutagenesis Kit (Stratagene, Santa Clara, CA) with the following primers 5'-CGTCGTACCACCTCTCACTAGAAAAAGAAACGAGCTG-3' and 5'-CAGCTCGTTTCTTTTCTAGTGAGAGGTGGTACGACG3'.

HEK293 cells stably transfected with pCDNA3 empty vector (control), pCDNA3-HJV, or co-transfected with both HJV and neogenin (HJV/neogenin) were generated previously. HEK293 cells stably expressing both HJV and truncated

neogenin with no cytoplasmic domain (truncated neogenin) were established by co-transfecting pcDNA3-HJV and pcDNA3-truncated neogenin plasmid DNA using Lipofectamine 2000 (Invitrogen). Generation of HepG2 cells stably expressing HJV (HepG2-HJV) was reported previously (Zhang et al., 2007).

RESULTS AND CONCLUSIONS

The cytoplasmic domain of neogenin is important for secretion of HJV from HEK293 cells. HEK293 cells are an easy to transfect kidney derived cell line that expresses low levels of endogenous neogenin. Stable cell lines were generated expressing neogenin and HJV. Stably transfected cell lines were used, because transient co-transfection of neogenin and HJV reduced the level of HJV expression in the lysate and the media (Figure A2 A), possibly due to competition of the two plasmids for the cellular protein synthesis machinery. This effect of co-transfection may explain the effect of neogenin on HJV secretion seen in the Lee et al. study. We compared the amount of HJV in the conditioned medium from HEK293 cells stably expressing HJV alone with those from HEK293 cells stably expressing both HJV and neogenin. Co-expression of neogenin with HJV increased the secretion of HJV relative to HJV alone (Figure A2 B). Interestingly, co-expression of HJV with a truncated form of neogenin lacking the cytoplasmic domain decreased secretion of HJV relative to full-length neogenin (Figure A2 B). The remaining secretion of HJV in the cells expressing truncated neogenin may be due to the presence of endogenous full-length neogenin. This data indicates that the secretion of HJV is dependent on the cytoplasmic domain of neogenin.

Together, our results support a model whereby cellular HJV release requires its interaction with full-length neogenin and that the cytoplasmic domain of neogenin plays a role in the release of HJV.

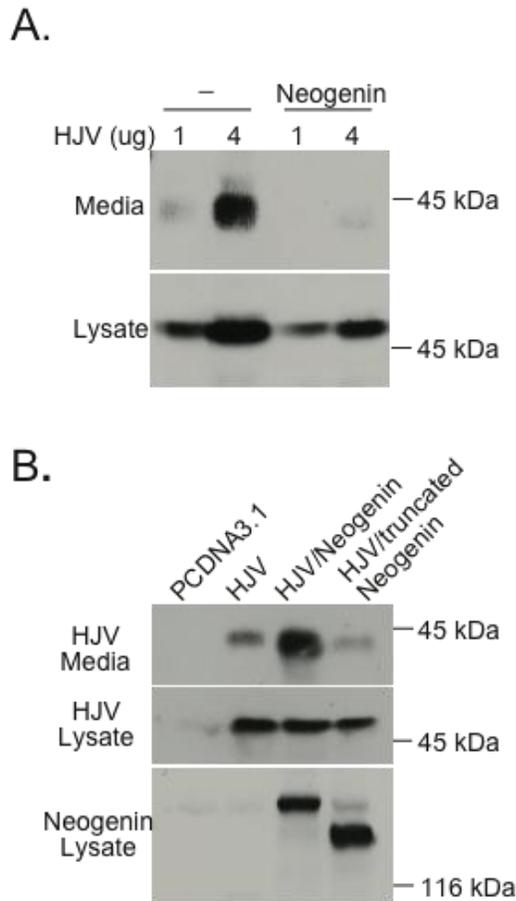


Figure A2. Cellular HJV release requires full-length neogenin.

A. Transient co-transfection of neogenin with HJV reduces the amount of HJV expressed by the cell. HEK293 cells were transfected with 1 or 4 μ g of HJV plasmid in the presence or absence of neogenin expression plasmid. B. The neogenin cytoplasmic domain is important for HJV secretion. HEK293 cells stably expressing HJV, HJV and neogenin, or HJV and truncated neogenin lacking the cytoplasmic domain were generated. Neogenin and HJV levels were detected in the lysate and HJV was detected in the media by immunoblot. All experiments were repeated with similar results.

APPENDIX B

Truncated HJV constructs have similar glycosylation profiles to WT HJV, but are secreted more rapidly from the cell

RATIONALE

We have shown previously that HJV constructs lacking a membrane anchor are cleaved by furin and also secreted in the absence of furin activity. We therefore wanted to analyze whether truncated forms of HJV have similar glycosylation profiles to WT HJV. Like WT HJV, truncated HJV (without a membrane anchor) was Endo H sensitive in the cell lysate and Endo H resistant in the medium. This indicates that truncated HJV has high-mannose glycosylation in the cell lysate and complex glycosylation when secreted into the medium.

METHODS

A stop codon was added in the coding region of HJV at amino acid 345 to create a soluble form of HJV that is not membrane tethered as described in Chapter 4. Endo H and PNGase F digestion, western analysis and pulse chase analysis were performed as described previously (Maxson et al., 2009).

RESULTS AND CONCLUSIONS

Removal of the membrane tether does not change the Endo H sensitivity of HJV in the lysate or the Endo H resistance of HJV in the media (Figure A3 A). These constructs were shown to be glycosylated by PNGase F digestion, which removes both high mannose and complex glycosylation. Removal of the membrane anchor of HJV did not alter glycosylation or cleavage of HJV by furin (Chapter 4), but it may change the kinetics of HJV secretion. To test this possibility, we analyzed the pool of nascently synthesized sHJV by pulse-chase analysis of the HJV 345X construct

(Figure A3 B). The HJV 345X construct disappeared more rapidly from the cell lysate, compared to WT HJV, which may indicate that it is rapidly secreted from cells. In summary, membrane anchoring of HJV is not required for HJV processing and cleavage but it does affect the rate of secretion. HJV 345X may be cleaved during the biosynthetic pathway because unlike GPI-HJV, it is conformationally accessible to proteases. Alternately, after being secreted it may bind to another protein on the cell surface and undergo retrograde trafficking prior to cleavage.

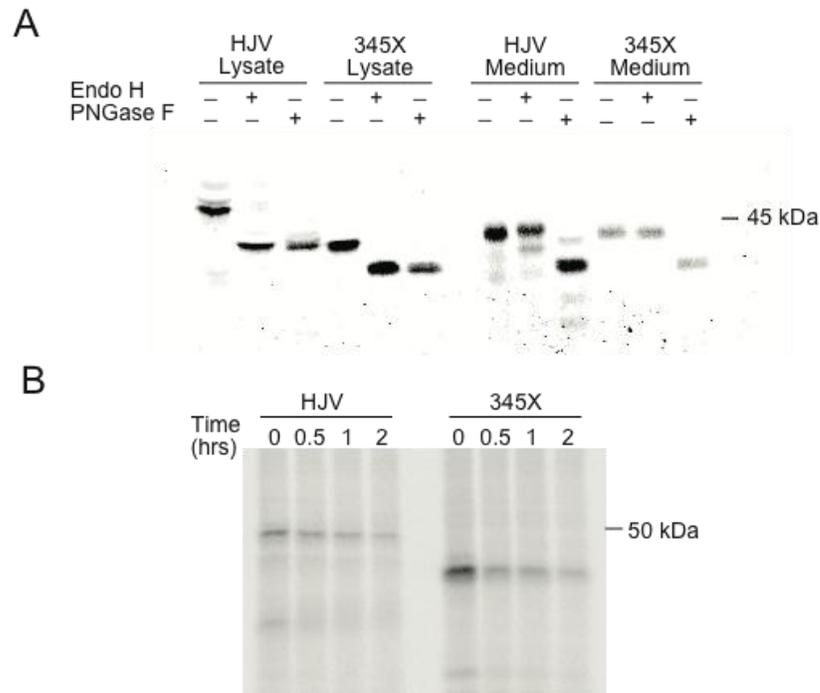


Figure A3. HJV constructs lacking a membrane anchor have a similar glycosylation profile to WT HJV, but are secreted more rapidly. (A) Endo H and PNGase F digest of the WT HJV and HJV 345X constructs. Constructs were transiently transfected into HEK293 cells and media and lysate were digested and analyzed by immunoblot. (B) Pulse-chase of WT HJV and HJV 345X. Constructs were transiently transfected into HEK293 cells and a pulse-chase analysis was performed. Cells in 35 mm dishes were labeled in 1 mL met/cys-free media with 100 μ Ci 35 S-(met/cys) for 30 minutes. Cells were then washed and incubated in unlabeled medium for 0, 0.5 1 and 2 hours. Immunoprecipitations were performed using 2 μ L rabbit anti-HJV antibody, 18745 (generated against residues 1-401 of HJV as described previously) (Zhang et al., 2008). Immunoprecipitated proteins were separated by SDS-PAGE, followed by soaking of the gel in Amplify (GE Healthcare, Chalfont St. Giles, United Kingdom) and drying of the gels prior to exposure to film.

APPENDIX C

BMP signaling induces tyrosine phosphorylation, but treatment with Dasatinib does not effect hepcidin expression.

RATIONALE

Neogenin has multiple tyrosines in its cytoplasmic domain. Tyrosine phosphorylation of a related receptor, DCC, is important for its function in neuron outgrowth and guidance (Li et al., 2004). DCC is phosphorylated on its cytoplasmic domain by the tyrosine kinases Src and focal adhesion kinase (FAK). Mutation of these tyrosine residues abolished the function of DCC (Li et al., 2004). We therefore investigated the role of tyrosine phosphorylation in the potentiation of BMP signaling by neogenin.

METHODS

To measure tyrosine phosphorylation in response to BMP4, tTA-HJV HepG2 cells were incubated in MEM with 1% FBS for 6 hours and then treated with doxycycline (2 μ g/mL), BMP4 (10 ng/mL) and/or dasatinib (100 nM, a gift from Brian Druker's lab) for 16 hours. Cells were lysed in the presence of the phosphatase inhibitors sodium orthovanadate (1 mM), sodium fluoride (50 mM) and beta glycerolphosphate (50 mM) to prevent dephosphorylation after cell lysis. Tyrosine phosphorylation was detected by immunoblotting using a mouse anti-phosphotyrosine antibody (1:2000, a gift from Brian Druker's Lab) and an Alexa Fluor 800 goat anti mouse antibody (1:1000, Invitrogen). The levels of hepcidin mRNA relative to GAPDH were measured by qRT-PCR as described previously (Zhang et al., 2009).

RESULTS AND CONCLUSIONS

Treatment of tTA-HJV HepG2 cells with BMP4 induces tyrosine phosphorylation.

This phosphorylation is inhibited by treatment with the Src/Abl tyrosine kinase inhibitor dasatinib. Despite this induction of tyrosine phosphorylation, treatment of cells with dasatinib has no effect on hepcidin expression in the presence or absence of BMP4 treatment. While tyrosine phosphorylation may mediated other effects downstream of BMP signaling, it does not appear to be involved in the transcriptional activation of hepcidin.

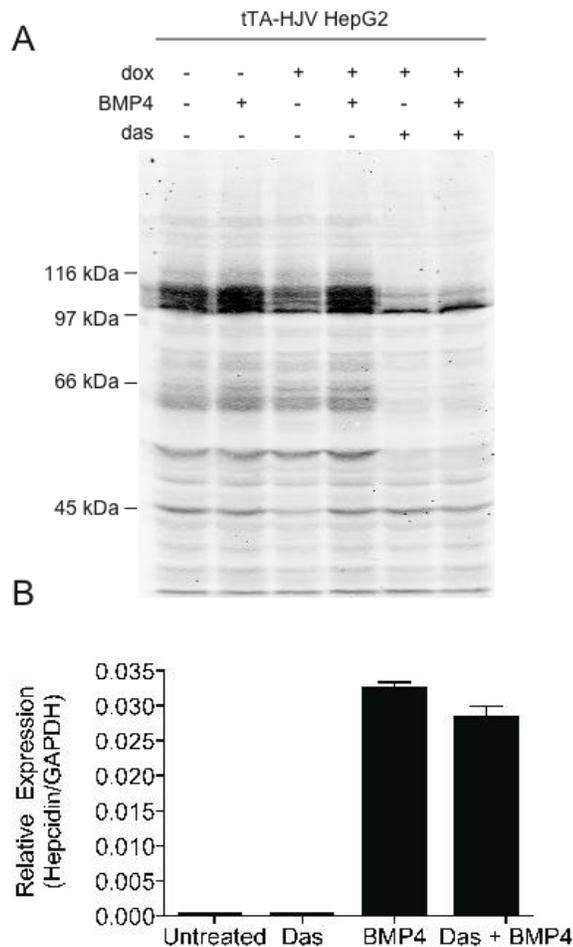


Figure A4. BMP signaling induces tyrosine phosphorylation, but treatment with Dasatinib does effect hepcidin expression.

(A) Treatment of cells with BMP4 induces tyrosine phosphorylation. tTA-HJV HepG2 cells were induced to express HJV using doxycycline (dox), treated with BMP4 and/or dasatinib (das). Levels of tyrosine phosphorylation were measured by immunoblotting. (B) The levels of hepcidin expression relative to GAPDH were measured by qRT-PCR in cells treated with BMP4 and/or dasatinib.

APPENDIX D

The ectodomain of neogenin is shed by proteolytic cleavage

RATIONALE

Neogenin has been proposed to undergo sequential alpha-secretase and gamma-secretase cleavages resulting in the release of an extracellular fragment and an intracellular fragment (Goldschneider et al., 2008). In this previous study, the intracellular fragment was detected using a tag on the cytoplasmic domain, but the presence of the extracellular domain was not assayed for (Goldschneider et al., 2008). We therefore assessed whether the neogenin extracellular domain was shed into the conditioned medium of cells using an antibody that recognizes the neogenin extracellular domain.

METHODS

Conditioned medium and cell lysate were collected from HEK293 cells stably expressing HJV, HJV and neogenin or a truncated form of neogenin lacking the cytoplasmic domain (see Appendix B). Neogenin was detected using a polyclonal rabbit anti-neogenin antibody generated against a portion of the neogenin ectodomain (21567, 1:1000). To assess whether shedding of the neogenin ectodomain was inhibited by a matrix metalloproteinase inhibitor, HJV/neogenin HEK293 cells were treated with 25 or 100 μ M TAPI-2 (using a 25 mM stock made in DMSO). A corresponding volume of DMSO (1 or 4 μ L) was used as a control.

RESULTS AND CONCLUSIONS

The ectodomain of neogenin is shed into the conditioned medium of HEK293 cells (Figure A5 A). A shed fragment was seen in the medium of HJV/neogenin HEK293 cells or HJV/truncated neogenin HEK293 cells, but not in control HEK293 cells or HEK293 cells expressing HJV alone. Interestingly, the shed fragment produced in cells expressing full-length neogenin or truncated neogenin (lacking a cytoplasmic domain) is the same size, indicating that the secreted product likely results from cleavage within the extracellular domain. Shedding of the HJV ectodomain was inhibited by the matrix metalloproteinase inhibitor, TAPI-2, which is know to inhibit alpha secretase cleavage. This indicates that the neogenin ectodomain may be cleaved by alpha secretase or a related protease. TAPI-2 does not alter hepcidin mRNA levels in tTA Neogenin HepG2 cells (data not shown), which indicates that this cleavage event may not be relevant to the regulation of hepcidin expression.

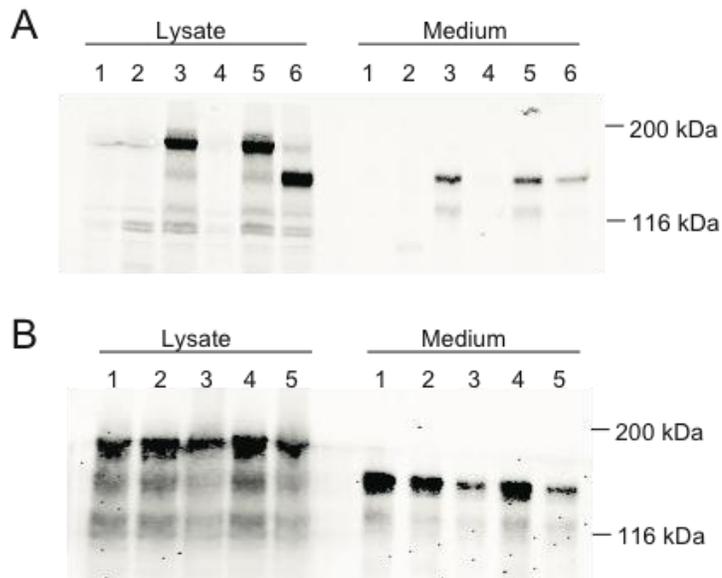


Figure A5. Shedding of neogenin into the conditioned medium is blocked by TAPI-2.

(A) Neogenin is shed from HEK293 cells. Neogenin was detected in the lysate and conditioned medium by immunoblotting. 1. HEK293 cells, 2. HJV HEK293 cells, 3. HJV/neogenin HEK293 cells, 4. HEK293 cells, 5. HJV/neogenin HEK293 cells, 6. HJV/truncated neogenin HEK293 cells. (B) TAPI-2 blocks the shedding of neogenin from HJV/neogenin HEK293 cells. Immunoblot analysis of neogenin in the cell lysate and conditioned medium. 1. untreated control, 2. DMSO control (1 μ L), 3. 25uM TAPI (1 μ L), 4. DMSO control (4 μ L), 5. 100uM TAPI (4 μ L).

APPENDIX E

Generation of flag-tagged mouse HJV constructs with mutations in the furin and matriptase-2 cleavage sites.

RATIONALE

In the liver-derived HepG2 cells there are two HJV products produced by furin and matriptase-2 cleavage. The relative role of these proteases in the regulation of HJV and hepcidin expression *in vivo* is not known. To test this, mouse HJV (Rgmc) constructs were created with Arg to Ala mutations in the residues corresponding to the cleavage sites in human HJV, which will ultimately be introduced into mice. Additionally, these constructs were flag-tagged to aid in detection *in vivo*.

METHODS

Human HJV was cut out of 3XFlag-hHJV p3XFlag-CMV-9 at XbaI/NotI sites. Rgmc PGMT was used to amplify Rgmc coding sequence minus the leader sequence with XbaI and NotI cut sites on primers: 5'-GCGGCCGCTCACTCCCAGTGCAAG-3' 5'-TCTAGACTACTTACTGAAGCAAAGCCACAGAAC-3'. The PCR product was cut and ligated into XbaI/NotI sites. Arg to Ala mutations were made at residues 281 and 325 of Rgmc, which corresponded to matriptase-2 and furin cleavage sites in human HJV when the sequences were aligned using the following primers: Rgmc R281A F 5'-ctacattggaacaactatcatcattgcacagacagctggg-3' and Rgmc R281A R 5'-ccagctgtctgtgcaatgatgatagttgttccaatgtag-3' or Rgmc R325A F 5'-ctctcgtctcagaggccaaccgctggg-3' and Rgmc R325A R 5'-cccacggcggttgccctctgagcgagag-3'. The expression of these constructs was tested by transient transfection of HEK293 or HepG2 cells using lipofectamine 2000 (Invitrogen) or PolyJet (SignaGen Laboratories) respectively.

RESULTS AND CONCLUSIONS

The flag-tagged Rgmc constructs express in HEK293 cells. It appears that the ratio of HJV in the media to the lysate is somewhat higher than flag-tagged human HJV, indicating that they are efficiently processed. The R325A mutation abolishes furin-mediated cleavage in HEK293 cells. These cells do not express matriptase-2, so the R281A mutation does not affect cleavage in these cells. In HepG2 cells, which express both furin and matriptase-2, the lower matriptase-2 cleavage product is reduced by the R281A mutation. Unlike HEK293 cells, the R325A mutation reduces but does not abolish the upper furin-mediated cleavage product in these cells. Thus in HepG2 cells, proprotein convertases are able to cleave at multiple sites within the furin cleavage cluster. These data indicate that the furin and matriptase-2 cleavage sites are conserved between human and mouse HJV. They also indicate that matriptase-2 cleavage does not require prior cleavage by furin.

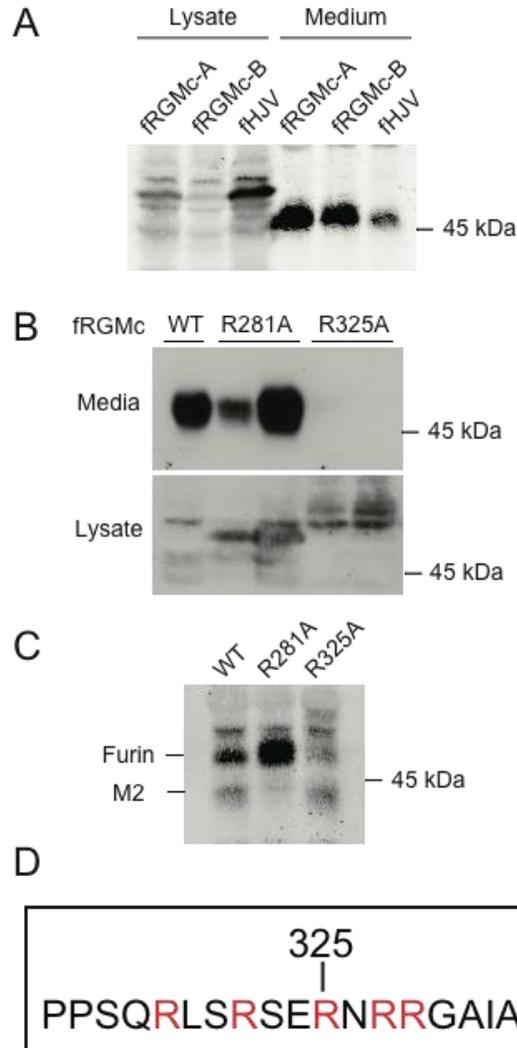


Figure A6. Generation of flag-tagged mouse HJV (fRgmc) constructs with mutations in the furin and matriptase-2 cleavage sites. (A) The flag-tagged Rgmc (fRgmc-A and B) constructs express and are secreted when transiently transfected into HEK293 cells. These two constructs are from two separate bacterial clones. HJV was detected in the lysate and the medium by immunoblot analysis using a rabbit-anti HJV antibody (18475, affinity purified, 0.22 μ g/ml). Flag-tagged human HJV (fHJV) serves as a positive control. These constructs are also detected using the M2 mouse anti-flag antibody (data not shown). (B) The R325A construct is not secreted from HEK293 cells. Cells were transiently transfected with the indicated flag-tagged Rgmc constructs. HJV was analyzed in the medium and lysate by immunoblot. (C) In HepG2 cells the R281A mutation reduces matriptase-2 cleavage and R325A mutation reduces the furin cleavage product. Flag-tagged Rgmc constructs were transiently transfected into HepG2 cells and the presence of HJV cleavage products was analyzed in the conditioned medium by immunoblot. The furin and matriptase-2 (M2) cleavage products are marked. (D) Schematic of the furin cleavage cluster in Rgmc.

APPENDIX F

Trafficking of Tf and TfR1

RATIONALE

HJV has an unusual pattern of glycosylation. The cellular receptor TfR1 and the secreted protein Tf were used as a control for the specificity of the Endo H digestion.

METHODS

A pulse chase analysis was performed by immunoprecipitating TfR1 and Tf from HepG2 cellular lysates and conditioned medium after 20 minutes of ^{35}S -(met/cys) labeling (Perkin Elmer) and the indicated chase periods as performed previously for HJV (Maxson et al., 2009). HepG2 cells at 30% confluency in 60 mm dishes were labeled using 2 mL met/cys-free media containing 200 μCi of ^{35}S -(met/cys). The immunoprecipitation was performed with 2 μL of sheep anti-TfR1 antibody (crude serum). This preparation of TfR1 had some contaminating Tf, so the antibody recognizes both proteins. This antibody was generated by Caroline Enns.

RESULTS AND CONCLUSIONS

TfR1 is initially Endo H sensitive a 0 time post labeling (Figure A7, upper fainter bands correspond to TfR1). By 20 minutes it has become partially Endo H resistant (one of the three glycosylation sites on TfR1 always remains Endo H sensitive). Endo H resistance indicates that TfR1 has obtained complex oligosaccharides in the Golgi. In contrast, Tf is Endo H sensitive in the cell lysate and then is thought to become Endo H resistant and quickly be secreted, which is why no Endo H resistant Tf is seen in the cell lysate (Figure A7, lower darker bands correspond to Tf). It

should be noted that the form of Tf in the medium is larger than in the lysate due to its complex glycosylation.

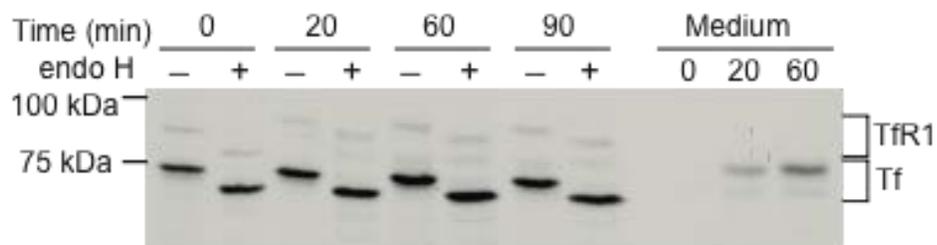


Figure A7. Pulse chase of TfR1 and Tf. HepG2 cells were labeled with ^{35}S for 30 minutes followed by the chase periods with unlabeled complete medium (0, 20, 60 or 90 minutes). Both TfR1 and Tf are detected in the cell lysates, but only Tf is detected in the medium.

REFERENCES

- Abboud, S. and Haile, D. J.** (2000). A novel mammalian iron-regulated protein involved in intracellular iron metabolism. *J Biol Chem* **275**, 19906-12.
- Ait-Slimane, T., Galmes, R., Trugnan, G. and Maurice, M.** (2009). Basolateral internalization of GPI-anchored proteins occurs via a clathrin-independent flotillin-dependent pathway in polarized hepatic cells. *Mol Biol Cell* **20**, 3792-800.
- Anderson, R. G., Vasile, E., Mello, R. J., Brown, M. S. and Goldstein, J. L.** (1978). Immunocytochemical visualization of coated pits and vesicles in human fibroblasts: relation to low density lipoprotein receptor distribution. *Cell* **15**, 919-33.
- Andrews, N. C. and Schmidt, P. J.** (2007). Iron homeostasis. *Annu Rev Physiol* **69**, 69-85.
- Andriopoulos, B., Jr., Corradini, E., Xia, Y., Faasse, S. A., Chen, S., Grgurevic, L., Knutson, M. D., Pietrangelo, A., Vukicevic, S., Lin, H. Y. et al.** (2009). BMP6 is a key endogenous regulator of hepcidin expression and iron metabolism. *Nat Genet* **41**, 482-7.
- Babitt, J. L., Huang, F. W., Wrighting, D. M., Xia, Y., Sidis, Y., Samad, T. A., Campagna, J. A., Chung, R. T., Schneyer, A. L., Woolf, C. J. et al.** (2006). Bone morphogenetic protein signaling by hemojuvelin regulates hepcidin expression. *Nat Genet* **38**, 531-9.
- Babitt, J. L., Huang, F. W., Xia, Y., Sidis, Y., Andrews, N. C. and Lin, H. Y.** (2007). Modulation of bone morphogenetic protein signaling in vivo regulates systemic iron balance. *J Clin Invest* **117**, 1933-9.
- Babitt, J. L., Zhang, Y., Samad, T. A., Xia, Y., Tang, J., Campagna, J. A., Schneyer, A. L., Woolf, C. J. and Lin, H. Y.** (2005). Repulsive guidance molecule (RGMa), a DRAGON homologue, is a bone morphogenetic protein co-receptor. *J Biol Chem* **280**, 29820-7.
- Beliveau, F., Desilets, A. and Leduc, R.** (2009). Probing the substrate specificities of matriptase, matriptase-2, hepsin and DESC1 with internally quenched fluorescent peptides. *FEBS J* **276**, 2213-26.
- Bennett, M. J., Lebron, J. A. and Bjorkman, P. J.** (2000). Crystal structure of the hereditary haemochromatosis protein HFE complexed with transferrin receptor. *Nature* **403**, 46-53.
- Brown, D. A. and London, E.** (2000). Structure and function of sphingolipid- and cholesterol-rich membrane rafts. *J Biol Chem* **275**, 17221-4.
- Calzolari, A., Raggi, C., Deaglio, S., Sposi, N. M., Stafsnes, M., Fecchi, K., Parolini, I., Malavasi, F., Peschle, C., Sargiacomo, M. et al.** (2006). TfR2 localizes in lipid raft domains and is released in exosomes to activate signal transduction along the MAPK pathway. *J Cell Sci* **119**, 4486-98.
- Camaschella, C.** (1998). Juvenile haemochromatosis. *Baillieres Clin Gastroenterol* **12**, 227-35.

- Camaschella, C., Roetto, A., Cali, A., De Gobbi, M., Garozzo, G., Carella, M., Majorano, N., Totaro, A. and Gasparini, P.** (2000). The gene TFR2 is mutated in a new type of haemochromatosis mapping to 7q22. *Nat Genet* **25**, 14-5.
- Camaschella, C., Roetto, A. and De Gobbi, M.** (2002). Juvenile hemochromatosis. *Semin Hematol* **39**, 242-8.
- Chadda, R., Howes, M. T., Plowman, S. J., Hancock, J. F., Parton, R. G. and Mayor, S.** (2007). Cholesterol-sensitive Cdc42 activation regulates actin polymerization for endocytosis via the GEEC pathway. *Traffic* **8**, 702-17.
- Chen, J., Chloupkova, M., Gao, J., Chapman-Arvedson, T. L. and Enns, C. A.** (2007). HFE modulates transferrin receptor 2 levels in hepatoma cells via interactions that differ from transferrin receptor 1-HFE interactions. *J Biol Chem* **282**, 36862-70.
- Cherukuri, S., Potla, R., Sarkar, J., Nurko, S., Harris, Z. L. and Fox, P. L.** (2005). Unexpected role of ceruloplasmin in intestinal iron absorption. *Cell Metab* **2**, 309-19.
- Dameshek, W.** (1931). Primary Hypochromic Anemic (Erythro-Normoblastic Anemia). A New Type of Idiopathic Anemia. *Am J Med Sci* **182**, 520-553.
- Davies, P. S., Zhang, A. S., Anderson, E. L., Roy, C. N., Lampson, M. A., McGraw, T. E. and Enns, C. A.** (2003). Evidence for the interaction of the hereditary haemochromatosis protein, HFE, with the transferrin receptor in endocytic compartments. *Biochem J* **373**, 145-53.
- De Domenico, I., McVey Ward, D. and Kaplan, J.** (2008). Regulation of iron acquisition and storage: consequences for iron-linked disorders. *Nat Rev Mol Cell Biol* **9**, 72-81.
- De Gobbi, M., Roetto, A., Piperno, A., Mariani, R., Alberti, F., Papanikolaou, G., Politou, M., Lockitch, G., Girelli, D., Fargion, S. et al.** (2002). Natural history of juvenile haemochromatosis. *Br J Haematol* **117**, 973-9.
- de Marco, M. C., Martin-Belmonte, F., Kremer, L., Albar, J. P., Correas, I., Vaerman, J. P., Marazuela, M., Byrne, J. A. and Alonso, M. A.** (2002). MAL2, a novel raft protein of the MAL family, is an essential component of the machinery for transcytosis in hepatoma HepG2 cells. *J Cell Biol* **159**, 37-44.
- Donovan, A., Brownlie, A., Zhou, Y., Shepard, J., Pratt, S. J., Moynihan, J., Paw, B. H., Drejer, A., Barut, B., Zapata, A. et al.** (2000). Positional cloning of zebrafish ferroportin1 identifies a conserved vertebrate iron exporter. *Nature* **403**, 776-81.
- Donovan, A., Lima, C. A., Pinkus, J. L., Pinkus, G. S., Zon, L. I., Robine, S. and Andrews, N. C.** (2005). The iron exporter ferroportin/Slc40a1 is essential for iron homeostasis. *Cell Metab* **1**, 191-200.
- Du, X., She, E., Gelbart, T., Truksa, J., Lee, P., Xia, Y., Khovananth, K., Mudd, S., Mann, N., Moresco, E. M. et al.** (2008). The serine protease TMPRSS6 is required to sense iron deficiency. *Science* **320**, 1088-92.
- Feder, J. N., Gnirke, A., Thomas, W., Tsuchihashi, Z., Ruddy, D. A., Basava, A., Dormishian, F., Domingo, R., Jr., Ellis, M. C., Fullan, A. et al.** (1996). A novel MHC class I-like gene is mutated in patients with hereditary haemochromatosis. *Nat Genet* **13**, 399-408.

Feng, Y. and Longmore, G. D. (2005). The LIM protein Ajuba influences interleukin-1-induced NF-kappaB activation by affecting the assembly and activity of the protein kinase Czeta/p62/TRAF6 signaling complex. *Mol Cell Biol* **25**, 4010-22.

Finberg, K. E., Heeney, M. M., Campagna, D. R., Aydinok, Y., Pearson, H. A., Hartman, K. R., Mayo, M. M., Samuel, S. M., Strouse, J. J., Markianos, K. et al. (2008). Mutations in Tmprss6 cause iron-refractory iron deficiency anemia (IRIDA). *Nat Genet* **40**, 569-71.

Finberg, K. E., Whittlesey, R. L., Fleming, M. D. and Andrews, N. C. (2010). Down-regulation of Bmp/Smad signaling by Tmprss6 is required for maintenance of systemic iron homeostasis. *Blood* **115**, 3817-26.

Fleming, M. D., Romano, M. A., Su, M. A., Garrick, L. M., Garrick, M. D. and Andrews, N. C. (1998). Nramp2 is mutated in the anemic Belgrade (b) rat: evidence of a role for Nramp2 in endosomal iron transport. *Proc Natl Acad Sci U S A* **95**, 1148-53.

Fleming, M. D., Trenor, C. C., 3rd, Su, M. A., Foernzler, D., Beier, D. R., Dietrich, W. F. and Andrews, N. C. (1997). Microcytic anaemia mice have a mutation in Nramp2, a candidate iron transporter gene. *Nat Genet* **16**, 383-6.

Folgueras, A. R., de Lara, F. M., Pendas, A. M., Garabaya, C., Rodriguez, F., Astudillo, A., Bernal, T., Cabanillas, R., Lopez-Otin, C. and Velasco, G. (2008). Membrane-bound serine protease matriptase-2 (Tmprss6) is an essential regulator of iron homeostasis. *Blood* **112**, 2539-45.

Goldschneider, D., Rama, N., Guix, C. and Mehlen, P. (2008). The neogenin intracellular domain regulates gene transcription via nuclear translocation. *Mol Cell Biol* **28**, 4068-79.

Gunshin, H., Fujiwara, Y., Custodio, A. O., Drenzo, C., Robine, S. and Andrews, N. C. (2005). Slc11a2 is required for intestinal iron absorption and erythropoiesis but dispensable in placenta and liver. *J Clin Invest* **115**, 1258-66.

Gunshin, H., Mackenzie, B., Berger, U. V., Gunshin, Y., Romero, M. F., Boron, W. F., Nussberger, S., Gollan, J. L. and Hediger, M. A. (1997). Cloning and characterization of a mammalian proton-coupled metal-ion transporter. *Nature* **388**, 482-8.

Harris, Z. L., Durley, A. P., Man, T. K. and Gitlin, J. D. (1999). Targeted gene disruption reveals an essential role for ceruloplasmin in cellular iron efflux. *Proc Natl Acad Sci U S A* **96**, 10812-7.

Heath, C. W., Strauss, M. B. and Castle, W. B. (1932). QUANTITATIVE ASPECTS OF IRON DEFICIENCY IN HYPOCHROMIC ANEMIA: (The Parenteral Administration of Iron). *J Clin Invest* **11**, 1293-312.

Hellman, N. E., Kono, S., Miyajima, H. and Gitlin, J. D. (2002). Biochemical analysis of a missense mutation in aceruloplasminemia. *J Biol Chem* **277**, 1375-80.

Horns, H. L. (1949). Hemochromatosis; cardiac failure associated with extensive hemosiderosis of the myocardium. *Am J Med* **6**, 272-4.

Huang, F. W., Pinkus, J. L., Pinkus, G. S., Fleming, M. D. and Andrews, N. C. (2005). A mouse model of juvenile hemochromatosis. *J Clin Invest* **115**, 2187-91.

Johnson, M. B. and Enns, C. A. (2004). Diferric transferrin regulates transferrin receptor 2 protein stability. *Blood* **104**, 4287-93.

- Kautz, L., Meynard, D., Monnier, A., Darnaud, V., Bouvet, R., Wang, R. H., Deng, C., Vaultont, S., Mosser, J., Coppin, H. et al.** (2008). Iron regulates phosphorylation of Smad1/5/8 and gene expression of Bmp6, Smad7, Id1, and Atoh8 in the mouse liver. *Blood* **112**, 1503-9.
- Klausner, R. D., Ashwell, G., van Renswoude, J., Harford, J. B. and Bridges, K. R.** (1983). Binding of apotransferrin to K562 cells: explanation of the transferrin cycle. *Proc Natl Acad Sci U S A* **80**, 2263-6.
- Knowles, B. B., Howe, C. C. and Aden, D. P.** (1980). Human hepatocellular carcinoma cell lines secrete the major plasma proteins and hepatitis B surface antigen. *Science* **209**, 497-9.
- Kuninger, D., Kuns-Hashimoto, R., Kuzmickas, R. and Rotwein, P.** (2006). Complex biosynthesis of the muscle-enriched iron regulator RGMc. *J Cell Sci* **119**, 3273-83.
- Kuninger, D., Kuns-Hashimoto, R., Nili, M. and Rotwein, P.** (2008). Pro-protein convertases control the maturation and processing of the iron-regulatory protein, RGMc/hemojuvelin. *BMC Biochem* **9**, 9.
- Kuns-Hashimoto, R., Kuninger, D., Nili, M. and Rotwein, P.** (2008). Selective Binding of RGMc/Hemojuvelin, a Key Protein in Systemic Iron Metabolism, to BMP-2 and Neogenin. *Am J Physiol Cell Physiol*.
- Laidlaw, P. P.** (1904). Some observations on blood pigments. *J Physiol* **31**, 464-72.
- Lajoie, P., Goetz, J. G., Dennis, J. W. and Nabi, I. R.** (2009). Lattices, rafts, and scaffolds: domain regulation of receptor signaling at the plasma membrane. *J Cell Biol* **185**, 381-5.
- Lang, T., Bruns, D., Wenzel, D., Riedel, D., Holroyd, P., Thiele, C. and Jahn, R.** (2001). SNAREs are concentrated in cholesterol-dependent clusters that define docking and fusion sites for exocytosis. *EMBO J* **20**, 2202-13.
- Larsson, S., Wierup, N., Sundler, F., Eliasson, L. and Holm, C.** (2008). Lack of cholesterol mobilization in islets of hormone-sensitive lipase deficient mice impairs insulin secretion. *Biochem Biophys Res Commun* **376**, 558-62.
- Lebron, J. A., West, A. P., Jr. and Bjorkman, P. J.** (1999). The hemochromatosis protein HFE competes with transferrin for binding to the transferrin receptor. *J Mol Biol* **294**, 239-45.
- Lee, D. H., Zhou, L. J., Zhou, Z., Xie, J. X., Jung, J. U., Liu, Y., Xi, C. X., Mei, L. and Xiong, W. C.** (2010). Neogenin inhibits HJV secretion and regulates BMP-induced hepcidin expression and iron homeostasis. *Blood* **115**, 3136-45.
- Li, W., Lee, J., Vikis, H. G., Lee, S. H., Liu, G., Aurandt, J., Shen, T. L., Fearon, E. R., Guan, J. L., Han, M. et al.** (2004). Activation of FAK and Src are receptor-proximal events required for netrin signaling. *Nat Neurosci* **7**, 1213-21.
- Lin, L., Goldberg, Y. P. and Ganz, T.** (2005). Competitive regulation of hepcidin mRNA by soluble and cell-associated hemojuvelin. *Blood* **106**, 2884-9.
- Lin, L., Nemeth, E., Goodnough, J. B., Thapa, D. R., Gabayan, V. and Ganz, T.** (2008). Soluble hemojuvelin is released by proprotein convertase-mediated cleavage at a conserved polybasic RNRR site. *Blood Cells Mol Dis* **40**, 122-31.

- Lin, L., Valore, E. V., Nemeth, E., Goodnough, J. B., Gabayan, V. and Ganz, T.** (2007). Iron transferrin regulates hepcidin synthesis in primary hepatocyte culture through hemojuvelin and BMP2/4. *Blood* **110**, 2182-9.
- Matsunaga, E., Tauszig-Delamasure, S., Monnier, P. P., Mueller, B. K., Strittmatter, S. M., Mehlen, P. and Chedotal, A.** (2004). RGM and its receptor neogenin regulate neuronal survival. *Nat Cell Biol* **6**, 749-55.
- Maxson, J. E., Enns, C. A. and Zhang, A. S.** (2009). Processing of hemojuvelin requires retrograde trafficking to the Golgi in HepG2 cells. *Blood* **113**, 1786-93.
- McKie, A. T., Barrow, D., Latunde-Dada, G. O., Rolfs, A., Sager, G., Mudaly, E., Mudaly, M., Richardson, C., Barlow, D., Bomford, A. et al.** (2001). An iron-regulated ferric reductase associated with the absorption of dietary iron. *Science* **291**, 1755-9.
- McKie, A. T., Marciani, P., Rolfs, A., Brennan, K., Wehr, K., Barrow, D., Miret, S., Bomford, A., Peters, T. J., Farzaneh, F. et al.** (2000). A novel duodenal iron-regulated transporter, IREG1, implicated in the basolateral transfer of iron to the circulation. *Mol Cell* **5**, 299-309.
- Mellman, I.** (1996). Endocytosis and molecular sorting. *Annu Rev Cell Dev Biol* **12**, 575-625.
- Merle, U., Theilig, F., Fein, E., Gehrke, S., Kallinowski, B., Riedel, H. D., Bachmann, S., Stremmel, W. and Kulaksiz, H.** (2007). Localization of the iron-regulatory proteins hemojuvelin and transferrin receptor 2 to the basolateral membrane domain of hepatocytes. *Histochem Cell Biol* **127**, 221-6.
- Merryweather-Clarke, A. T., Pointon, J. J., Shearman, J. D. and Robson, K. J.** (1997). Global prevalence of putative haemochromatosis mutations. *J Med Genet* **34**, 275-8.
- Meynard, D., Kautz, L., Darnaud, V., Canonne-Hergaux, F., Coppin, H. and Roth, M. P.** (2009). Lack of the bone morphogenetic protein BMP6 induces massive iron overload. *Nat Genet* **41**, 478-81.
- Minot, G. R. a. H., C.W.** (1932). The Response of the Reticulocytes to Iron. *Am J Med Sci* **183**, 110-121.
- Molloy, S. S., Bresnahan, P. A., Leppla, S. H., Klimpel, K. R. and Thomas, G.** (1992). Human furin is a calcium-dependent serine endoprotease that recognizes the sequence Arg-X-X-Arg and efficiently cleaves anthrax toxin protective antigen. *J Biol Chem* **267**, 16396-402.
- Molloy, S. S., Thomas, L., VanSlyke, J. K., Stenberg, P. E. and Thomas, G.** (1994). Intracellular trafficking and activation of the furin proprotein convertase: localization to the TGN and recycling from the cell surface. *Embo J* **13**, 18-33.
- Montosi, G., Donovan, A., Totaro, A., Garuti, C., Pignatti, E., Cassanelli, S., Trenor, C. C., Gasparini, P., Andrews, N. C. and Pietrangelo, A.** (2001). Autosomal-dominant hemochromatosis is associated with a mutation in the ferroportin (SLC11A3) gene. *J Clin Invest* **108**, 619-23.
- Muniz, M., Nuoffer, C., Hauri, H. P. and Riezman, H.** (2000). The Emp24 complex recruits a specific cargo molecule into endoplasmic reticulum-derived vesicles. *J Cell Biol* **148**, 925-30.

- Nemeth, E., Tuttle, M. S., Powelson, J., Vaughn, M. B., Donovan, A., Ward, D. M., Ganz, T. and Kaplan, J.** (2004). Hepcidin regulates cellular iron efflux by binding to ferroportin and inducing its internalization. *Science* **306**, 2090-3.
- Nichols, B. J., Kenworthy, A. K., Polishchuk, R. S., Lodge, R., Roberts, T. H., Hirschberg, K., Phair, R. D. and Lippincott-Schwartz, J.** (2001). Rapid cycling of lipid raft markers between the cell surface and Golgi complex. *J Cell Biol* **153**, 529-41.
- Nicolas, G., Bennoun, M., Devaux, I., Beaumont, C., Grandchamp, B., Kahn, A. and Vaulont, S.** (2001). Lack of hepcidin gene expression and severe tissue iron overload in upstream stimulatory factor 2 (USF2) knockout mice. *Proc Natl Acad Sci USA* **98**, 8780-5.
- Nicolas, G., Chauvet, C., Viatte, L., Danan, J. L., Bigard, X., Devaux, I., Beaumont, C., Kahn, A. and Vaulont, S.** (2002). The gene encoding the iron regulatory peptide hepcidin is regulated by anemia, hypoxia, and inflammation. *J Clin Invest* **110**, 1037-44.
- Niederkofler, V., Salie, R. and Arber, S.** (2005). Hemojuvelin is essential for dietary iron sensing, and its mutation leads to severe iron overload. *J Clin Invest* **115**, 2180-6.
- Niederkofler, V., Salie, R., Sigrist, M. and Arber, S.** (2004). Repulsive guidance molecule (RGM) gene function is required for neural tube closure but not retinal topography in the mouse visual system. *J Neurosci* **24**, 808-18.
- Ohgami, R. S., Campagna, D. R., Greer, E. L., Antiochos, B., McDonald, A., Chen, J., Sharp, J. J., Fujiwara, Y., Barker, J. E. and Fleming, M. D.** (2005). Identification of a ferrireductase required for efficient transferrin-dependent iron uptake in erythroid cells. *Nat Genet* **37**, 1264-9.
- Opie, E. L.** (1899). A Case of Haemochromatosis.-the Relation of Haemochromatosis to Bronzed Diabetes. *J Exp Med* **4**, 279-306.
- Orlandi, P. A. and Fishman, P. H.** (1998). Filipin-dependent inhibition of cholera toxin: evidence for toxin internalization and activation through caveolae-like domains. *J Cell Biol* **141**, 905-15.
- Papanikolaou, G., Samuels, M. E., Ludwig, E. H., MacDonald, M. L., Franchini, P. L., Dube, M. P., Andres, L., MacFarlane, J., Sakellaropoulos, N., Politou, M. et al.** (2004). Mutations in HFE2 cause iron overload in chromosome 1q-linked juvenile hemochromatosis. *Nat Genet* **36**, 77-82.
- Park, C. H., Bacon, B. R., Brittenham, G. M. and Tavill, A. S.** (1987). Pathology of dietary carbonyl iron overload in rats. *Lab Invest* **57**, 555-63.
- Park, C. H., Valore, E. V., Waring, A. J. and Ganz, T.** (2001). Hepcidin, a urinary antimicrobial peptide synthesized in the liver. *J Biol Chem* **276**, 7806-10.
- Peters, R. A.** (1912). Chemical nature of specific oxygen capacity in haemoglobin. *J Physiol* **44**, 131-49.
- Pigeon, C., Ilyin, G., Courselaud, B., Leroyer, P., Turlin, B., Brissot, P. and Loreal, O.** (2001). A new mouse liver-specific gene, encoding a protein homologous to human antimicrobial peptide hepcidin, is overexpressed during iron overload. *J Biol Chem* **276**, 7811-9.

- Rajagopalan, S., Deitinghoff, L., Davis, D., Conrad, S., Skutella, T., Chedotal, A., Mueller, B. K. and Strittmatter, S. M.** (2004). Neogenin mediates the action of repulsive guidance molecule. *Nat Cell Biol* **6**, 756-62.
- Robb, A. and Wessling-Resnick, M.** (2004). Regulation of transferrin receptor 2 protein levels by transferrin. *Blood* **104**, 4294-9.
- Roebroek, A. J., Taylor, N. A., Louagie, E., Pauli, I., Smeijers, L., Snellinx, A., Lauwers, A., Van de Ven, W. J., Hartmann, D. and Creemers, J. W.** (2004). Limited redundancy of the proprotein convertase furin in mouse liver. *J Biol Chem* **279**, 53442-50.
- Sabharanjak, S., Sharma, P., Parton, R. G. and Mayor, S.** (2002). GPI-anchored proteins are delivered to recycling endosomes via a distinct cdc42-regulated, clathrin-independent pinocytic pathway. *Dev Cell* **2**, 411-23.
- Samad, T. A., Rebbapragada, A., Bell, E., Zhang, Y., Sidis, Y., Jeong, S. J., Campagna, J. A., Perusini, S., Fabrizio, D. A., Schneyer, A. L. et al.** (2005). DRAGON, a bone morphogenetic protein co-receptor. *J Biol Chem* **280**, 14122-9.
- Schaffar, G., Taniguchi, J., Brodbeck, T., Meyer, A. H., Schmidt, M., Yamashita, T. and Mueller, B. K.** (2008). LIM-only protein 4 interacts directly with the repulsive guidance molecule A receptor Neogenin. *J Neurochem* **107**, 418-31.
- Schell, M. J., Maurice, M., Stieger, B. and Hubbard, A. L.** (1992). 5'nucleotidase is sorted to the apical domain of hepatocytes via an indirect route. *J Cell Biol* **119**, 1173-82.
- Seidah, N. G., Mayer, G., Zaid, A., Rousselet, E., Nassoury, N., Poirier, S., Essalmani, R. and Prat, A.** (2008). The activation and physiological functions of the proprotein convertases. *Int J Biochem Cell Biol* **40**, 1111-25.
- Sheldon, J. H.** (1934). Haemochromatosis. *The Lancet*, 1031-1036.
- Shi, Y. and Massague, J.** (2003). Mechanisms of TGF-beta signaling from cell membrane to the nucleus. *Cell* **113**, 685-700.
- Silvestri, L., Pagani, A. and Camaschella, C.** (2008a). Furin-mediated release of soluble hemojuvelin: a new link between hypoxia and iron homeostasis. *Blood* **111**, 924-31.
- Silvestri, L., Pagani, A., Fazi, C., Gerardi, G., Levi, S., Arosio, P. and Camaschella, C.** (2007). Defective targeting of hemojuvelin to plasma membrane is a common pathogenetic mechanism in juvenile hemochromatosis. *Blood* **109**, 4503-10.
- Silvestri, L., Pagani, A., Nai, A., De Domenico, I., Kaplan, J. and Camaschella, C.** (2008b). The serine protease matriptase-2 (TMPRSS6) inhibits hepcidin activation by cleaving membrane hemojuvelin. *Cell Metab* **8**, 502-11.
- Snider, M. D. and Rogers, O. C.** (1985). Intracellular movement of cell surface receptors after endocytosis: resialylation of asialo-transferrin receptor in human erythroleukemia cells. *J Cell Biol* **100**, 826-34.
- Snider, M. D. and Rogers, O. C.** (1986). Membrane traffic in animal cells: cellular glycoproteins return to the site of Golgi mannosidase I. *J Cell Biol* **103**, 265-75.
- Sun, B., Zhang, H., Franco, L. M., Brown, T., Bird, A., Schneider, A. and Koeberl, D. D.** (2005). Correction of glycogen storage disease type II by an adeno-associated virus vector containing a muscle-specific promoter. *Mol Ther* **11**, 889-98.

Takida, S., Maeda, Y. and Kinoshita, T. (2008). Mammalian GPI-anchored proteins require p24 proteins for their efficient transport from the ER to the plasma membrane. *Biochem J* **409**, 555-62.

Teasdale, R. D. and Jackson, M. R. (1996). Signal-mediated sorting of membrane proteins between the endoplasmic reticulum and the golgi apparatus. *Annu Rev Cell Dev Biol* **12**, 27-54.

Theil, E. C. (2003). Ferritin: at the crossroads of iron and oxygen metabolism. *J Nutr* **133**, 1549S-53S.

Thomas, G. (2002). Furin at the cutting edge: from protein traffic to embryogenesis and disease. *Nat Rev Mol Cell Biol* **3**, 753-66.

VanSlyke, J. K. and Musil, L. S. (2005). Cytosolic stress reduces degradation of connexin43 internalized from the cell surface and enhances gap junction formation and function. *Mol Biol Cell* **16**, 5247-57.

Velasco, G., Cal, S., Quesada, V., Sanchez, L. M. and Lopez-Otin, C. (2002). Matriptase-2, a membrane-bound mosaic serine proteinase predominantly expressed in human liver and showing degrading activity against extracellular matrix proteins. *J Biol Chem* **277**, 37637-46.

Viatte, L., Lesbordes-Brion, J. C., Lou, D. Q., Bennoun, M., Nicolas, G., Kahn, A., Canonne-Hergaux, F. and Vaulont, S. (2005). Deregulation of proteins involved in iron metabolism in hepcidin-deficient mice. *Blood* **105**, 4861-4.

Vikman, J., Jimenez-Feltstrom, J., Nyman, P., Thelin, J. and Eliasson, L. (2009). Insulin secretion is highly sensitive to desorption of plasma membrane cholesterol. *FASEB J* **23**, 58-67.

Vulpe, C. D., Kuo, Y. M., Murphy, T. L., Cowley, L., Askwith, C., Libina, N., Gitschier, J. and Anderson, G. J. (1999). Hephaestin, a ceruloplasmin homologue implicated in intestinal iron transport, is defective in the sla mouse. *Nat Genet* **21**, 195-9.

Wang, R. H., Li, C., Xu, X., Zheng, Y., Xiao, C., Zervas, P., Cooperman, S., Eckhaus, M., Rouault, T., Mishra, L. et al. (2005). A role of SMAD4 in iron metabolism through the positive regulation of hepcidin expression. *Cell Metab* **2**, 399-409.

West, A. P., Jr., Giannetti, A. M., Herr, A. B., Bennett, M. J., Nangiana, J. S., Pierce, J. R., Weiner, L. P., Snow, P. M. and Bjorkman, P. J. (2001). Mutational analysis of the transferrin receptor reveals overlapping HFE and transferrin binding sites. *J Mol Biol* **313**, 385-97.

Whitlock, E. P., Garlitz, B. A., Harris, E. L., Beil, T. L. and Smith, P. R. (2006). Screening for hereditary hemochromatosis: a systematic review for the U.S. Preventive Services Task Force. *Ann Intern Med* **145**, 209-23.

Wouters, S., Leruth, M., Decroly, E., Vandenbranden, M., Creemers, J. W., van de Loo, J. W., Ruyschaert, J. M. and Courtoy, P. J. (1998). Furin and proprotein convertase 7 (PC7)/lymphoma PC endogenously expressed in rat liver can be resolved into distinct post-Golgi compartments. *Biochem J* **336 (Pt 2)**, 311-6.

Xia, Y., Babitt, J. L., Sidis, Y., Chung, R. T. and Lin, H. Y. (2008). Hemojuvelin regulates hepcidin expression via a selective subset of BMP ligands and receptors independently of neogenin. *Blood*.

Xia, Y., Sidis, Y., Mukherjee, A., Samad, T. A., Brenner, G., Woolf, C. J., Lin, H. Y. and Schneyer, A. (2005). Localization and action of Dragon (repulsive guidance molecule b), a novel bone morphogenetic protein coreceptor, throughout the reproductive axis. *Endocrinology* **146**, 3614-21.

Yang, F., West, A. P., Jr., Allendorph, G. P., Choe, S. and Bjorkman, P. J. (2008). Neogenin interacts with hemojuvelin through its two membrane-proximal fibronectin type III domains. *Biochemistry* **47**, 4237-45.

Yoshimori, T., Yamamoto, A., Moriyama, Y., Futai, M. and Tashiro, Y. (1991). Bafilomycin A1, a specific inhibitor of vacuolar-type H(+)-ATPase, inhibits acidification and protein degradation in lysosomes of cultured cells. *J Biol Chem* **266**, 17707-12.

Zacchigna, L., Vecchione, C., Notte, A., Cordenonsi, M., Dupont, S., Maretto, S., Cifelli, G., Ferrari, A., Maffei, A., Fabbro, C. et al. (2006). Emilin1 links TGF-beta maturation to blood pressure homeostasis. *Cell* **124**, 929-42.

Zhang, A. S., Anderson, S. A., Meyers, K. R., Hernandez, C., Eisenstein, R. S. and Enns, C. A. (2007). Evidence that inhibition of hemojuvelin shedding in response to iron is mediated through neogenin. *J Biol Chem* **282**, 12547-56.

Zhang, A. S., Gao, J., Koeberl, D. D. and Enns, C. A. (2010). The role of hepatocyte hemojuvelin in the regulation of bone morphogenic protein-6 and hepcidin expression in vivo. *J Biol Chem* **285**, 16416-23.

Zhang, A. S., West, A. P., Jr., Wyman, A. E., Bjorkman, P. J. and Enns, C. A. (2005). Interaction of hemojuvelin with neogenin results in iron accumulation in human embryonic kidney 293 cells. *J Biol Chem* **280**, 33885-94.

Zhang, A. S., Xiong, S., Tsukamoto, H. and Enns, C. A. (2004). Localization of iron metabolism-related mRNAs in rat liver indicate that HFE is expressed predominantly in hepatocytes. *Blood* **103**, 1509-14.

Zhang, A. S., Yang, F., Meyer, K., Hernandez, C., Chapman-Arvedson, T., Bjorkman, P. J. and Enns, C. A. (2008). Neogenin-mediated hemojuvelin shedding occurs after hemojuvelin traffics to the plasma membrane. *J Biol Chem* **283**, 17494-502.

Zhang, A. S., Yang, F., Wang, J., Tsukamoto, H. and Enns, C. A. (2009). Hemojuvelin-neogenin interaction is required for bone morphogenic protein-4-induced hepcidin expression. *J Biol Chem* **284**, 22580-9.

Zhou, Z., Xie, J., Lee, D., Liu, Y., Jung, J., Zhou, L., Xiong, S., Mei, L. and Xiong, W. C. (2010). Neogenin regulation of BMP-induced canonical Smad signaling and endochondral bone formation. *Dev Cell* **19**, 90-102.

Julia Elizabeth Maxson

Education:

- Scripps Women's College, B.A., Awarded May 2005.
Honors in Biology, Summa Cum Laude, GPA: 3.94.
- Graduate Student OHSU, 2005-2011, GPA: 4.0.

Research Experience:

- Undergraduate research assistant to Dr. Gretchen Edwalds-Gilbert, Claremont Colleges. Subject of research: The yeast spliceosome protein Prp43. September 2002-May 2003.
- Undergraduate research assistant to Dr. Emily Wiley, Claremont Colleges. Thesis title: Regulation of Chromatin Structure and Gene Expression by Histone Deacetylases in *Tetrahymena thermophila*. June 2003- June 2005.
- Summer Research Student in the lab of Dr. Toshio Tsukiyama, Fred Hutchinson Cancer Research Center. Subject of research: ATP dependant chromatin remodeling factors. June 2004-August 2004.
- Graduate Student at OHSU in Caroline Enns' Lab. Processing and Trafficking of the Iron Regulatory Protein, Hemojuvelin. 2007-2011.

Honors Societies:

- Sigma Xi.
- Phi Beta Kappa.

Awards:

- Isabel Fothergill Smith Award for excellence in the Physical Sciences and the Humanities.
- Barbara McClintock Award for the best senior thesis project in the sciences, Scripps College.
- Herbert Award for Graduate Studies at OHSU.
- NSF Graduate Research Fellowship Program, Honorable Mention.
- 2009 OHSU Student Research Forum best oral presentation.
- 2009 PMCB best poster presentation.

Scholarships and Fellowships:

- Earthwatch Research Fellowship.
- Autodesk Inc. Design Your Future Scholarship.
- James E. Scripps Merit Scholarship.
- W.M. Keck Summer Research Fellowship.
- NIH Training Grant Recipient, PMCB Program, OHSU.
- Training Program in Embryonic Development Grant Recipient, OHSU.
- ARCS Scholarship.
- Vertex Scholarship.

- American Heart Association Predoctoral Fellowship.

Journal Club and Committee Membership:

- Developmental Biology Journal Club, 2006-2009
- Cell Biology Journal Club, 2007-2010.
- Conjoint Curriculum Committee, 2007-2010.

Publications:

- Parker K, **Maxson J**, Mooney A, Wiley EA. Class I Histone Deacetylase Thd1p Promotes Global Chromatin Condensation in *Tetrahymena thermophila*. *Eukaryotic Cell*. 2007 Oct;6(10):1913-24.
- Smith JJ, Torigoe SE, **Maxson J**, Fish LC, Wiley EA. A class II histone deacetylase acts on newly synthesized histones in *Tetrahymena*. *Eukaryotic Cell*. 2008 Mar;7(3):471-82.
- **Maxson JE**, Enns CA, and Zhang A-S. Processing of hemojuvelin requires retrograde trafficking to the Golgi in HepG2 cells. *Blood*. 2009 Feb 19;113(8):1786-93.
- **Maxson JE**, Chen J, Enns CA, and Zhang A-S. Matriptase-2 and furin cleaved forms of hemojuvelin have different functions in the down-regulation of hepcidin expression. *Journal of Biological Chemistry*. 2010 Dec 10;285(50):39021-8.
- Pratt EB, Wentzell JS, **Maxson JE**, Courter L, Hazelett D, Christian JL. The cell giveth and the cell taketh away: An overview of Notch pathway activation by endocytic trafficking of ligands and receptors. *Acta Histochemistry*. 2011 May;113(3):248-55.
- **Maxson JE**, Enns CA, and Zhang A-S. The GPI-anchor of hemojuvelin potentiates signaling, but is not required for proteolytic processing. Submitted.